h) AIRRIG : Figs. 4.59 and 4.60 show that an increase in irrigated area is primarily responsible for reduced base flows, and base loads, with resultant decrease in the corresponding means, and a small rise in the standard deviations. The mean salt concentrations will inevitably rise but the effect upon the standard deviation depends upon the input pollutograph, although an increase is the most common result as base flow salt concentrations are usually higher than those during floods.

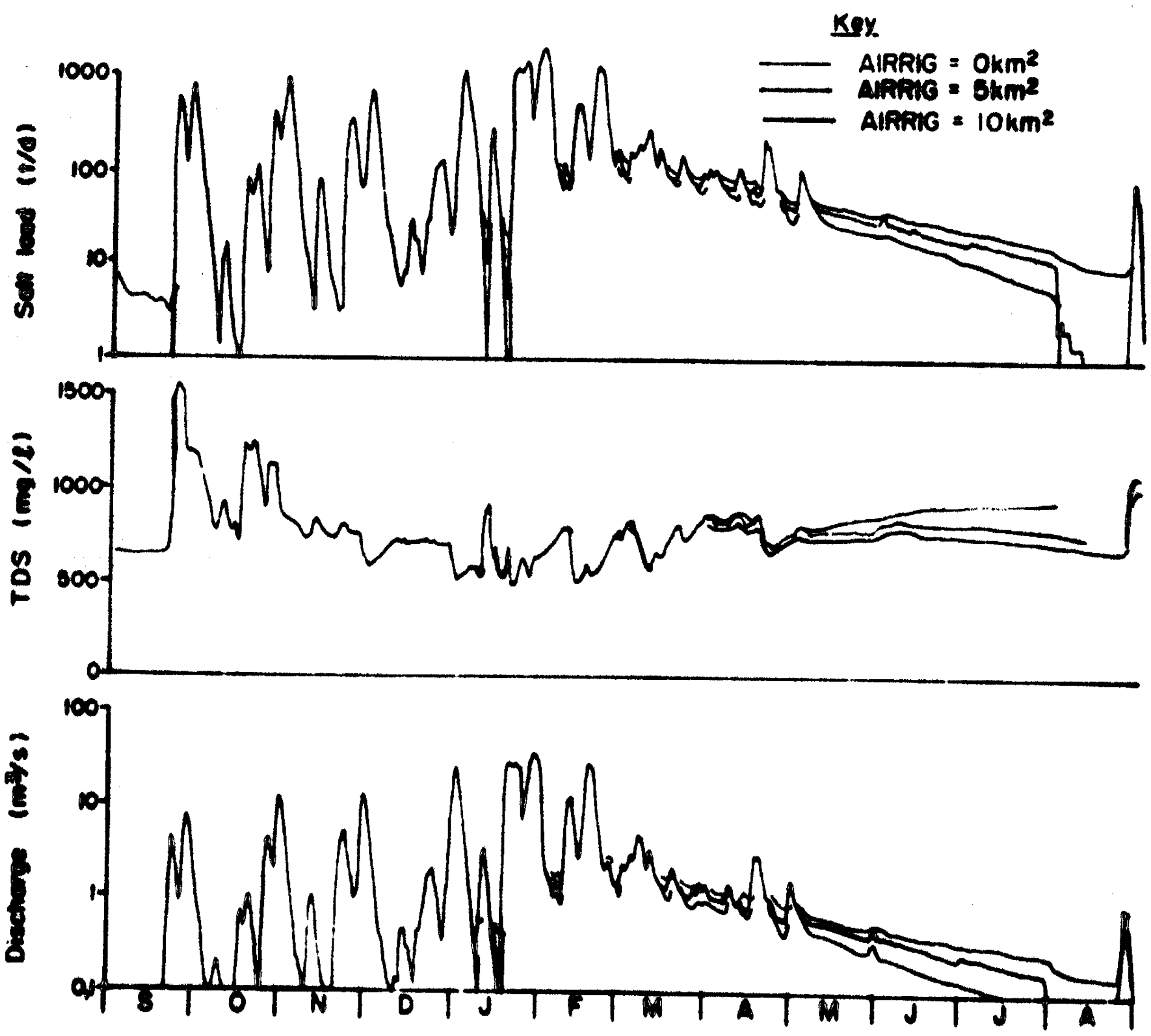

Fig.4.59: Sensitivity of modelled daily discharges, salt concentrations and salt loads to changes in AIRRIG.

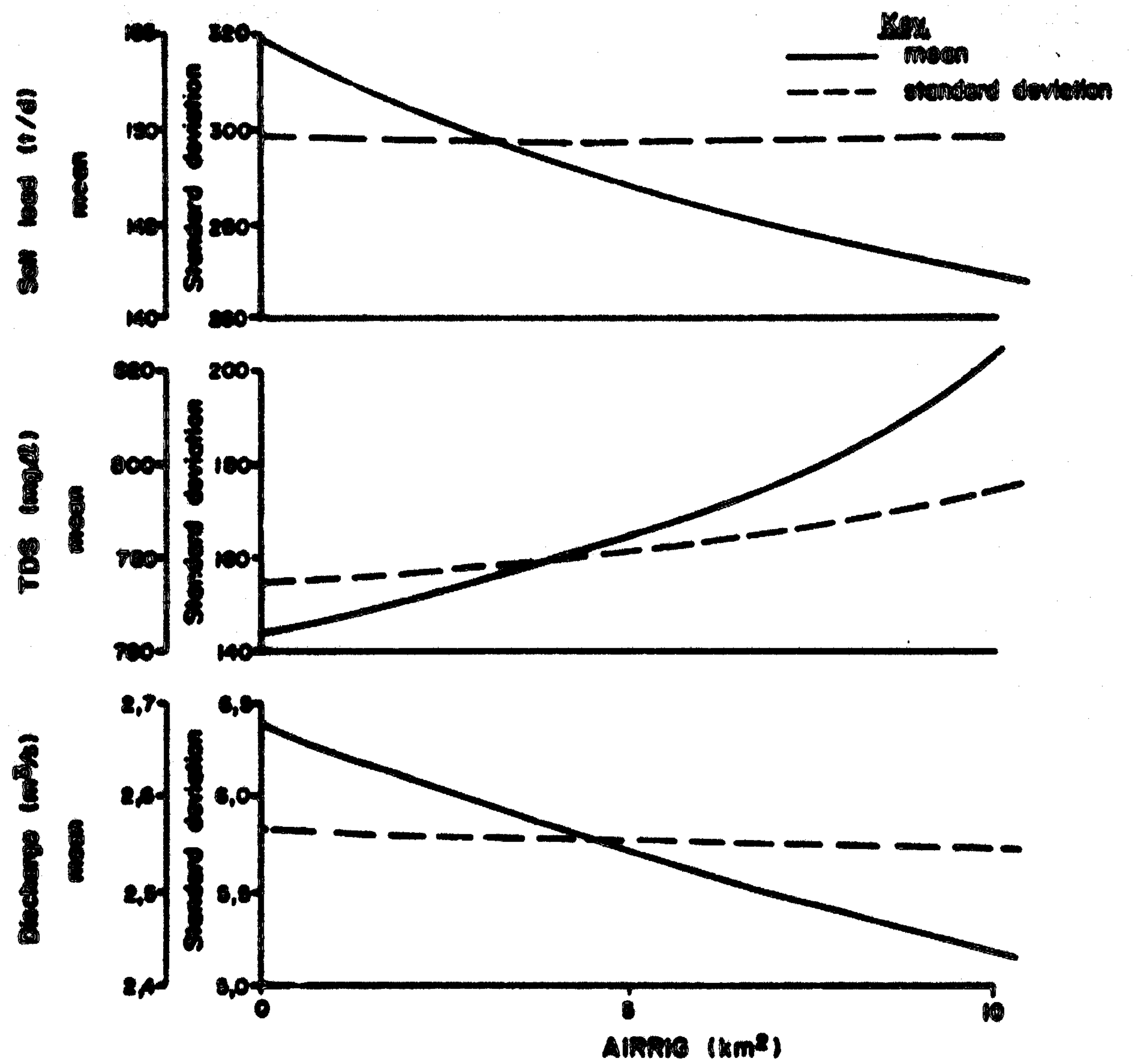

Fig.4.60: Sensitivity of modelled means and standard deviations to changes in AIRRIG.

i) <u>RETURN</u> : Varying the proportion of irrigation demand returned to the stream between 0,1 and 0,3 produced little change in modelled daily discharges and salinities. The sensitivity of modelled values to changes in RETURN were therefore not plotted. An increase in RETURN is accompanied by a small increase in the mean discharge and a small decrease in the standard deviations of modelled daily discharges and salt loads. The mean salt load is unaffected and base flow salt concentrations decline slightly.

j) __FIX__ : Figs. 4.61 and 4.62 show that an increase in FIX, the proportion of the irrigated salt load retained on irrigated lands, causes a decline in mean salt loads and concentrations due to reduced base loads. The increase in the standard deviation of daily salt loads is too small to be detected in Fig. 4.62 because of the very small changes in base flow salt loads. The standard deviation of modelled daily salt concentrations increases as FIX increases because in the example used the base flow salt concentrations are generally higher than those during most floods.

k) __FIRRIG__ : Figs. 4.63 and 4.64 show that an increase in FIRRIG causes a reduction in base flows and consequently reduces the mean discharge and mean salt load. Base flow salt concentrations also increase with a consequent rise in the corresponding mean and standard deviation. The increases in the standard deviations of modelled daily discharges and salt loads are small.

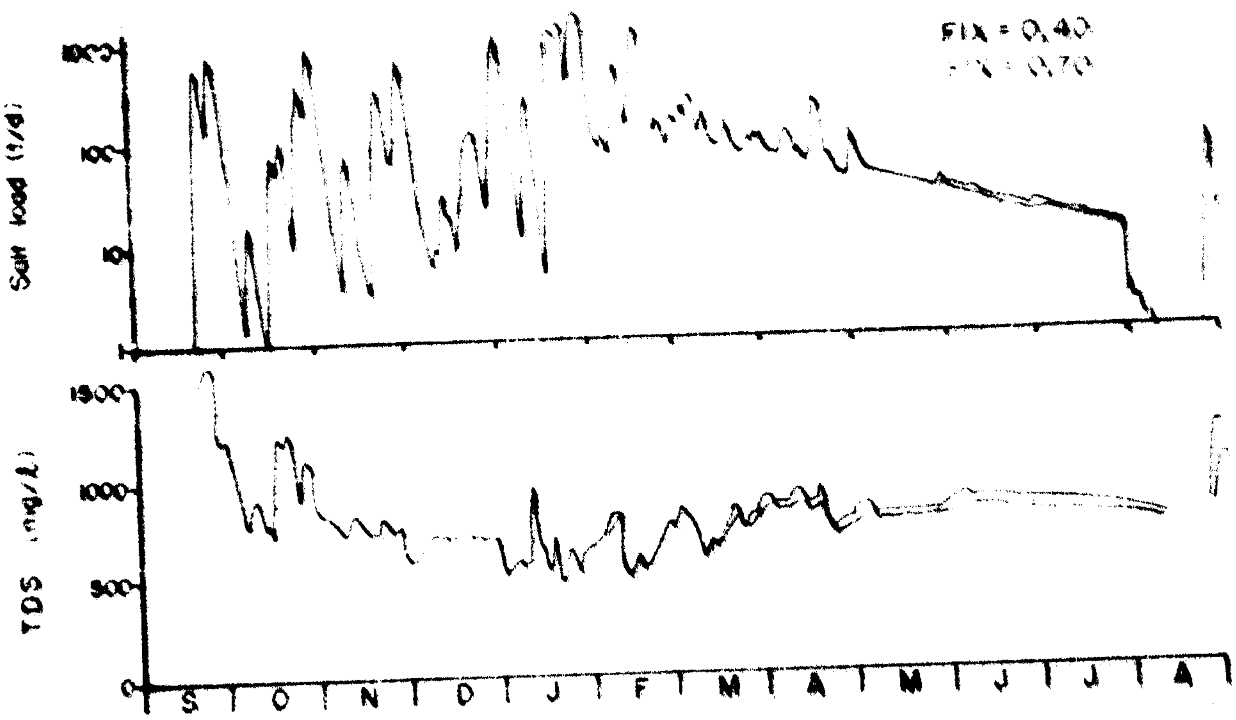

Fig. 4.61 Sensitivity of modelled daily discharges, salt concentrations and salt loads to changes in FIX

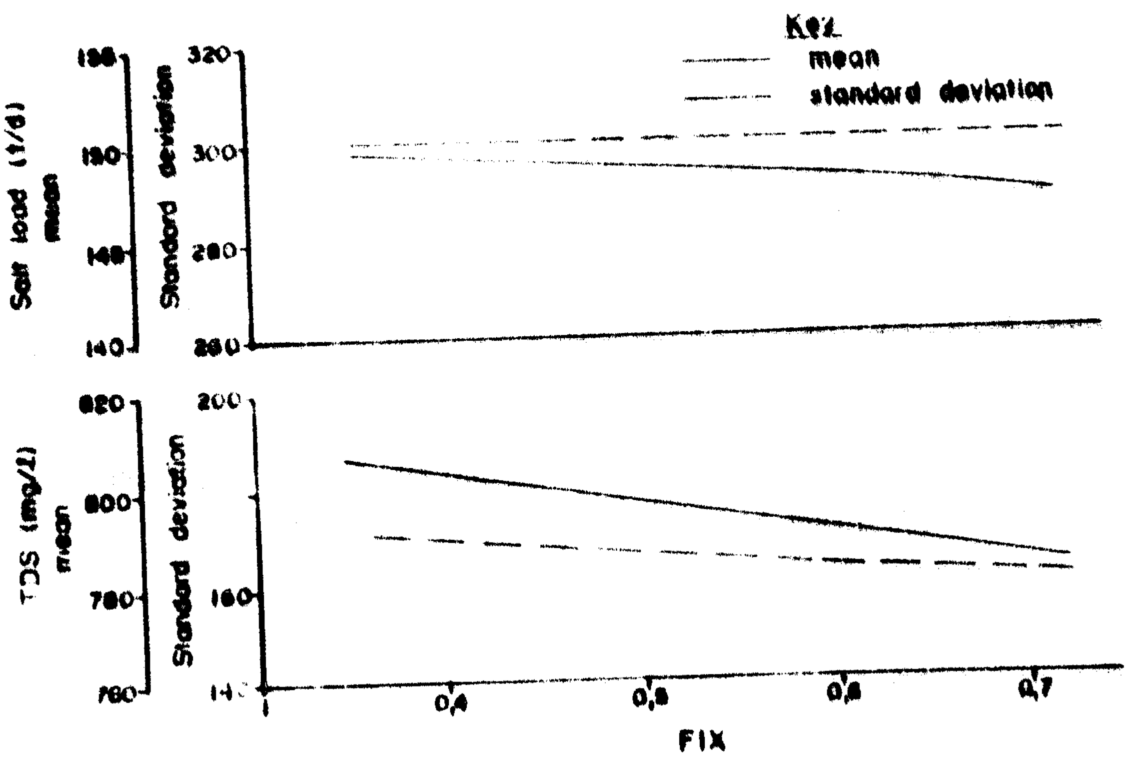

Fig 4.62 Sensitivity of modelled means and standard deviations to changes in FIX

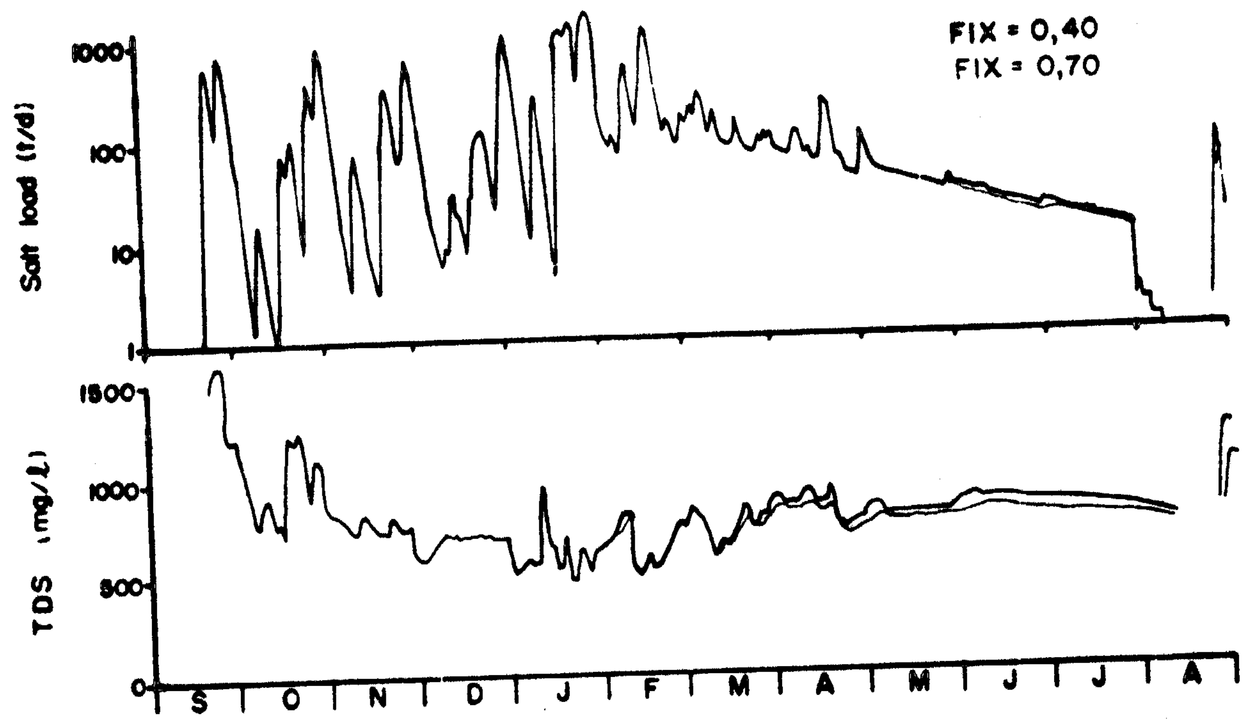

Fig. 4.61 Sensitivity of modelled daily discharges, salt concentrations and salt loads to changes in FIX

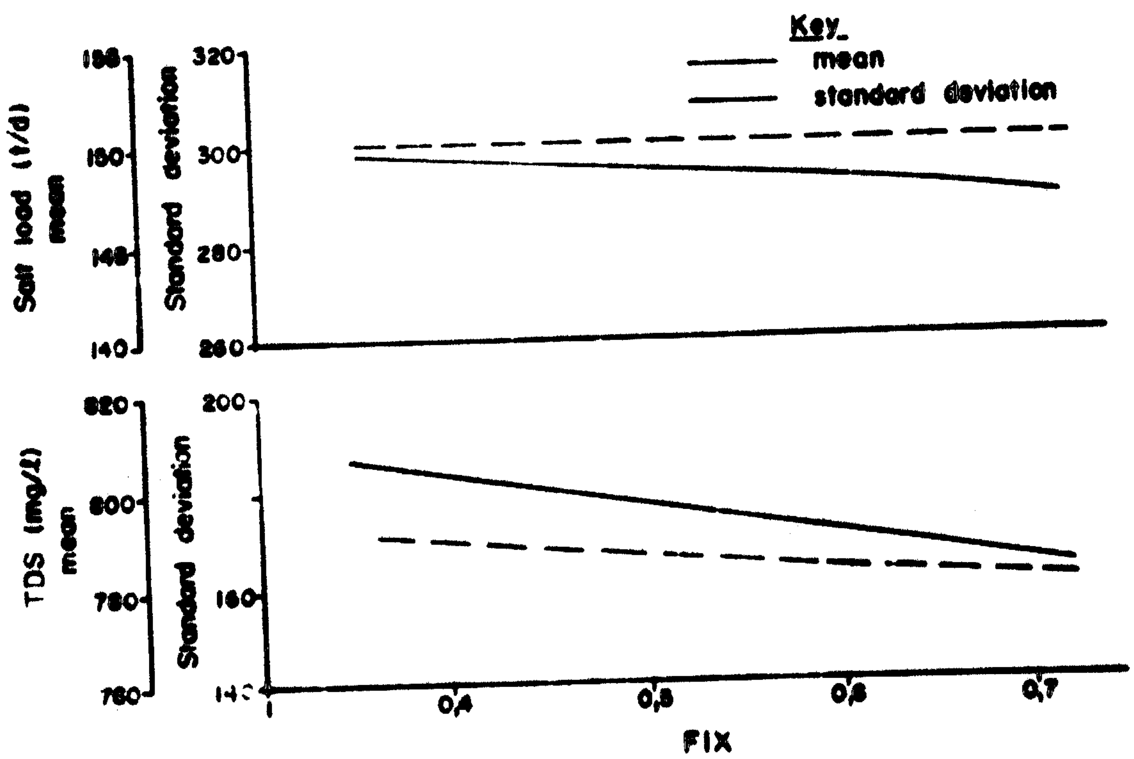

Fig. 4.62. Sensitivity of modelled means and standard deviations to changes in FIX

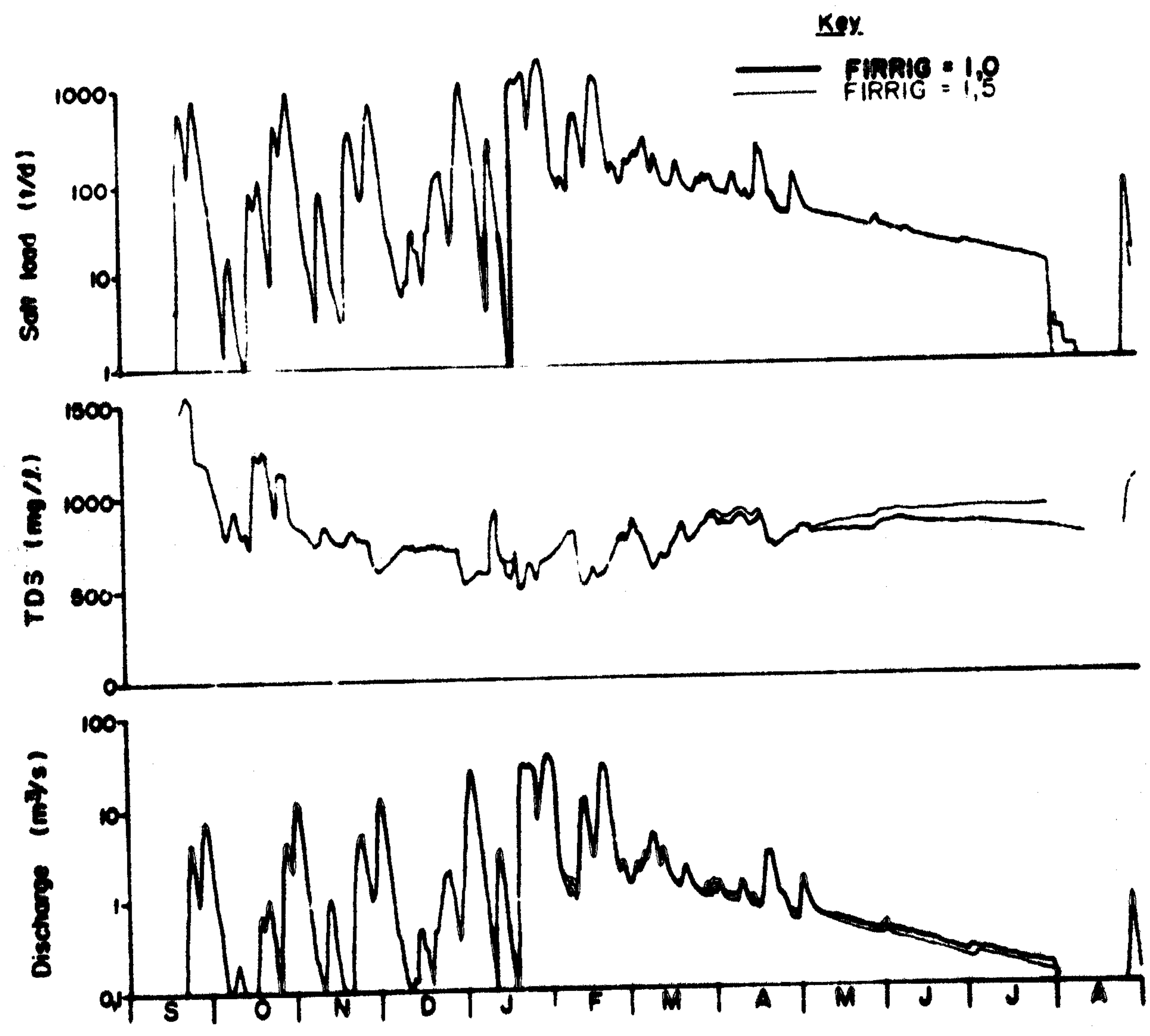

Fig.4.63: Sensitivity of modelled daily discharges, salt concentrations and salt loads to changes in FIRRIG.

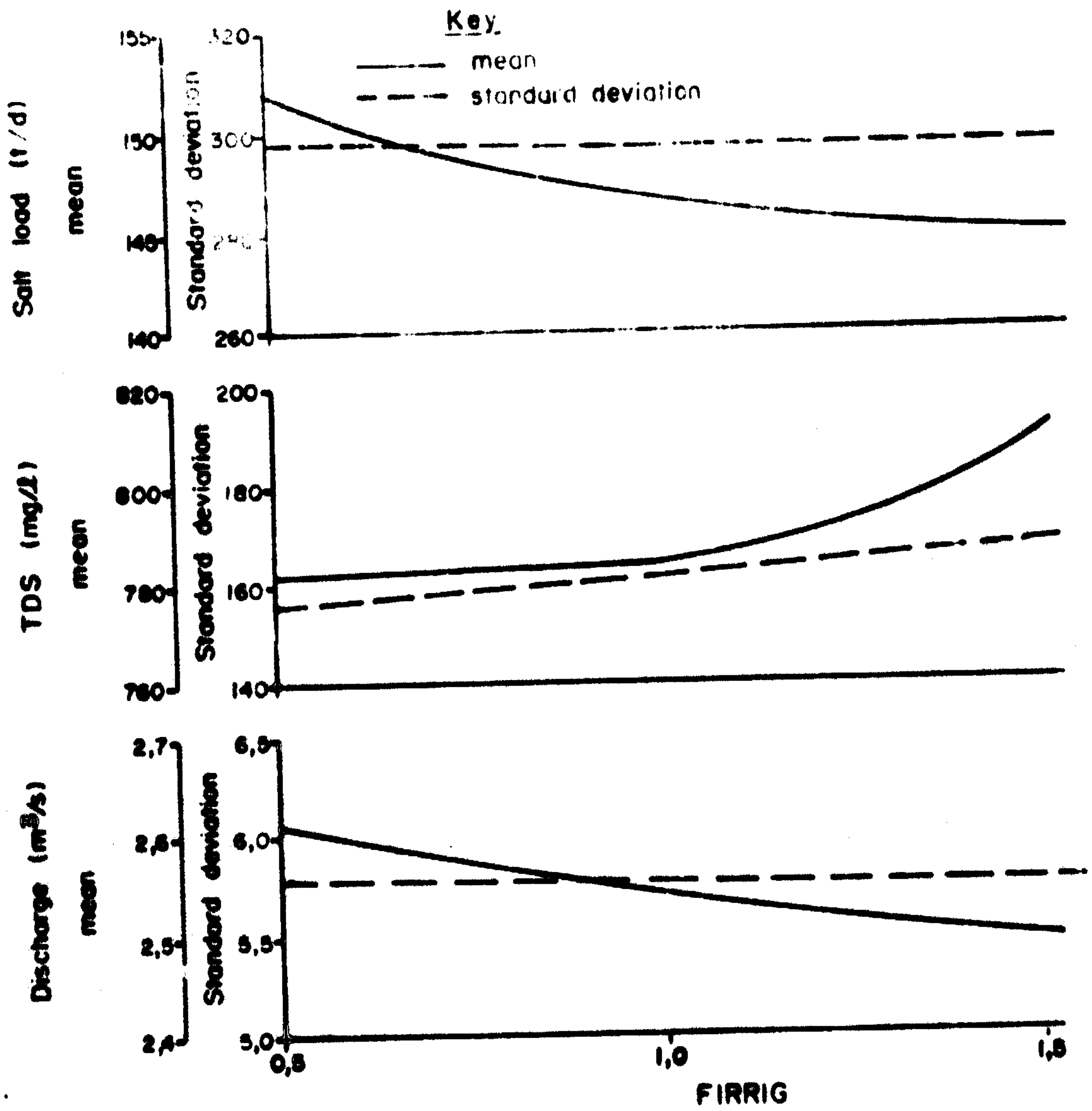

Fig. 4.64: Sensitivity of modelled means and standard deviations to changes in FIRRIG.

CHAPTER 5 MODEL CALIBRATION

This chapter comprises a guide to calibration of model parameters used in programs NACLØ1 and NACLØ2. Section 5.1 provides guidance as to initial selection of each parameter while section 5.2 discusses how each should be adjusted in subsequent calibration runs. Section 5.3 contains worked examples based on the Natalspruit and Rietspruit catchments (subcatchment 1 and 9).

5.1 Initial parameter selection

5.1.1 Program NACLØ1

Guidelines for the selection of initial calibration parameters are discussed in sub-sections a) to x). Parameters AREA, AI are not included in the discussion as these are physical properties which can be measured directly from maps.

a) POW: Pitman (1976) found that for most applications the values as determined for his monthly model (Pitman 1973) are also the optimum values for the daily model. For a wide range of South African catchments Pitman (1973) obtained values in the range 1 to 3. A value of 1 is applicable to dolomitic catchments exhibiting strong base flows. For most other catchments a value of 3 produced the best results. Fig. 5.1 shows Pitman's regionalisation of this parameter for the Republic of South Africa. Dolomitic areas are shown in Fig. 5.2. In the arid "B" zone of Fig. 5.1 the parameter POW has little significance because of the small base flows involved. The early cessation of base flow can best be modelled by adopting a small FT value and a high SL value. A value of 3 is therefore also adequate for the "B" zone.

For regions other than that shown in Fig. 5.1 an initial value of 3 is recommended, unless base flows are known to be exceptionally strong, in which case a smaller value would be appropriate.

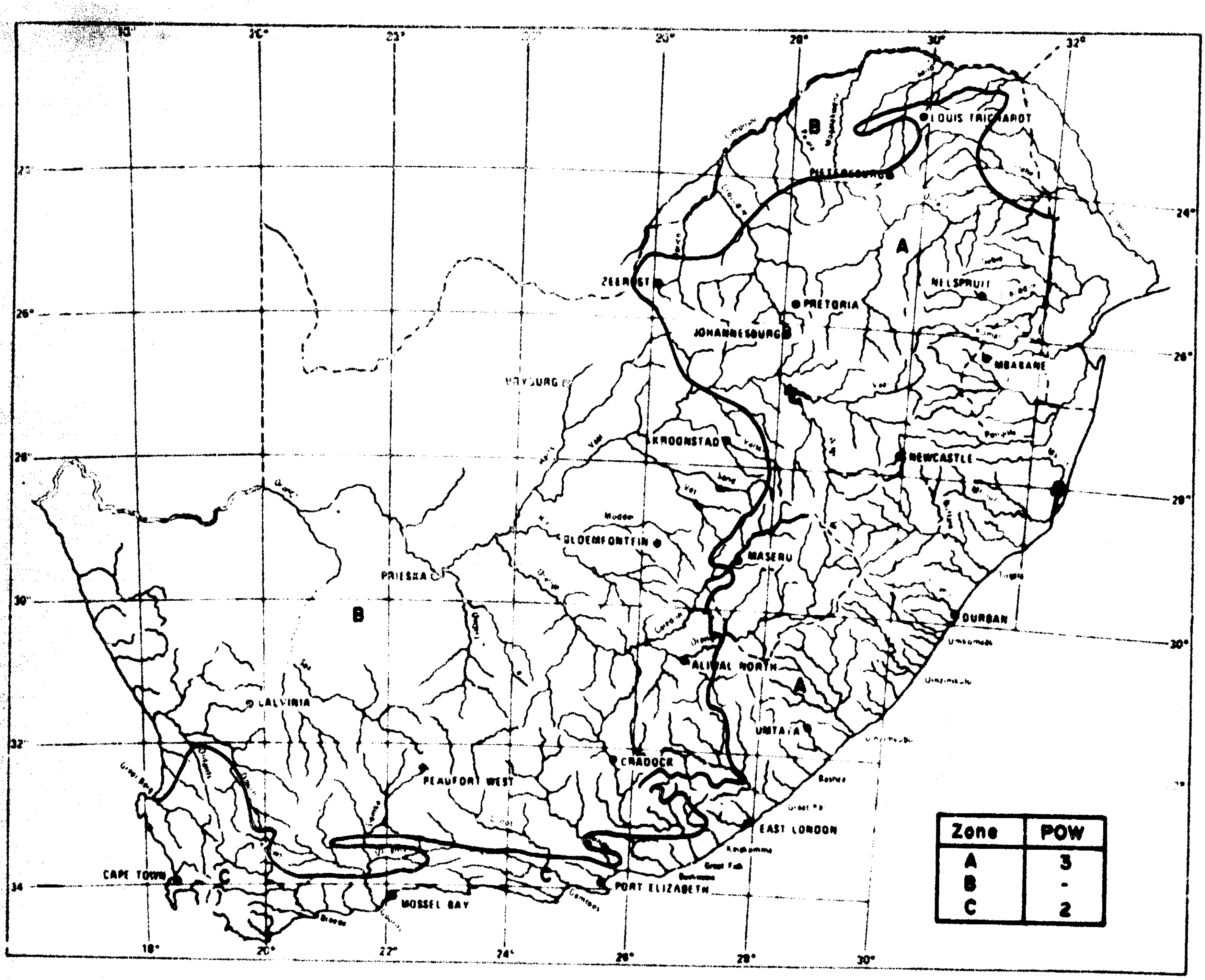

Fig.5.1: Suggested values of parameter POW.

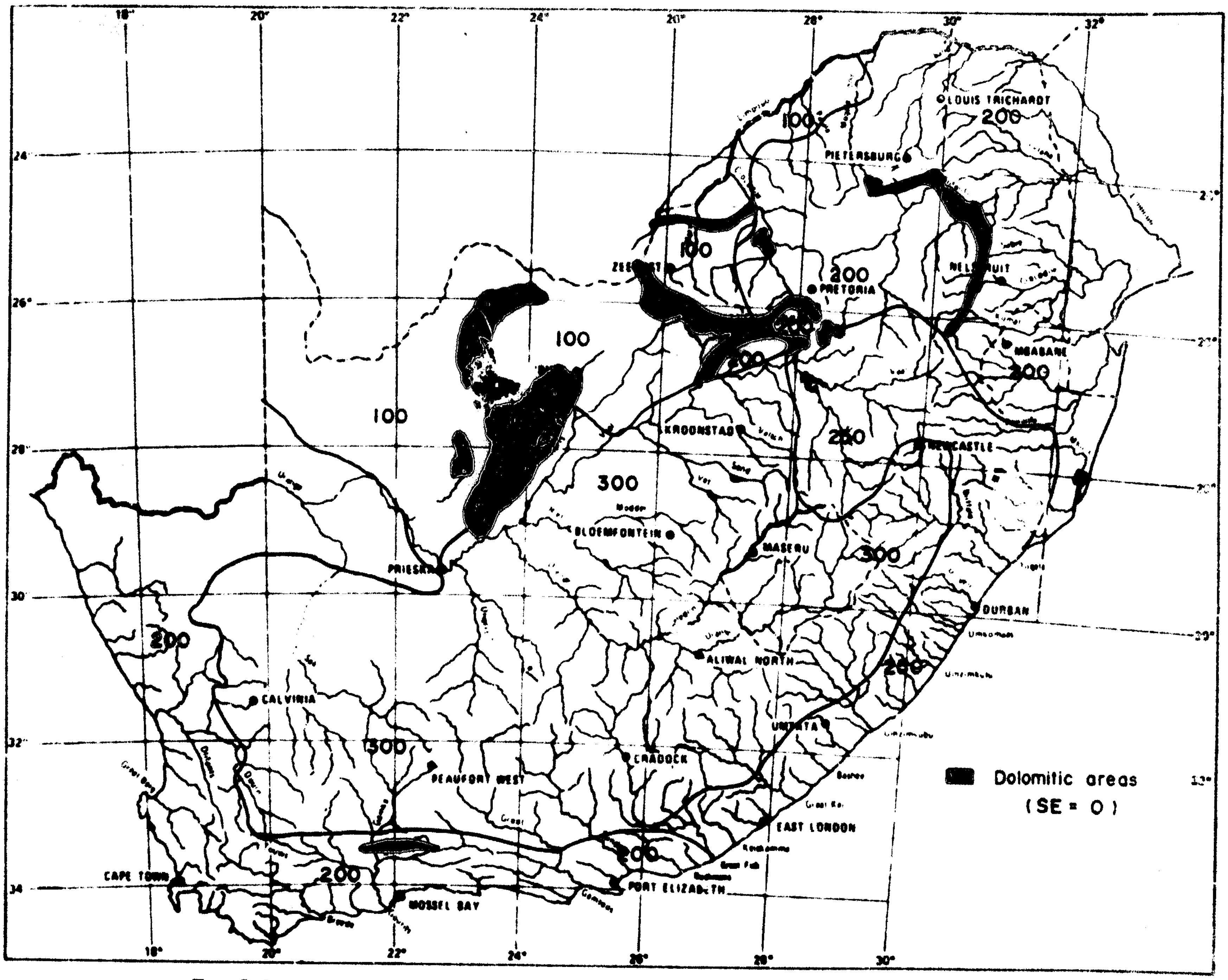

Fig. 5.2. Suggested values of parameter SE (mm)

b) SL: As stated in section 4.1.1(b), it is possible to duplicate closely the effect of parameter SL on modelled discharge by adjusting POW and FT, and for this reason Pitman (1976) advocates setting SL equal to zero in all cases. It is recommended that this procedure should be followed for the initial selection of SL. Water quality considerations might, however, necessitate a later revision of the initial estimate.

c) SE: In the Pitman model evaporation is assumed to cease when the soil moisture storage is at or near zero. Furthermore, with POW equal to 3, percolation losses have very little influence upon the soil moisture storage when the storage is less than SE (the storage at which evaporation is assumed to cease). The storage below SE can therefore be assumed to be little more than dead storage in so far as streamflow modelling is concerned and the soil moisture storage between SE and ST can be considered roughly equivalent to the total storage (ST) of the Pitman model.

Sufficient attenuation of soil moisture salt concentrations was obtained for the sub-catchments of the southern PWV region (see Table 3.1) when the total soil moisture storage was set equal to 400mm and this value is therefore recommended as an initial value of ST. The initial value of SE can then be estimated by subtracting, from 400, Pitman's recommended ST value. (Pitman (1973) has produced regionalised values of ST for the Republic of South Africa).

Pitman's ST values have been adjusted in this manner to yield recommended starting values of SE (see Fig. 5.2).

SE will subsequently have to be adjusted in order to improve the modelled mean and standard deviation of modelled daily discharges.

d) ST: As discussed in (c) above a value of 400mm should serve as a reasonable starting value. For very flat catchments, such as the Taaibosspruit catchment (subcatchment 10), it may prove necessary to reduce ST, although an increase in SE and SL should have the same effect. After the streamflow parameters have been successfully calibrated it may be found that base flow salt concentrations drop too low immediately after floods, in which case ST, SE and SL will have to be increased in order to dampen the model response.

e) FT: Pitman (1976) suggests an initial FT value approximately half that of the monthly model equivalent. Pitman's suggested monthly model values for South Africa (Pitman 1973) have accordingly been adjusted and are plotted in Fig. 5.3.

f) ZMINN: Pitman (1976) found that optimum values of ZMINN, the nominal minimum infiltration capacity, varied between 0 and 3 mm/h. An initial value of zero is suggested. The relative magnitudes of successive flood peaks will dictate subsequent parameter adjustments.

g) ZMAXN: For a large number of dissimilar test catchments Pitman (1976) found that, in combination with ZMINN equal to zero, the optimum value of ZMAXN resided within the range 10 to 20 mm/h. His suggested starting value of 15 mm/h is therefore recommended.

h) PI: Wide usage of the Pitman model (1976) has proved that a value of 1,5 mm is appropriate to all but heavily forested catchments. This value should therefore be adopted.

i) TL: Output from program NACLØ1 is fed as input to NACLØ2, the channel routing model. Pitman's method of estimating TL from inspection of the recession limbs of flood hydrographs (Pitman 1976) therefore cannot be used. Instead, TL has to be adjusted by trial until a good fit is obtained.

The initial value of TL should be quite small because much of the flood attenuation is achieved by means of the channel routing model. For catchment areas between 200 and 1000 km^2 a starting value in the range 0,5 to 1,0 is suggested.

j) LAG: For catchment areas between 200 and 1000 km^2 a starting value of zero is suggested.

k) GL: Pitman (1976) suggests an initial value equal to the initial TL value. This policy cannot be adopted in the present context, however, because with the introduction of the channel routing model the value of TL has to be reduced. The value of GL should lie in the range 1 to 20. An initial estimate can be made

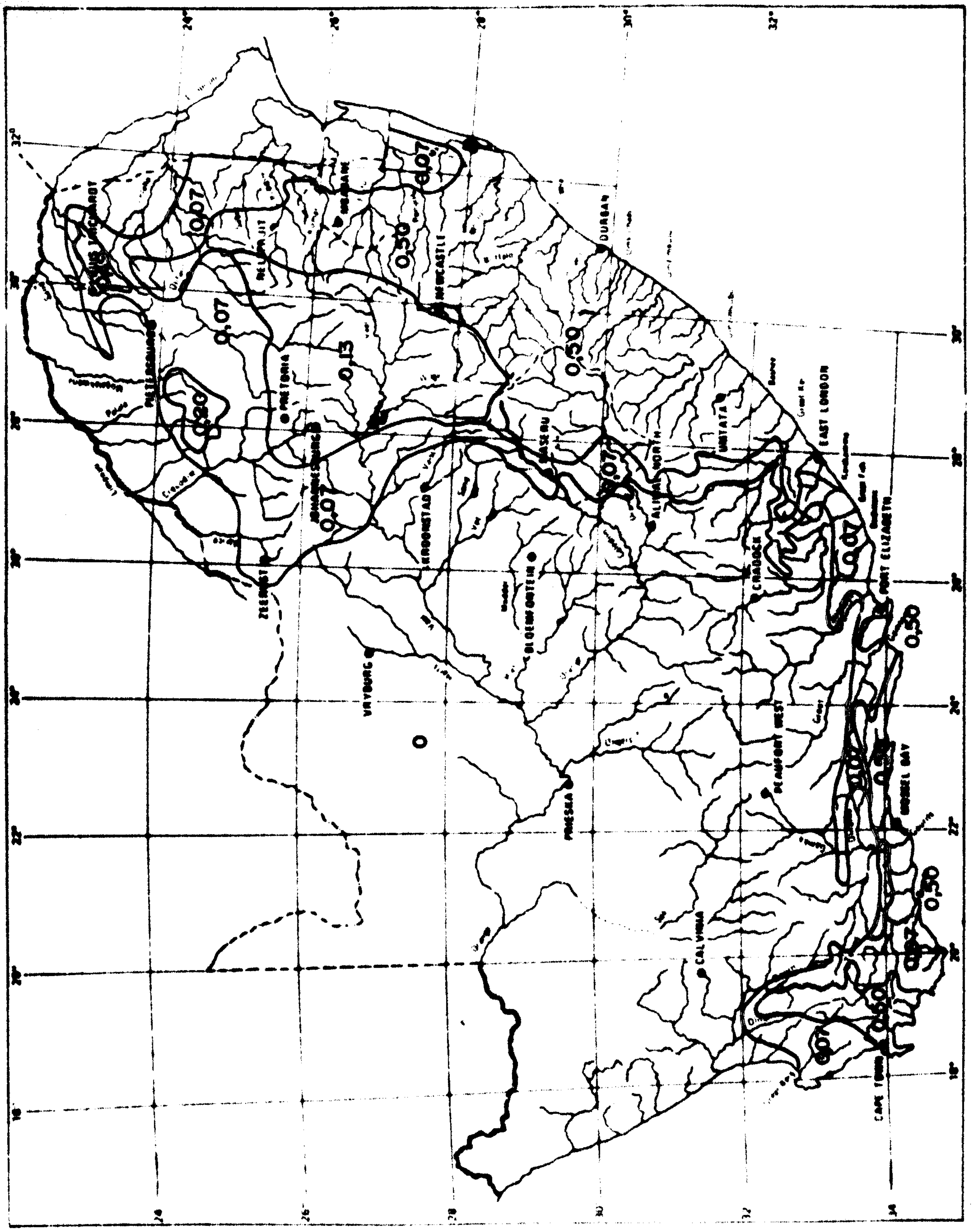

Fig. 5.3. Suggested values of Model parameter FT (mm/d)

by examination of available hydrographs. If the base flows appear to persist with little decline during the dry season, then a value approaching 20 should be used. If base flows decline rapidly, then a value nearer 1 would be more appropriate.

l) <u>QOBS</u>: This is not a calibration parameter, but rather an initial value. The observed base flow at the start of the simulation is usually difficult to measure because in most situations where water qualities are of concern effluent discharges are also involved. These point flows tend to mask the natural base flow. The requirement of a very long running-in period to warm up the water quality component of the model, however, makes the initial choice of QOBS irrelevant.

m) <u>DGL</u>: Unless there is positive evidence of a substantial loss to deep groundwater (for example due to mine dewatering) DGL should be set to zero. A value of zero was found to be the most appropriate even in the case of the southern Witwatersrand (subcatchments 1,2, 3, 4a and 4b), where underlying dolomitic compartments have been dewatered to great depths by gold mining activities.

n) <u>APARR</u>: Values of APARR in the range -0,0007 to -0,001 were found to produce reasonable results for most of the catchments modelled in the southern PWV region. A starting value within this range is therefore recommended.

o) <u>BPARR</u>: In cases where details of industrial water supply are readily available equation 3.4 can be used to estimate the initial total salt recharge rate per unit area. The salt recharge rate per unit of pervious area can then be approximated as follows:

$$BPARR = BPART.10^{-3} - AI.1{,}00 \quad (t/km^2/d) \quad \ldots\ldots\ldots\ldots(5.1)$$

where BPART = total salt generation rate per unit area as computed using equation 3.4. $(kg/km^2/d)$

Equation 5.1 is based upon the assumption that the salt recharge rate for impervious catchment surfaces is equal to 1,00 $t/km^2/d$ (the value most commonly encountered for catchments of the southern PWV region).

If details of industrial water supply are not readily available, BPART can be estimated using the relationship between impervious area and salt generation rate (see Table 3.8 of section 3.3). The linear regression equation for catchments of the southern PWV region is given by:

$$BPART = 1,92.AI + 0,046 \quad (t/km^2/d) \quad ....(5.2)$$

with a linear correlation coefficient of 0,726 for the catchments studied in section 3.3.

p) <u>APARU</u>: Experience gained from the modelling of southern PWV catchments suggests that reasonable values of APARU range between -0,001 and -0,015. A starting value of -0,01 is recommended.

q) <u>BPARU</u>: From Table 3.4 it can be seen that the calibrated values vary between 0,4 and 1,2, with most values falling within the range 0,8 to 1,2. An initial value of 1,0 $t/km^2/d$ is therefore recommended.

r) <u>PDEPS</u>: A starting value of 0,9 is recommended unless there is evidence of increasing base flow salt concentrations towards the end of the dry season, in which case lower values would be more appropriate.

s) <u>CONCBG</u>: Rainfall salt concentrations can in fact be measured directly, but in many instances the data may not be available. From various sources*, Betson (1978) compiled bulk precipitation and rainfall water quality data for four rural and three urban catchments. The total dissolved solids concentrations for the four rural catchments varied between 2,2 and 5,3 mg/ℓ with a mean of 4,3, while the maximum concentration for the three urban catchments was 17,8 mg/ℓ. It should be noted, however, that most of

---

* The sources cited by Betson include studies of the following localities: St. Louis, Missouri; Gottingen, Germany; Gatlinburg, Tennessee; Oak Ridge, Tennessee; Blairoville, Georgia and Canton-Clyde, North Carolina.

these values are based on bulk precipitations, not on actual rainfall concentrations. Part of the salt load associated with bulk precipitation is in fact accounted for in the model as salt storage recharge (parameters BPARR and BAPRU). Values slightly lower than those given above should therefore be used. Gat (1979) suggests that the major constituent of the salt load of natural rainfall is NaCl and quotes continental precipitation chloride concentrations in the range 0,1 to 10 mg/ℓ. The assumption that the cation is sodium suggests TDS concentrations in the range 0,2 to 16 mg/ℓ for undeveloped catchments (the higher values being more appropriate to coastal catchments). It should, however, be borne in mind that rural catchment rainfall concentrations can also be influenced by atmospheric pollution originating in adjacent urbanised catchments.

For inland catchments concentrations of 4 and 10 mg/ℓ are recommended as starting values of CONCBG for rural and developed catchments respectively.

t) PINTM: The interflow through the soil moisture storage will depend upon catchment slopes, lateral and vertical permeabilities and other geographical features. PINTM values calibrated for the southern PWV catchments varied between 0,6 and 0,9 with an average of 0,8. The average value (0,8) is therefore recommended as a starting value.

u) APARG: As most catchments are in a state of equilibrium it follows that leaching rates will be very small. It is therefore suggested that APARG be set equal to zero. This value should be increased only if there is an unaccountable growth in base flow salt concentrations. Even then it is possible to achieve similar results by adjusting other water quality parameters (such as PDEPS and PINTM).

v) SALTR: This is in fact an initial value and not really a calibration parameter. The long-lasting influence of the starting soil moisture salt storage, however, lends importance to careful selection of the initial SALTR value (if SALTR is much too large, then, although the pervious surface salt storage will quickly stabilise, most of the additional starting load will enter the soil moisture where its influence will be felt for a much longer time (see Fig. 4.42), thereby necessitating a longer running-in period. It is important, therefore, to adjust SALTR in such a way that initial and final surface salt storages are mutually compatible.

If the value of APARR is in the range -0,0007 to -0,001 and the mean annual precipitation is in the range 600-800 mm (as is the case in the southern PWV region), then the initial value of SALTR should be between 600 and 1000 times greater than BPARR.

w) <u>SALTU</u>: The value of SALTU is not at all critical as the impervious surface salt storage stabilises very rapidly (see Fig. 4.41) and SALTU has no influence on the soil moisture salt storage. A value about 100 times that of BPARU is recommended.

x) <u>CONCS</u>: As can be seen from Fig. 4.41, an error in the estimation of the initial soil moisture salt storage persists for a long time. This storage, however, can be estimated with reasonable accuracy only if both QOBS and CONCS, the starting base flow discharge and salt concentration, are known. In practice, however, point discharges mask both QOBS and CONCS and render direct estimation of the soil moisture salt storage virtually impossible.

No guide can be given as to the initial estimate of CONCS, other than to recommend a value of about 150 mg/ℓ for undeveloped catchments, and higher values for urbanised catchments. Even this estimate for rural catchments could be way off the mark as natural groundwater salt concentrations can vary widely. (For example, Tordiffe (1973) encountered TDS concentrations as high as 12000 mg/ℓ in parts of the Fish river basin).

It is essential that CONCS be adjusted after every calibration run in order to balance initial and final soil moisture salt loads. A long running-in period (of the order of ten years) is also recommended in order to reduce errors introduced by inaccuracies in the starting conditions.

5.1.2 Program NACLØ2

Guidelines for the selection of initial calibration parameter values are given in sub-sections a) to i). Table 5.1 has recommended values for the parameters controlling the computational accuracy. Parameters describing the physical characteristics of the channel which can be measured directly are not discussed. HSTART, CONSU and CONSL are also omitted from the discussion as these starting values can be measured directly and in any case have little influence on results because of the short memory of the channel routing model.

Table 5.1 : Recommended values for parameters controlling computational accuracy

Parameter	NMAX	NMIX	NQMAX	NSTEP	ERROR
Value	10	2	10	3	0,001

a) RETURN: Of the water applied to irrigated lands, the proportion returned to the stream is extremely difficult to estimate because of the relatively small quantities involved and the masking effect of base flows. Studies in the Coachella Valley, California, between 1957 and 1965 indicated a 22 percent irrigation return flow (Bower et al., 1969). A value of 0,2 is therefore recommended.

b) FIX: The Coachella Valley study (Bower et al., 1969) also indicated an increase in TDS from 800 to 2600 mg/ℓ, suggesting that 72 percent of the applied salt load was returned to stream (the equivalent value of FIX would be 0,28). Hall and Görgens (1978), however, point out that part of the salt load associated with return seepage can sometimes be attributable to the displacement of saline groundwater into the river channel. Such processes might well occur in the Coachella Valley. Furthermore, the salt load returned to the stream is almost certainly affected by other factors (such as topography).

Unfortunately only extreme cases (such as that of the Coachella Valley, where saline return flows are problematic) tend to be published. It is therefore most difficult to arrive at reasonable average condition values for the parameter FIX.

In the case of the southern PWV region irrigation losses are generally small compared with the base flows (consisting mostly of effluent point inputs) and consequently have no noticeable effect on water quality. The present study cannot therefore shed any further light on the modelling of irrigation return flows. In modelling the southern PWV region it was assumed that the dewatering of underlying dolomitic compartments would reduce the salt load returned to the stream via irrigation return seepage and FIX was thus (arbitrarily) set equal to 0,7. For most applications lower values would be more appropriate.

c) <u>FLEACH</u>: The choice of this parameter is also rather arbitrary. An initial value of 0,5 is recommended. Only after calibration of the other parameters (of both programs NACLØ1 and NACLØ2) should this parameter be changed to test whether any improvement in fit can be attained.

d) <u>GLOSS</u>: Initially the bed loss should be set to zero. If the reduction in flow in the reach cannot otherwise be accounted for (such as in the case of station B9 discussed in section 3.2.1), a bed loss can be introduced.

e) <u>AMANC and AMANF</u>: Manning n values for various conditions are dealt with extensively in the literature. (Rouse (1949) gives a useful table of Manning n values for several channel types, while Chow (1959) devotes an entire chapter to the subject). For most natural streams n values for the river channel vary between 0,03 and 0,1. A value of 0,15 is suggested for flood plains.

f) <u>FEVAP</u>: The choice of monthly evaporation factors depends upon the aquatic vegetation. For most rivers a value of 1,0 is recommended. For large stands of reeds or other vegetation a lower value of FEVAP is recommended, combined with a suitable choice of monthly values of FTRANS. Rijks (1969) concluded that evaporation from an African swamp about 500m wide is 60 ±15 percent of the evaporation from open water. Other studies indicated higher ratios. (Penman (1963), using data collected by Migahid, found a ratio of about unity for recently transplanted papyrus in a 10m^2 tank, while Gel'bukh (1964) reported measurements on reeds in tanks with ratios between 0,8 and 2,5). It should be noted, however, that results for small evaporation pans can be highly misleading. Rijks (1969), for example, reports other measurements by Migahid (1952) from which it can be concluded that the mean evaporation from papyrus that had grown undisturbed for a longer period (6½ years) was only 55 per-cent of the equivalent open water evaporation. It is clear there-fore that the age of swamp vegetation has an important influence upon evaporation.

A study of 30 km² Australian swamp by Linacre et al. (1970) tends to confirm Rijks's assertion that swamp evaporation is significant-ly lower than lake evaporation, except immediately after rain. Linacre et al. suggest further that although in dry climates reeds tend to lower the evaporation loss, the reverse might be the case in wet climates.

For dry climatic conditions (such as those of Southern Africa) Rijks's estimate is recommended (i.e. the annual average sum of FEVAP and FTRANS should equal 0,6). In the present study (see Table 4.5 of section 4.2.1) it has been assumed that half of the swamp evaporation is from the water surface and the remainder attributable to evapotranspiration from the vegetation. The evaporation component was assumed to remain constant. The value of FEVAP was thus set equal to 0,3 for each month. This arbitrary estimate had to be made in view of the present lack of knowledge concerning the balance between evaporation and evapotranspiration losses.

g) <u>FTRANS</u>: If the vlei area (AVLEI) is equal to zero, then FTRANS has no influence upon modelled output. When AVLEI is greater than zero then, following the reasoning of section 5.1.2(f), the average annual value of FTRANS should equal 0,3. In the case of the present study it was assumed that vlei evapotranspiration would vary according to a sine curve with the higher values corres-ponding to the summer months. This pattern was adopted as the swamp vegetation of the vleis of the southern PWV region were observed to become dry and straw-coloured during the winter.

Table 4.5 of section 4.2.1 gives the monthly values adopted. In the absence of any better data it is suggested that these values be used.

h) FIRRIG: The irrigation demand factor will vary according to the crops and the agricultural practices involved. If details concerning crops are available, reference can be made to various publications such as those by Olivier (1961,1972), Israelson and Hansen (1962) and many others. Most of the irrigation by riparian farmers of the southern PWV continues unabated throughout the year with a wide variety of crops. The value of FIRRIG was therefore set equal to 1,0 for all months.

5.2 Subsequent parameter adjustments

The adjustments that have to be made to the calibration parameters of programs NACLØ1 and NACLØ2 in order to improve the fit between modelled and observed daily discharges are discussed in section 5.2.1 while section 5.2.2 describes the adjustments needed to improve the fit between modelled and observed water qualities. The recommended approach is to optimise the streamflow parameters first, before attempting to adjust water quality parameters.

5.2.1 Optimisation of streamflow parameters

The different stages in the parameter optimisation process are discussed below:

a) Primary parameter adjustment: The long term mean discharge is of the utmost importance and the error between modelled and observed means (E_1) should therefore be minimised. At the same time the error between modelled and observed base flows should also be minimised (the plotting program, NACL23, prints average monthly modelled and observed discharges). These criteria can be satisfied by adjusting any number of parameters, but it is suggested that changes during any one simulation be limited to two, or at most three, parameters. The flow parameters that have the greatest influence on E_1 and base flow discharges are SE, ST, ZMAXN and FT. In order to ensure sufficient depth to the soil moisture storage (note the water quality considerations discussed in section 5.1.1(a) and (b)) it is recommended that ST be left unaltered in the initial stages. Changes should therefore be confined to parameters SE, ZMAXN and FT. Table 5.2 gives recommendations for the adjustment of these three parameters.

Table 5.2 : Primary parameter adjustments - SE, ZMAXN and FT

Condition of modelled output		Parameter adjustment		
Mean	Base flows	SE	ZMAXN	FT
high	high	decrease	-	decrease
	low	-	increase	increase
	correct	-	increase	decrease
low	high	-	decrease	decrease
	low	increase	-	-
	correct	-	decrease	increase
correct	high	-	decrease	decrease
	low	-	increase	increase

b) Secondary parameter adjustment: Once E_1 has been minimised and the modelled and observed base flows are of the same order of magnitude, further refinements can be made.

First, should it be noticed that simulated peaks are consistently earlier than those observed, the parameter LAG should be set equal to the time displacement.

Secondly, if on examination of the flood hydrographs the modelled flood recession limbs should be found to fall too rapidly, TL should be increased.

Thirdly, the base flows should be examined. If base flows at the end of the rainy season are too high and those at the end of the dry season too low, GL ought to be increased (see Fig. 4.21).

None of the above changes will in any way alter the mean discharge or the total base flow discharge and will therefore not necessitate further changes in SE, ZMAXN and FT. LAG, TL and GL should be adjusted until the correlation coefficient is maximised.

c) Fine tuning: The final calibration entails a certain amount of trial-and-error to improve the model fit. It may be found at this stage that it had been impossible to reduce base flows sufficiently by means of any of the adjustments discussed in a) and b) above. This could occur if, for example, recorded point discharges are significantly higher than those recorded at the catchment outlet. In such a case the catchment should first be closely examined (in the field) to ascertain whether there is an obvious explanation (such as illegal abstractions or irrigated lands which had previously been overlooked). If no obvious cause can be found, a channel bed loss (GLOSS) should be specified to account for the lost water. It may be wise at this stage to repeat steps a) and b) as previous attempts to reduce base flows by adjustments only to the catchment model parameters may have resulted in unrealistic values (in particular there could have been too little dilution of point discharges).

It may also be found that base flows cease entirely early in the dry season, in which case SL should be increased (see Fig. 4.3). Adjustments to GL as described in b) above may not completely succeed in restoring the balance between base flows at the beginning and end of the dry season. In this case the parameter POW will also have to be adjusted. An increase in POW will have to be accompanied by an increase in FT if the mean is to remain unaltered (see Figs. 4.1 and 4.2).

Finally, the modelled flood peaks should be closely examined. If the modelled peaks at the start of the wet season are consistently too high, while those later in the season are too low or approximately correct, this is an indication that ZMINN should be increased (this should also increase the standard deviation of modelled daily discharges). The balance between modelled and observed means and base flows will then have to be restored by increasing SE, reducing ZMAXN, or a combination of both. If SE is increased, then FT will have to be reduced to prevent base flows from becoming too high. Pitman (1976) found that the value of ZMAXN required to maintain the same overall volume of surface runoff for an increase of ZMINN from zero can be approximated as:

$$ZMAXN' = ZMAXN_o . (0,8)^{ZMINN'} \qquad \text{..................} (5.3)$$

where ZMAXN' = new value of ZMAXN
$ZMAXN_o$ = value of ZMAXN for ZMINN = zero
ZMINN' = new value of ZMINN

Fine tuning of the parameters should be continued in this manner until E_1 and E_2 (see equations 3.1 and 3.2) are minimised, the correlation coefficient is maximised and the visual fit is good.

Table 5.3 summarises the effect on the mean and standard deviation of daily discharges, flood hydrographs and base flows of increases in each of the calibration parameters.

5.2.2 Optimisation of water quality parameters

The various stages in the optimisation of water quality parameters are discussed below:

a) Primary parameter adjustment: It is of paramount importance that the modelled mean salt load be as close as possible to that observed. At the same time, however, a reasonable balance between initial and final salt storages should be maintained so as to avoid the systematic depletion or growth of unrealistically high or low initial storages. Particular attention should be paid to the balance of the soil moisture salt storage.

After the first calibration simulation, using the initial values suggested in section 5.1, parameters BPARR and BPARU should be adjusted in such a manner as to minimise the error between modelled and observed mean salt loads, and initial storages (SALTR, SALTU and CONCS) should be adjusted accordingly. The following procedure is recommended:

(i) Assuming that the initial value of BPARU is reasonable, adjust BPARR to reduce the error between modelled and observed mean salt loads. The new value of BPARR can be approximated as:

$$BPARR' = BPARR + \left(\frac{\bar{x}_{LO} - \bar{x}_{LM}}{AREA}\right) \quad \ldots\ldots\ldots\ldots\ldots\ldots\ldots (5.4)$$

Table 5.3 : Effect on modelled discharges of increases in model parameter values

Parameter	Change in modelled discharges			
	Mean	Std. dev.	Flood peaks	Base flows
POW	decrease	increase	indeterminate	increased
SL	decrease	increase	-	decreased - base flows can be made to cease entirely early in dry season
SE	increase	increase	increase	increase
ST	decrease	decrease	decrease	decrease
T	increase	decrease	-	increase
ZMINN	decrease	increase	decrease - earlier peaks decrease more relative to later peaks; some later peaks can be increased	small increase - after very wet rainy season no change
ZMAXN	decrease	indeterminate	decrease - earlier peaks decrease more than later peaks; some later peaks can be increased	increase
PI	decrease	decrease	decrease - small peaks decrease more relative to large peaks	decrease
TL	-	decrease	decrease - flood recession limbs fall more gradually	-
LAG	-	-	no change - peaks delayed	-
GL	-	small decrease	-	volume unaltered - early dry season flows decreased; late dry season flows increased
DGL	decrease	-	small decrease	decrease
GLOSS	decrease	-	small decrease	decrease - base flows can be made to cease entirely early in dry season

where BPARR' = new estimate of BPARR ($t/km^2/d$)

$\bar{x}_{LO}$ = mean observed salt load (t/d)

$\bar{x}_{LM}$ = mean modelled salt load (t/d)

Equation 5.4 will not entirely eliminate the error, however, because it takes no account of antecedent conditions. (The salt load washed off during the calibration period need not be the same as the recharge during the same period). More than one iteration may therefore be required before the error is entirely eliminated.

$\bar{x}_{LO}$ and $\bar{x}_{LM}$, the mean observed and modelled loads used in equation 5.4, are included in the printed output of the plotting programs NACLØ3 and NACL23.

(ii) Adjust SALTR and SALTU to balance initial and final storages:

$$SALTR' = SALTR.\frac{TSALTR_F}{TSALTR_I}\cdot\frac{GROW_O}{GROW_N}\cdot\frac{BPARR'}{BPARR} \quad \ldots\ldots\ldots (5.5)$$

where SALTR' = new estimate of SALTR (t/km^2)

$TSALTR_F$ = final total rural surface salt storage (t)

$TSALTR_I$ = initial total rural surface salt storage (t)

$GROW_O$ = growth factor at start of simulation

$GROW_N$ = growth factor at end of simulation

$$SALTU' = SALTU.\frac{TSALTU_F}{TSALTU_I}\cdot\frac{GROW_O}{GROW_N}\cdot\frac{BPARU'}{BPARU} \quad \ldots\ldots\ldots (5.6)$$

where SALTU' = new estimate of SALTU (t/km^2)

$TSALTU_F$ = final total urban surface salt storage (t)

$TSALTU_I$ = initial total urban surface salt storage (t)

BPARU' = new estimate of BPARU (in this case BPARU' = BPARU)

Initial and final total rural and urban salt storages are part of the printed output from program NACLØ1.

Equations 5.5 and 5.6 are exact relationships provided that parameters APARR and APARU are not altered.

(iii) Balance initial and final soil moisture salt storages. Provided that QOBS is kept constant, this can be achieved by adjusting CONCS:

$$CONCS' = CONCS \cdot \frac{SLOAD_F}{SLOAD_I} \cdot \frac{GROW_O}{GROW_N} \cdot \frac{BPARR'}{BPARR} \quad \ldots\ldots\ldots\ldots(5.7)$$

where $CONCS'$ = new estimate of CONCS (mg/ℓ)
$SLOAD_F$ = final soil moisture salt storage (t)
$SLOAD_I$ = initial soil moisture salt storage (t)

Initial and final soil moisture salt storages are printed by program NACLØ1.

If parameters FT or PINTM are increased, the flow through the soil moisture storage will be increased, thereby reducing the average salt storage. The average equilibrium salt storage is approximately inversely proportional to the outflow (excluding evaporation) from the soil moisture.

The new equilibrium salt load due to a change in outflow from the soil moisture can thus be estimated as:

$$SLOAD' = SLOAD \cdot \left(\frac{TQPERC + TQINT}{TQPERC' + TQINT'}\right) \quad \ldots\ldots\ldots\ldots\ldots(5.8)$$

where SLOAD' = new equilibrium salt load (t)
SLOAD = old equilibrium salt load before changing QPERC and QINT (t)
TQPERC' = new value of TQPERC, the total percolation during the simulation (mm)
TQINT' = new value of TQINT, the total interflow during the simulation (mm)

Now from equations 2.41 and 2.42 of section 2.2.2 it can be deduced that:

$$\frac{TQPERC}{TQINT} = \frac{TLOADG}{TLOADI}$$

Hence: $$TQPERC = \frac{TLOADG}{TLOADI} \cdot TQINT \quad \ldots\ldots\ldots\ldots\ldots\ldots\ldots\ldots (5.9)$$

where TLOADG = total salt load percolating from soil moisture storage to groundwater during simulation (t)

TLOADI = total salt load leaving soil moisture storage as interflow during simulation (t)

The cumulative totals TLOADG and TLOADI are part of the printed output of program NACLØ1.

Furthermore the following relationships also exist:

$$TQPERC' = TQPERC \cdot \frac{FT'}{FT} \quad \ldots\ldots\ldots\ldots\ldots\ldots\ldots\ldots (5.10)$$

$$TQINT' = TQINT \cdot \frac{PINTM'}{PINTM} \quad \ldots\ldots\ldots\ldots\ldots\ldots\ldots\ldots (5.11)$$

where FT' = new value of parameter FT (mm/d)

PINTM' = new value of parameter PINTM

Equation 5.10 is only an approximate relationship as the percolation is limited by the availability of water in the soil moisture.

Substituting equations 5.9, 5.10 and 5.11 in equation 5.8 yields:

$$SLOAD' = SLOAD \left\{ \frac{1 + (\frac{TLOADG}{TLOADI})}{(\frac{TLOADG}{TLOADI}) \cdot (\frac{FT'}{FT}) + \frac{PINTM'}{PINTM}} \right\} \quad \ldots\ldots\ldots (5.12)$$

If QOBS is kept constant, SLOAD can be replaced by CONCS in equation 5.12. Combining equations 5.7 and 5.12 yields:

$$CONCS' = CONCS.\left\{\frac{1 + \frac{TLOADG}{TLOADI}}{\frac{TLOADG.FT'}{TLOADI.FT} + \frac{PINTM'}{PINTM}}\right\}.\frac{SLOAD_F}{SLOAD_I}.\frac{GROW_O}{GROW_N}.$$

$$\frac{BPARR'}{BPARR} \quad ....(5.13)$$

Equation 5.13 provides a basis for estimating CONCS' given any changes in FT, PINTM and BPARR together with an imbalance between starting and ending soil moisture salt storages. It should be noted, however, that equation 5.13 is also merely an approximate relationship.

Steps (i) - (iii) should be carried out at the end of every calibration simulation in order to maintain the correct balance between initial and final values, especially in cases where the running-in period is relatively short (less than ten years).

b) Secondary parameter adjustments: After the modelled and observed mean salt loads have been brought into good agreement and a reasonable equilibrium between initial and final storages has been achieved, consideration should be given to the distribution of salt loads during the wet season as well as to the base flow salt concentrations. The salt load distribution during the rainy season is controlled primarily by the relative magnitudes of BPARR and BPARU, but is also affected by parameters APARR, BPARR and PINTM, while base flow salinities are controlled by BPARR, APARR, PDEPS and PINTM.

If peak salt loads at the start of the wet season are too low and those later in the season too high, BPARU should be increased and BPARR decreased as follows:

$$BPARR' = BPARR - (BPARU' - BPARU).AI \quad ....(5.14)$$

where BPARU' = new value of BPARU ($t/km^2/d$)

After adjusting BPARU it may be found that salt loads washed off during smallish floods later in the wet season are still too low while salt loads produced during larger floods are too high. In such a case the fit can be improved by increasing the magnitude of APARR. If APARR is increased, however, SALTR must be decreased. If the calibration period is short (one or two years) then BPARR may also have to be adjusted to achieve the correct mean salt load. The required change in BPARR depends on the antecedent hydrology.

If salt loads during floods are too high while those during the dry season are too low, PINTM should be decreased. This will also have the effect of decreasing peak salt loads later in the wet season relative to those at the start of the season.

If modelled salt concentrations are found to rise too rapidly during the dry season, PDEPS should be increased.

Two worked examples illustrating the calibration process are given in section 5.3.

5.3 Worked examples of model calibration

Sections 5.3.1 describe the calibration of the model for the Natalspruit and R..etspruit catchments (subcatchments 2 and 9 of Fig. 3.2). Data for the period 1977.09 to 1978.08 were used for both so as to limit the number of plots needed to illustrate the calibration process. As a result (because of the shorter calibration period for modelled discharges) the optimum parameters differ from those obtained in section 3.2.

The period 1965.09 to 1977.08 was used for running-in program NACLØ1, while a one-month period (August 1977) was used to warm up program NACLØ2. Fig. 3.2 shows the locations of the two test catchments, while Appendix A gives details of catchment characteristics and effluent point sources.

5.3.1 Natalspruit catchment

a) Initial parameter selection

Initial parameter values were selected according to the principles set out in section 5.1 and are given in Tables 5.4 and 5.5.

b) Subsequent parameter adjustments

Model parameters controlling modelled streamflow were first adjusted until a reasonable fit between modelled and observed discharges was achieved. Streamflow parameter values used in each calibration run are listed in Table 5.6 together with the statistical parameters representing the goodness-of fit. Modelled and observed daily discharges for each calibration run are plotted in Fig. 5.4.

Once a reasonable fit between modelled and observed daily discharges had been achieved, the water quality parameters were progressively adjusted until a good fit between modelled and observed daily salt loads was obtained. Water quality parameter values used for each calibration run, together with the statistical properties of the fit obtained between modelled and observed values are given in Table 5.7. Figs. 5.5 and 5.6 show the fit between observed and modelled daily salt loads and salt concentrations for each simulation.

The parameters that were changed during each simulation are indicated with asterisks in Tables 5.6 and 5.7.

Table 5.4 : Initial parameter values used in program MACLØ1 for the Natalspruit catchment

Parameter	Value	Units	Derivation of parameter value
AREA	392	km^2	Measurement
POW	3	-	Fig. 5.1
SL	0	mm	Recommended value (section 5.1.1(b))
SE	100	mm	From Fig. 5.2, the catchment is situated partly in a region having a recommended value of 200 mm and partly on dolomite (SE=0). Hence adopt the average

Table 5.4 - cont.

Parameter	Value	Units	Derivation of parameter value
ST	400	mm	Recommended value (section 5.1.1(d))
FT	0,13	mm/d	Fig. 5.3
AI	0,089	-	Measurement (20% of the urbanised area shown on 1:50 000 maps was assumed to be impervious)
ZMINN	0	mm/h	Recommended value (section 5.1.1(f))
ZMAXN	15	mm/h	Recommended value (section 5.1.1(g))
PI	1,5	mm	Recommended value (section 5.1.1(h))
TL	0,75	days	Recommended value (section 5.1.1(i))
LAG	0	days	Recommended value (section 5.1.1(j))
GL	10	days	Value chosen from the middle of the recommended range (section 5.1.1(k))
QOBS	0,05	m^3/s	The simulation commences at the end of the dry season, therefore an arbitrary (small) discharge was chosen
DGL	0	-	Recommended value (section 5.1.1(m))
SALTR	102	t/km^2	800xBPARR (see section 5.1.1(v))
APARR	-0,001	mm^{-1}	Recommended value (section 5.1.1(n))
BPARR	0,1279	$t/km^2/d$	From equations 5.2 and 5.1 (section 5.1.1 (o))
SALTU	100	t/km^2	100xBPARU (section 5.1.1(w))
APARU	-0,01	mm^{-1}	Recommended value (section 5.1.1(p))
BPARU	1,00	$t/km^2/d$	Recommended value (section 5.1.1(q))
PDEPS	0,9	-	Recommended value (section 5.1.1(r))
CONCS	500	mg/l	Arbitrary choice (section 5.1.1(x))
CONCBG	10	mg/l	Recommended value for urbanised catchment (section 5.1.1(s))
PINTM	0,8	-	Recommended value (section 5.1.1(t))
APARG	0	$t/km^2/mm/d$	Recommended value (section 5.1.1 (u))

Table 5.5 : Initial parameter values used in program NACLØ2 for the Natalspruit catchment

Parameter	Value		Units	Derivation of parameter
	Reach 1	Reach 2		
AVLEI	1,0	6,9	km^2	Measurement
AIRRIG	0	3,0	km^2	Measurement
CHAIN	7,5	17,0	km	Measurement
RETURN	0,2	0,2	-	Recommended value (section 5.1.2(a))
F[illegible]X	0,7	0,7	-	Estimate (see section 5.1.2(b))
[illegible]EACH	0,5	0,5	-	Recommended value (section 5.1.2.(c))
PLAT	0,40	0,46	-	Measurement
PUP	0,14	0	-	Measurement
HSTART	1,50	1,50	m	Arbitrary choice
CONSU	1500	1500	mg/l	Observed TDS at start of simulation
CONSL	1500	1500	mg/l	Observed TDS at start of simulation
GLOSS	0	0	Ml/d	Recommended value (section 5.1.2(d))
SLOPE	0,0024	0,0024	-	Measurement
AMANC	0,04	0,08	-	Manning n estimated for channel
AMANF	0,06	0,10	-	Manning n estimated for flood plain
FEVAP	0,3	0,3	-	Assumed (see section 5.1.2.(f))
FTRANS	As per Table 4.5			Assumed (see section 5.1.2(g))
FIRRIG	1,0	1,0	-	Assumed (see section 5.1.2(h))

Table 5.6 : Optimisation of streamflow parameters (Natalspruit catchment)

	Item	Observed	Calibration run number 1	2	3	4	7
Model parameters	POW		3	3	3	3	3
	SL		0	0	0	0	0
	SE		100	100	90*	90	90
	ST		400	400	400	400	400
	FT		0,13	0,30*	0,35*	0,35	0,50*
	AI		0,089	0,089	0,089	0,089	0,089
	ZMINN		0	1*	1	1	1
	ZMAXN		15	12*	12	14*	14
	PI		1,5	1,5	1,5	1,5	1,5
	TL		0,75	0,75	1,00*	1,00	1,00
	LAG		0	1*	1	1	1
	GL		10	10	5*	5	5
	QOBS		0,05	0,05	0,05	0,05	0,05
	DGL		0	0	0	0	0
	GLOSS		0	0	0	0	10*
Statistical parameters	Mean discharge (m^3/s)	2,982	3,031	3,147	3,122	3,033	2,964
	Standard deviation	2,202	3,009	3,097	2,942	2,542	2,339
	E_1	-	1,64	5,53	4,69	1,71	0,60
	E_2	-	36,65	40,64	33,61	15,44	6,22
	Correlation coefficient	-	0,817	0,867	0,875	0,874	0,864

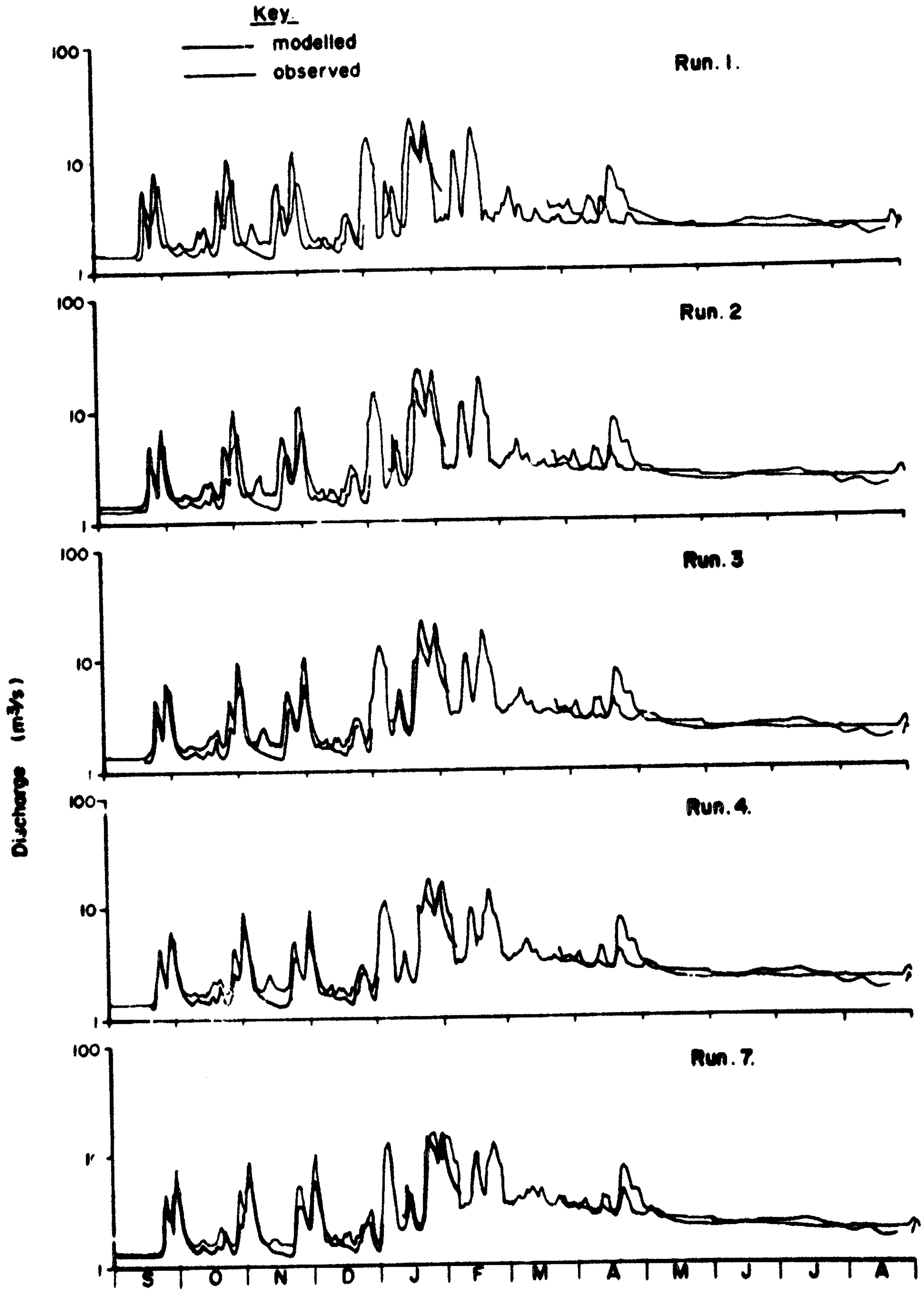

Fig. 5.4: Model calibration for Natalspruit: Discharges.

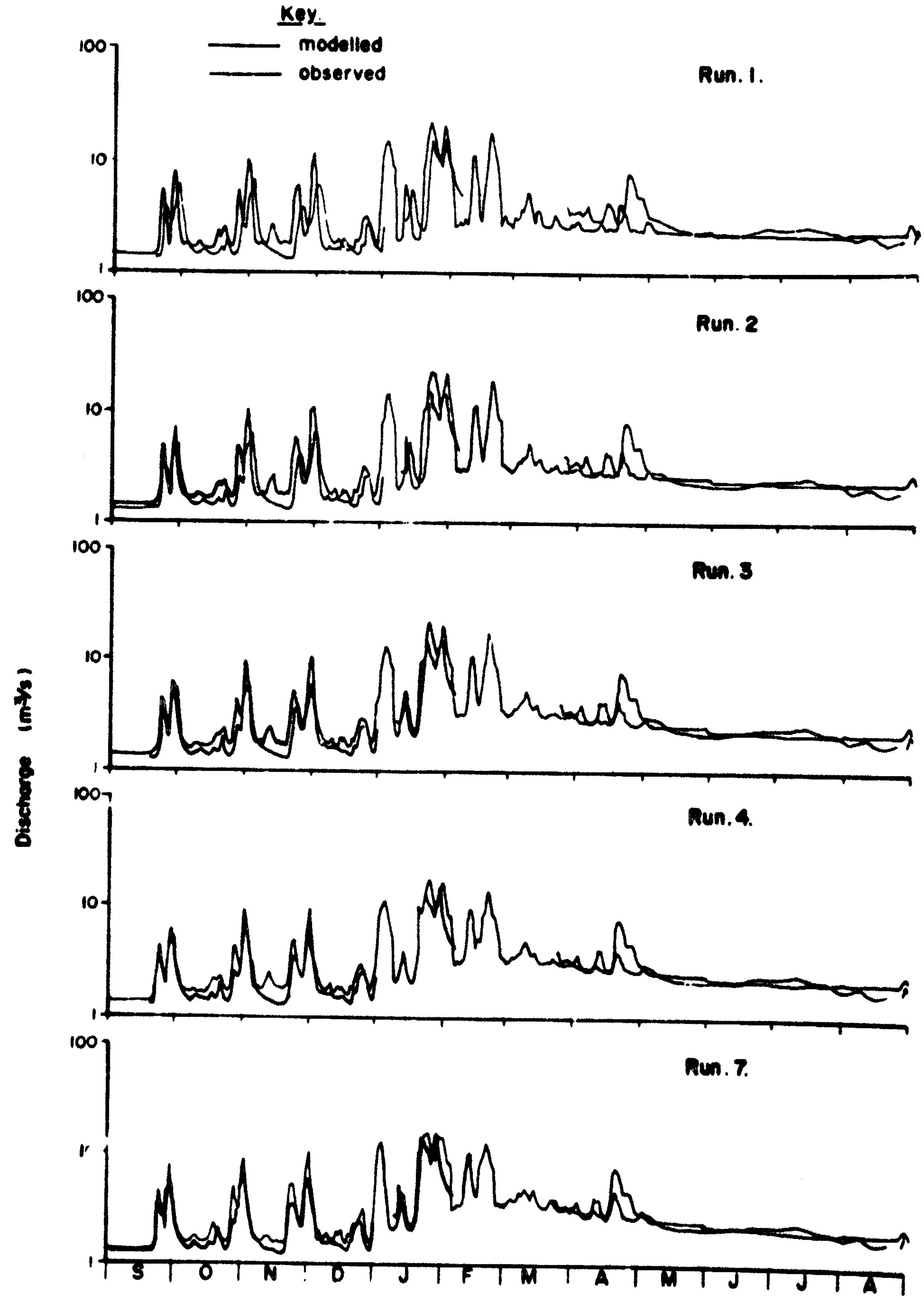

Fig. 5.4: Model calibration for Natalspruit: Discharges.

Table 5.7 : Optimisation of water quality parameters (Natalspruit catchment)

Item			Observed	Calibration run number				
				4	5	6	7	8
Model parameters		SALTR		102	63*	35*	90*	90
		APARR		-0,001	-0,001	-0,001	-0,001	-0.001
		BPARR		0,1279	0,0865*	0,0476*	0,1232*	0,1232
		SALTU		100	187*	187	187	187
		APARU		-0,01	-0,01	-0,01	-0,01	-0,01
		BPARU		1,00	1,00	1,00	1,00	1,00
		PDEPS		0,90	0,90	0,90	0,90	0,90
		CONCS		500	900*	670*	1455*	1335*
		CONCBG		10	10	10	10	10
		PINTM		0,8	0,8	0,9	0,9	0,9
		APARG		0	0	0	0	0
Statistical parameters	Salt loads (t/d)	Mean	319,9	336,1	327,7	314,9	321,3	320,4
		Standard deviation	141,2	123,9	110,3	92,9	145,0	143,7
		E_1	-	5,07	2,46	1,56	0,44	0,16
		E_2	-	12,31	21,93	34,21	2,69	1,77
		Corr.coeff.	-	0,737	0,732	0,710	0,765	0,764
	TDS (mg/ℓ)	Mean	1225	1337	1310	1267	1270	1267
		Standard deviation	235	279	289	305	239	240
		E_1	-	9,12	6,96	3,43	3,67	3,43
		E_2	-	18,62	23,15	29,79	1,70	2,13
		Corr.coeff.	-	0,737	0,800	0,813	0,769	0,771
Salt storage states (t)		$TSALTU_I$		3489	6524	6524	6524	6524
		$TSALTU_F$		6510	6510	6510	6510	6510
		$TSALTR_I$		39984	24696	13720	35280	32144
		$TSALTR_F$		36518	24694	13587	34751	31975
		$SLOAD_I$		74004	131464	97868	211726	194264
		$SLOAD_F$		192419	157564	98512	194270	190589
		TLOADG		77329	79154	52477	150319	143504
		TLOADI		66058	78413	60275	119499	112553

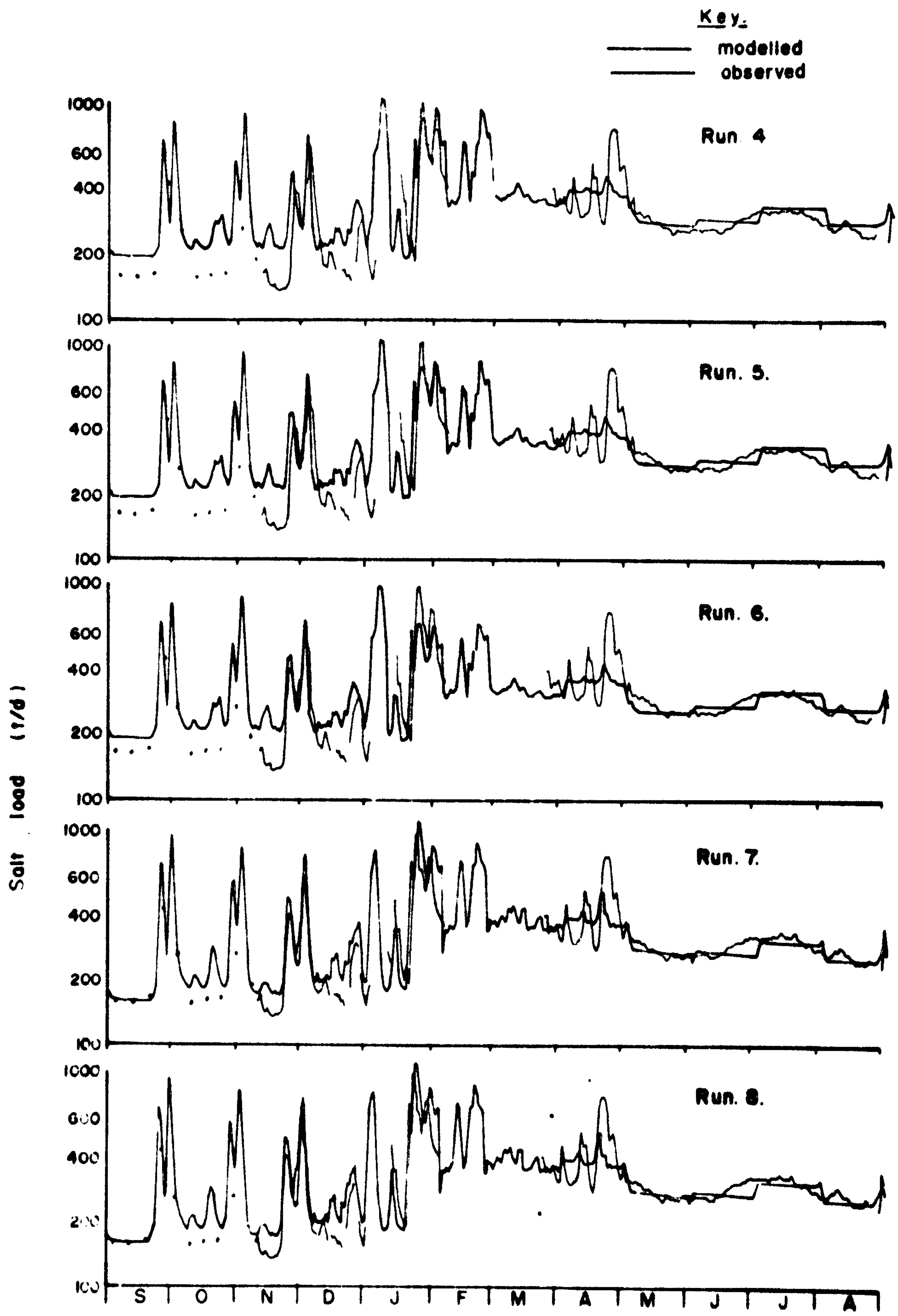

Fig. 5.5. Model calibration for the Natalspruit: Salt loads

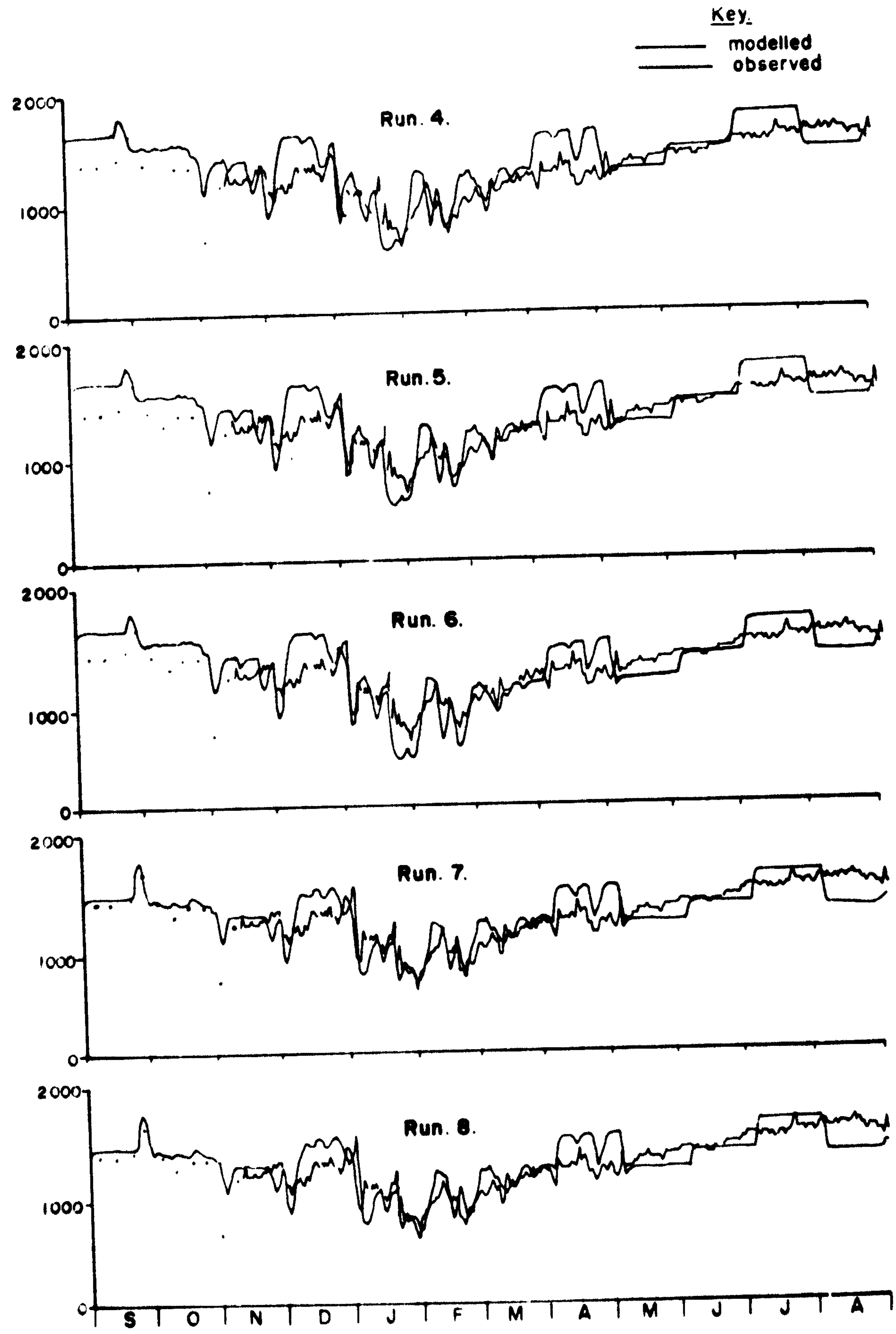

Fig. 5.6: Model calibration for the Natalspruit: Salt concentration.

A full description of the parameter adjustments made after each calibration run is given below. During the first stage of the calibration process (runs 1 to 4) only streamflow parameters are adjusted; thereafter (runs 5 to 10) the water quality parameters are optimised.

<u>Run 1</u>: The initial parameter values discussed in section 5.3.1(a) were used for the first simulation.

From Table 5.6 it can be seen that the mean discharge is very nearly correct, but the standard deviation is too high. Furthermore, Fig. 5.4 shows that the smaller modelled flood peaks early in the wet season are too high. This can be corrected by increasing ZMINN, say to 1 mm/h. In order to preserve the same mean discharge, ZMAXN must be reduced to compensate for the change in ZMINN. From equation 5.3 (see section 5.2.1(c)):

$$ZMAXN^{1} = 15.(0,8)^{1} = 12 \text{ mm/h.}$$

It can also be seen from Fig. 5.4 that the modelled hydrograph is in advance of the observed. LAG must therefore be increased, say to 1 day.

Finally, the modelled base flows are too low, therefore FT must be increased, say to 0,3 mm/d. Normally ZMAXN would also be increased to compensate for the increased mean due to the increase in FT. This is not done at this stage, however, as both ZMINN and ZMAXN have already been altered, and further changes in the first calibration step would merely obscure the effects of the other parameter adjustments. The mean can be re-adjusted after the next simulation.

<u>Run 2</u> : Table 5.6 shows that the mean and standard deviation are both too high and Fig. 5.4 shows that the base flows are still a little low. Modelled flood peaks are too high, but are now in phase with the observed peaks (i.e. LAG need not be adjusted any further).

The mean, standard deviation and flood peaks can be lowered by reducing SE, say to 90 mm, while the base flows can be raised by slightly increasing FT, say to 0,35 mm/h. From Table 5.6 it can be seen that E_2 is very much greater than E_1, indicating that the relative decrease in the modelled standard deviation needs to be greater than the decrease in the mean. This can be achieved by increasing TL (which is a shape parameter, and therefore does not alter the mean), say to 1,0.

It is apparent from Fig. 5.4 that the modelled base flows early in the dry season (March and April, 1978) are too low, while those towards the end of the dry season (August, 1978) are too high. The base flows can be re-distributed (without altering the total volume) by decreasing GL, say to 5 days.

<u>Run 3</u>: Table 5.6 indicates that both mean and standard deviation are still too high, and Fig. 5.4 shows that most of the flood peaks are too high. The fit between modelled and observed base flows appears to be good. The best way to decrease the flood peaks without greatly affecting base flows is to increase ZMAXN, say to 14 mm/h (decreasing SE would also have reduced base flows, while increasing ZMINN would severely affect the smaller flood peaks whereas it is the larger peaks that need the greatest reduction).

<u>Run 4</u>: Table 5.6 and Fig. 5.4 indicate a reasonably good fit between modelled and observed daily discharges. We are now in a position to start optimising water quality parameters.

Table 5.7 gives statistical details of the fit between modelled and observed daily salt loads and salt concentrations for run 4 while Figs 5.5 and 5.6 are the corresponding plots.

From Table 5.7 it can be seen that the mean salt load is too high, indicating that BPARR should be reduced. Other water quality parameters will have to be adjusted to correct the balance between initial and final storages.

Using equation 5.4 (see section 5.2.2(a)):

$$BPARR' = 0{,}1279 + \frac{(319{,}9-336{,}1)}{392}$$

$$= \underline{0{,}0865}\ t/km^2/d$$

From equation 5.5:

$$SALTR' = 102.\frac{36518}{39984}.\frac{1{,}0}{1{,}0}.\frac{0{,}0865}{0{,}1279}$$

$$= \underline{65}\quad t/km^2$$

Similarly, from equation 5.6:

$$SALTU' = 100.\frac{6510}{3489}.\frac{1{,}0}{1{,}0}.\frac{1{,}0}{1{,}0}$$

$$= \underline{187}\quad t/km^2$$

Finally, the initial soil moisture salt storage must be adjusted by means of a change in the initial soil moisture salt concentration. From equation 5.13:

$$CONCS' = 500.\left[\frac{1 + \frac{77329}{66058}}{\frac{77329}{66058}.\frac{0{,}35}{0{,}35}+\frac{0{,}8}{0{,}8}}\right].\ \frac{192419}{74004}.\frac{1{,}0}{1{,}0}.\frac{0{,}0865}{0{,}1279}$$

$$= 879$$

The new CONCS value can be rounded up to 900 mg/l, as an increase in the initial soil moisture salt storage will in itself have the effect of slightly increasing the final storage over and above the value predicted by equation 5.13.

It should be noted that $GROW_O$ and $GROW_N$ in equations 5.5, 5.6 and 5.13 have values of unity because the salt recharge rate has been assumed to be zero for the purposes of the two examples in this section.

<u>Run 5</u>: Table 5.7 again shows that the mean salt load is too high, indicating that BPARR must be still further reduced. Equation 5.5 can now be abandoned in favour of simple proportionality:

A reduction in BPARR from 0,1279 to 0,0865 $t/km^2/d$ reduced the modelled mean from 336,1 to 327,7 t/d. The required BPARR value to bring the mean to 319,9 t/d (the observed value) can thus be computed as:

$$BPARR' = 0,0865 - \frac{(0,1279 - 0,0865)}{(336,1 - 327,7)} \cdot (327,7-319,9)$$

$$= \underline{0,0476}\ t/km^2/d.$$

Using equation 5.5, SALTR is adjusted to 35 t/km^2.

From Figs. 5.5 and 5.6 it can be seen that salt loads (and concentrations) during floods tend to be a little low, while base flow salinities are a little high. An increase in PINTM will have the effect of increasing the flushing of the soil moisture storage, thereby increasing salt loads during floods and reducing base flow salt concentrations. PINTM is therefore increased to 0,9.

CONCS is now adjusted to balance the soil moisture salt storage. From equation 5.13, CONCS' = 559. This reduction in CONCS, however, seems to be too drastic. Bearing in mind that equation 5.13 is only an approximate relationship we can increase CONCS' by say 20% to 670 mg/l. (This is a judgement decision based on extensive experience of the model behaviour and is used here simply to reduce the number of simulations in the example. Following the method outlined in section 5.2.2 an extra simulation would be required).

Run 6: At this stage E_1 has been reduced to only 1,56% and a reasonable balance has been obtained between $SLOAD_I$ and $SLOAD_F$ and between $TSALT_I$ and $TSALT_F$ (see Table 5.7). Base flow salt concentrations, however, tend to be too high, especially in the September-December, 1977 period (see Figs. 5.5 and 5.6). Moreover, the modelled standard deviation of daily salt loads and the peak salt loads are too low. The balance could be restored partially by further increasing PINTM, but the interflow component already comprises 90 percent of the surface runoff from pervious catchment surfaces. Any further increase in PINTM would therefore be unrealistic. Other strategies which might be employed to increase the flood peak salt loads will inevitably also increase the base flow salt concentrations and will lead to a deterioration of the fit between modelled and observed means.

A careful examination of the catchment reveals that a substantial portion of the course of the Natalspruit traverses dolomite (see Fig. 5.7). It is also clear that base flows are dominated by effluent inputs, especially the highly saline water pumped from the workings of the ERPM gold mine. Fig. 5.7 shows the location of the major point inputs while Table 5.8 gives average discharges and salt concentrations for the period 1977.09 to 1978.08.

From the disposition of the effluent point sources it is clear that even a small bed loss downstream of the ERPM gold mine could substantially reduce the base flow salt concentrations. The assumption of such a bed loss is tenable because of the location of the lower Elsburgspruit on the contact of the dolomitic area. Even a small outcrop of fissured dolomite in the river bed could account for the loss.

Assuming such a bed loss, say GLOSS=10 Ml/d, FT must be increased (say to 0,50 mm/d) to balance the base flow discharges, and BPARR must also be increased to balance the mean salt loads.

With the further assumption that about half of the bed loss will be derived from the mine effluent (because the effluent is mixed with catchment runoff) we can deduce that the salt lost due to the increase in GLOSS will be approximately:

$$(\tfrac{1}{2}\cdot \mathrm{GLOSS}\cdot 10^{-3})\cdot 3998$$
$$= 20 \text{ t/d}$$

Compensating for this loss and for the difference between the modelled and observed mean salt loads using simple proportion-

Table 5.8: Average discharges and salt concentrations of effluent point flows entering the Natalspruit

Serial no.	Description	Average discharge (Ml/d)	Average TDS (mg/l)
1	ERPM gold mine	48	3998
2	Germiston (Rondebult) sewage works	39	746
3	Germiston (Dekema) sewage works	56	563
4	Boksburg (Vlakplaats) sewage works	44	678

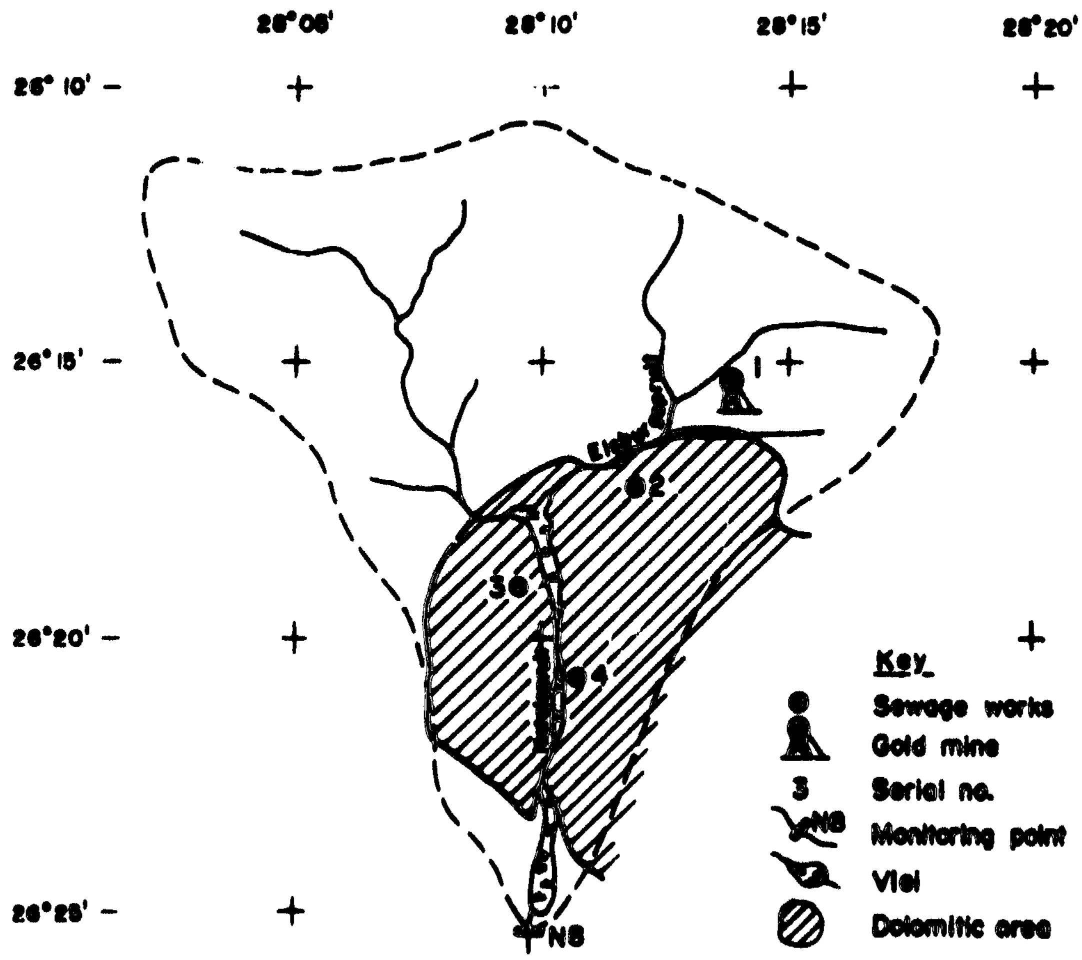

Fig. 5.7: Location of major effluent point sources and dolomitic areas in the Natalspruit catchment

ality yields:

$$BPARR' = 0{,}0476 + \frac{(0{,}0865-0{,}0476)}{327{,}7-314{,}9}\cdot(319{,}9-314{,}9+20)$$
$$= 0{,}1232\ t/km^2/d$$

CONCS is then adjusted to accommodate the changes in BPARR' and FT and the imbalance between initial and final soil moisture salt storages by means of equation 5.13:

$$CONCS' = 670\left[\frac{1+\dfrac{52477}{60275}}{\dfrac{52477}{60275}\cdot\dfrac{0{,}50}{0{,}35}+\dfrac{0{,}9}{0{,}9}}\right]\frac{98512}{97868}\cdot\frac{1{,}0}{1{,}0}\cdot\frac{0{,}1232}{0{,}0476}$$
$$= 1455\ mg/\ell$$

Run 7: Table 5.6 and Fig. 5.4 indicate a small improvement in the fit between modelled and observed daily discharges, further adjustment of streamflow parameters is not required. Figs. 5.5 and 5.6 and Table 5.7 show a substantial improvement in the fit between modelled and observed daily salt loads and daily salt concentrations, thereby justifying the assumption of a bed loss from the Elsburgspruit. Although the fit between modelled and observed values is good, further parameter adjustment is desirable in order to improve the balance between initial and final soil moisture salt storages.

From equation 5.13 the new estimate of CONCS becomes 1335 mg/l. BPARR is not adjusted as the modelled mean salt load is only slightly higher than observed, and the reduction in CONCS will in any case reduce the modelled mean.

Run 8: The statistical parameters of Table 5.7 show that an acceptable fit has been achieved. Furthermore, the 8,2 percent decrease in CONCS has produced only a 0,3 percent change in the mean modelled salt load, indicating that any remaining imbalance between initial and final soil moisture salt loads is inconsequential.

Marginal improvements to the model fit could be achieved by means of a further small increase in GLOSS and by finer adjustment of parameters such as APARR, APARU, PDEPS, CONCBG, PINTM and

FLEACH, but the large number of simulations required cannot be justified by the small improvement in fit which can be gained.

5.3.2 Rietspruit catchment

a) Initial parameter selection

Initial parameter values were selected according to the guidelines given in section 5.1 and are listed in Tables 5.9 and 5.10

b) Subsequent parameter adjustment

Streamflow parameter values used in each calibration run and statistical parameters representing the goodness-of-fit are listed in Table 5.11; modelled and observed daily discharges are plotted in Fig. 5.8.

Water quality parameter values together with the statistical properties of the fit obtained between modelled and observed daily salinities for each calibration run are given in Table 5.12. Modelled and observed daily salt loads and salt concentrations are plotted in Figs. 5.9 and 5.10.

The parameter adjustments made after each calibration run are described below.

Run 1: The initial parameter values given in Tables 5.9 and 5.10 were used for the first simulation.

From Table 5.11 it can be seen that the mean discharge is too low. Fig. 5.8 shows that modelled base flows are a little high during the early part of September 1977, but nearly correct during the period May-August 1978. FT is therefore left unaltered at this stage. It is also apparent that the modelled flood peaks early in the wet season are too high, while those later in the wet season are low, indicating that ZMINN should be increased and ZMAXN decreased. It would be unwise to do so at this stage, however, because the mean discharge must first be corrected. This can be done by increasing SE, say to 210 mm.

Table 5.9 : Initial parameter values used in program NACLØ1 for the Rietspruit catchment

Parameter	Value	Units	Derivation of parameter value
AREA	1116	km^2	Measurement
POW	3	-	Fig. 5.1
SL	0	mm	Recommended value (section 5.1.1(b))
SE	200	mm	Fig. 5.2
ST	400	mm	Recommended value (section 5.1.1(d))
FT	0,10	mm/d	Fig. 5.3
AI	0,006	-	Measurement
ZMINN	0	mm/h	Recommended value (section 5.1.1(f))
ZMAXN	15	mm/h	Recommended value (section 5.1.1(g))
PI	1,5	mm	Recommended value (section 5.1.1(h))
TL	0,75	days	Recommended value (section 5.1.1(i))
LAG	0	days	Recommended value (section 5.1.1(j))
GL	10	days	Recommended value (section 5.1.1(k))
QOBS	0,05	m^3/s	Arbitrary small dry season discharge
DGL	0	-	Recommended value (section 5.1.1(m))
SLATR	72	t/km^2	800xBPARR (section 5.1.1(v))
APARR	-0,008	mm^{-1}	Recommended value (section 5.1.1(n))
BPARR	0,0903	$t/km^2/d$	From equations 3.4 and 5.1 (section 5.1.1(o))
SALTU	100	t/km^2	100xBPARU (section 5.1.1(w))
APARU	-0,01	mm^{-1}	Recommended value (section 5.1.1(p))
BPARU	1,00	$t/km^2/d$	Recommended value (section 5.1.1(q))
PDEPS	0,90	-	Recommended value (section 5.1.1(r))
CONCS	500	mg/l	Arbitrary choice (section 5.1.1(x))
CONCBG	10	mg/l	Recommended value (section 5.1.1(s))
PINTM	0,80	-	Recommended value (section 5.1.1(t))
APARG	0	$t/km^2/$ mm/d	Recommended value (section 5.1.1(u))

Table 5.10: Initial parameter values used in program NACLØ2 for the Rietspruit catchment

Parameter	Value	Units	Derivation of parameter value
AVLEI	0	km^2	Measurement
AIRRIG	4,0	km^2	Measurement
CHAIN	17,0	km	Measurement
RETURN	0,2	-	Recommended value (section 5.1.2(a))
FIX	0,7	-	Estimate (see section 5.1.2(b))
FLEACH	0,5	-	Recommended value (section 5.1.2(c))
PLAT	0,28	-	Measurement
PUP	0,72	-	Measurement
HSTART	1,00	m	Arbitrary choice
CONSU	800	mg/l	Observed TDS at start of simulation
CONSL	800	mg/l	Observed TDS at start of simulation
GLOSS	0	Ml/d	Recommended value (section 5.1.2(d))
SLOPE	0,0015	-	Measurement
AMANC	0,04	-	Manning n estimated for channel
AMANF	0,10	-	Manning n estimated for flood plain
FEVAP	1,00	-	Value for open water surface (section 5.1.2(f))
FTRANS	0	-	Value for open water surface (section 5.1.2.(g))
FIRRIG	1,00	-	Value for open water surface (section 5.1.2(h))

Table 5.11 : Optimisation of streamflow parameters (Rietspruit catchment)

	Item	Observed	Calibration run number						
			1	2	3	4	5	9	10
Model parameters	POW		3	3	3	3	3	3	3
	SL		0	0	0	0	0	0	0
	SE		200	210*	210	220*	222*	122*	132*
	ST		400	400	400	400	400	300*	300
	FT		0,10	0,10	0,10	0,10	0,10	0,10	0,12*
	AI		0,006	0,006	0,006	0,006	0,006	0,006	0,006
	ZMINN		0	0	2*	2	2	2	2
	ZMAXN		15	15	10*	12*	12	12	10*
	PI		1,5	1,5	1,5	1,5	1,5	1,5	1,5
	TL		0,75	0,75	0,75	1,0*	1,0	1,0	1,0
	LAG		0	0	1*	1	1	1	1
	GL		10	10	10	10	10	10	10
	QOBS		0,05	0,05	0,05	0,05	0,05	0,05	0,05
	DGL		0	0	0	0	0	0	0
	GLOSS		0	0	0	0	0	0	0
Statistical parameters	Mean discharge (m^3/s)	3,557	3,254	3,527	3,512	3,494	3,568	3,211	3,544
	Standard deviation	8,972	6,869	7,502	8,080	8,189	8,389	8,424	9,106
	E_1	-	8,52	0,84	1,27	1,77	0,25	9,73	0,37
	E_2	-	23,44	16,38	9,94	8,73	6,50	6,11	1,49
	Correlation coefficient	-	0,432	0,463	0,609	0,653	0,652	0,649	0,690

Run 2: Table 5.11 now shows that the mean discharge is nearly correct. ZMINN can therefore be adjusted so as to reduce the earlier flood peaks, say to 2 mm/h. ZMAXN must then be decreased to preserve the modelled mean. Using equation 5.3:

$$ZMAXN' = 15.(0,8)^2$$
$$= 9,6 \text{ say } \underline{10} \text{ mm/h.}$$

Fig. 5.8 shows that the modelled flood peaks are about one day earlier than those observed. This can be corrected by setting LAG equal to 1 day.

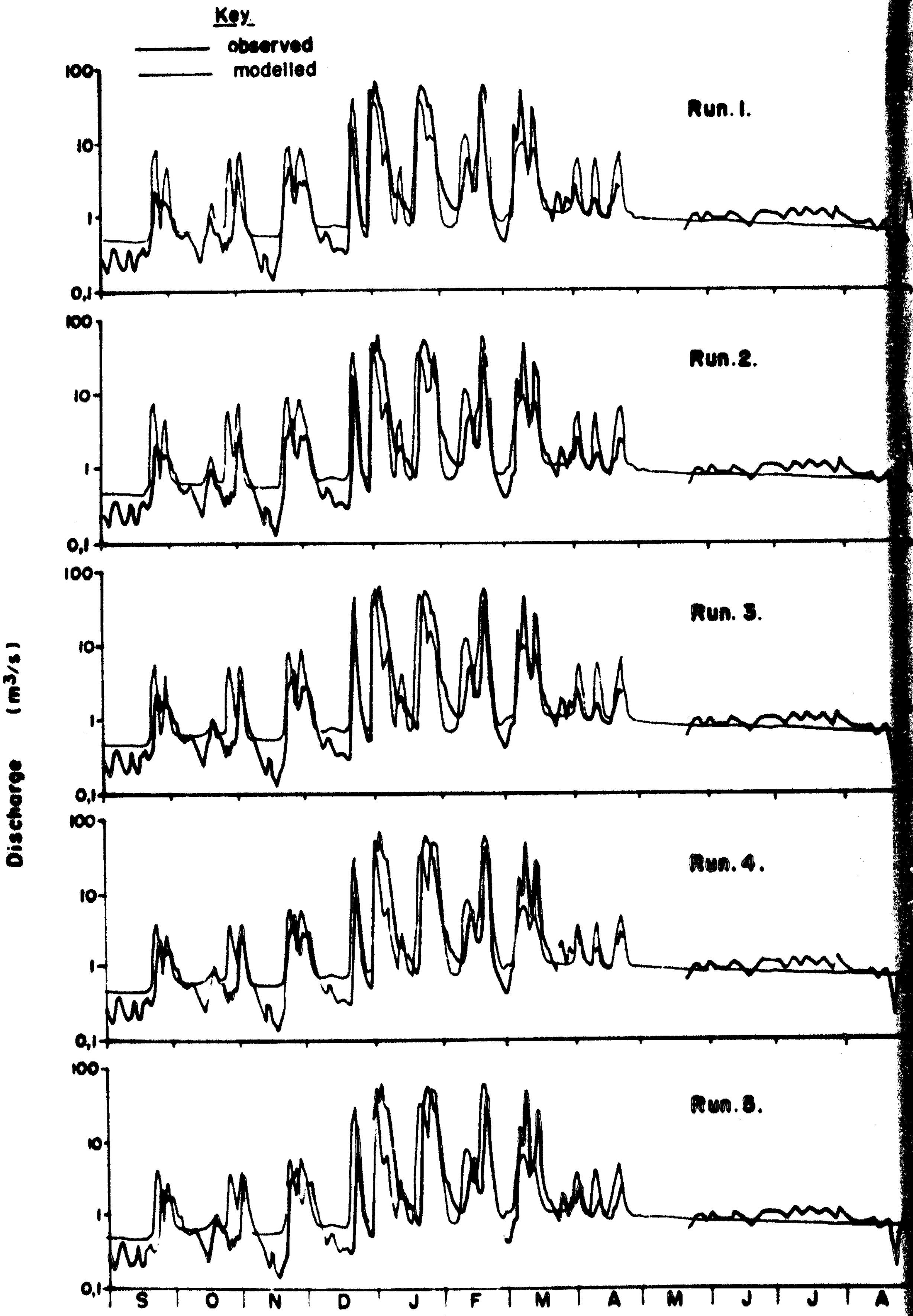

Fig. 5.8: Model calibration for the Rietspruit at C2M05: Discharges.

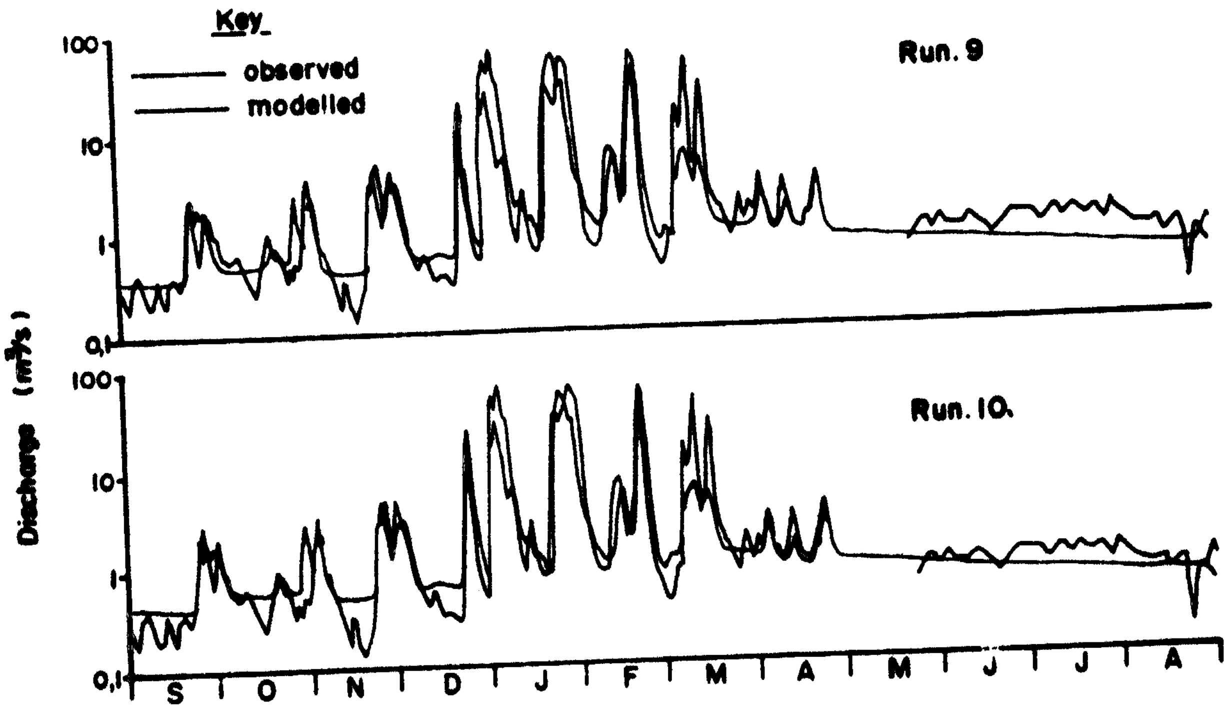

Fig. 5.8: Model calibration for the Rietspruit at C2M05 discharges

Run 3: From Table 5.11 it is seen that the mean discharge is a little low, but Fig. 5.8 shows that the early wet season flood peaks are still too high. Experience has shown that once ZMINN has been increased beyond 2 mm/h, further increases in ZMINN (together with a corresponding decrease in ZMAXN) produce only marginal differences in the distribution of floods during the rainy season. A more effective method of reducing the smaller early floods relative to the larger floods later in the wet season would be to increase the potential infiltration rates at the same time as increasing SE (i.e. reducing the effective soil moisture capacity). The early rains are then rapidly absorbed by the catchment, but during the heavier rains later in the season the soil moisture quickly reaches capacity giving rise to larger floods. In this way the flood distribution can be altered without affecting the mean discharge.

Table 5.12 : Optimisation of water quality parameters (Rietspruit catchment)

		Item	Observed	Calibration number 5	6	7	8	9	10	11	12
Model parameters		SALTR		72	35*	40*	39*	40*	40	39*	38*
		APARR		-0,008	-0,008	-0,008	-0,008	-0,008	-0,008	-0,008	-0,008
		BPARR		0,0903	0,0436*	0,0493*	0,0487*	0,0492*	0,0492	0,0484*	0,0469*
		SALTU		100	165*	199*	199	199	199	199	199
		APARU		-0,01	-0,01	-0,01	-0,01	-0,01	-0,01	-0,01	-0,01
		BPARU		1,00	1,00	1,20*	1,20	1,20	1,20	1,20	1,20
		PDEPS		0,9	0,9	0,9	0,7*	0,7	0,7	0,7	0,7
		CONCS		500	350*	570*	550*	605*	680*	645*	630*
		CONCBG		10	10	10	10	10	10	10	10
		PINTM		0,8	0,8	0,6*	0,6	0,6	0,6	0,6	0,6
		APARG		0	0	0	0	0	0	0	0
Statistical parameters	Salt load (t/d)	Mean	134,1	186,3	125,1	135,2	131,5	133,8	139,3	137,5	135,3
		Standard deviation	195,6	381,1	221,6	232,2	218,9	258,2	260,5	255,9	250,0
		E_1	-	38,88	6,71	0,82	1,91	0,22	3,88	2,56	0,89
		E_2	-	94,80	13,29	18,71	11,90	32,00	33,18	30,83	2[illegible]
		Corr.coeff.	-	0,711	0,718	0,719	0,722	0,701	0,741	0,741	
	TDS (mg/l)	Mean	871,9	815,0	642,4	711,9	708,1	822,7	763,8	758,1	
		Standard deviation	286,3	167,1	180,3	197,3	202,0	238,4	219,1	219,3	
		E_1	-	6,52	26,32	18,35	18,79	5,64	12,40	13,05	13,07
		E_2	-	41,64	37,02	31,09	29,45	16,73	23,47	23,40	23,33
		Correlation coeff.	-	0,814	0,842	0,838	0,844	0,855	0,856	0,856	0,856
Salt storage states (t)		$TSALTU_I$		670	1105	1333	1333	1333	1333	1333	1333
		$TSALTU_F$		1109	1109	1331	1331	1331	1331	1331	1331
		$TSALTR_I$		80352	39060	44640	43524	44640	44640	43524	42408
		$TSALTR_F$		81670	39465	44602	44058	44367	44158	43438	42094
		$SLOAD_I$		208430	145901	237610	196780	162343	181106	171785	167790
		$SLOAD_F$		299031	170730	231896	214363	191316	175633	172385	168346
		$TLOAD_G$		112955	68001	98075	93805	78346	98361	95521	93319
		$TLOAD_I$		333312	204831	228227	205712	214558	228684	221044	215941

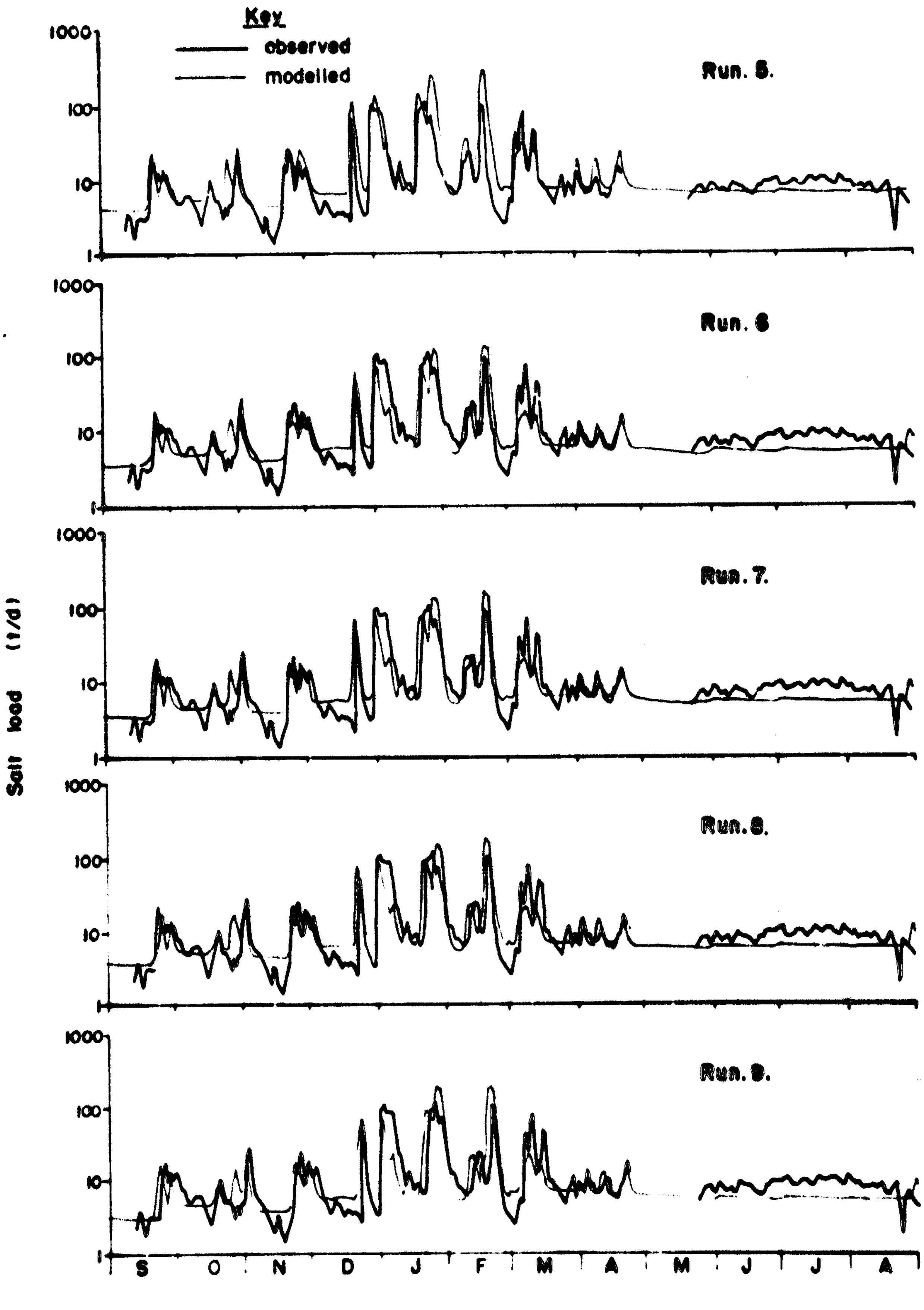

Fig. 5.9. Model calibration for the Rietspruit at C2M05: Salt loads.

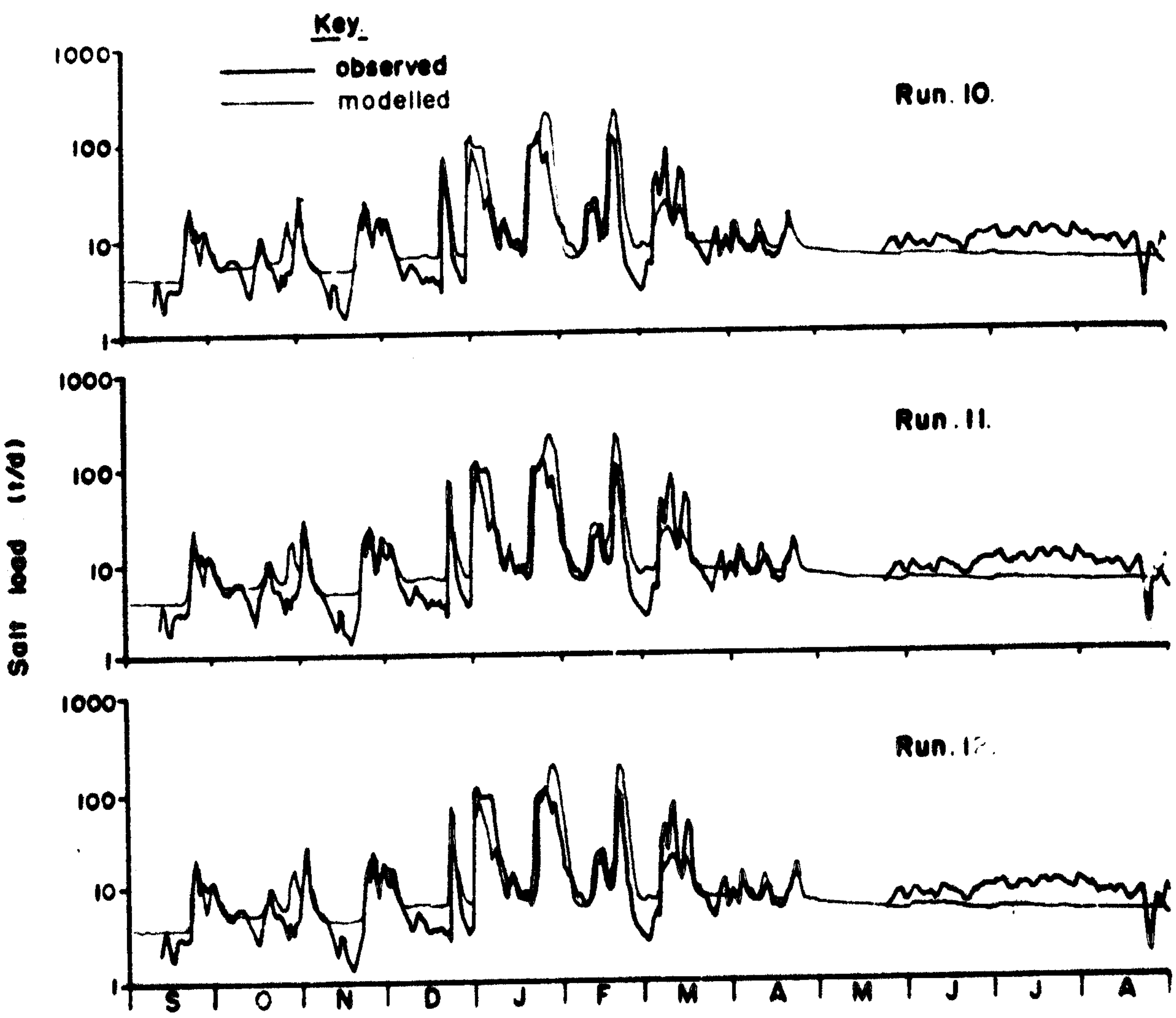

Fig. 5.9: Model calibration for the Rietspruit at C2M05 salt loads.

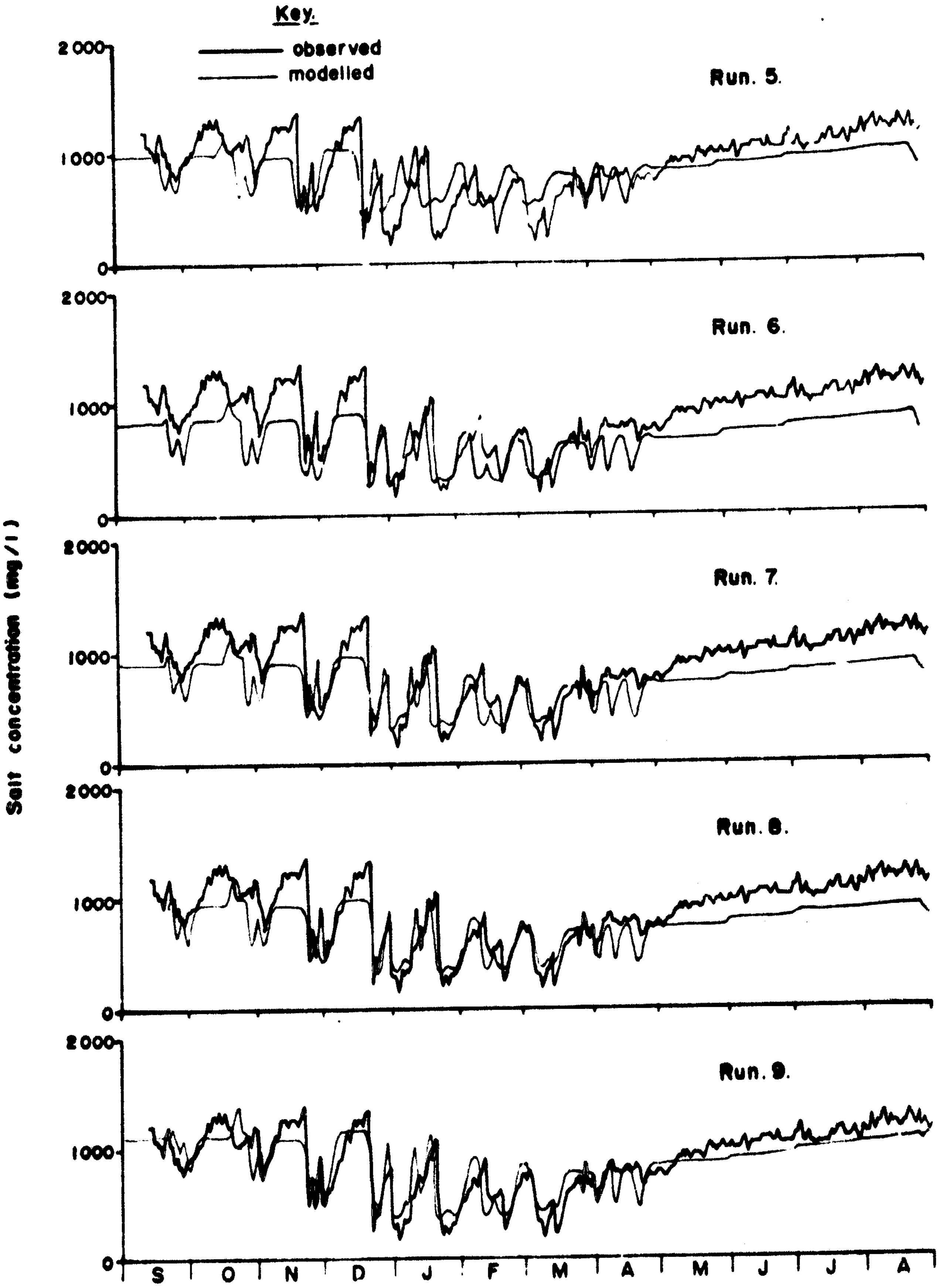

Fig. 5.10: Model calibration for the Rietspruit at C2M05 salt concentrations.

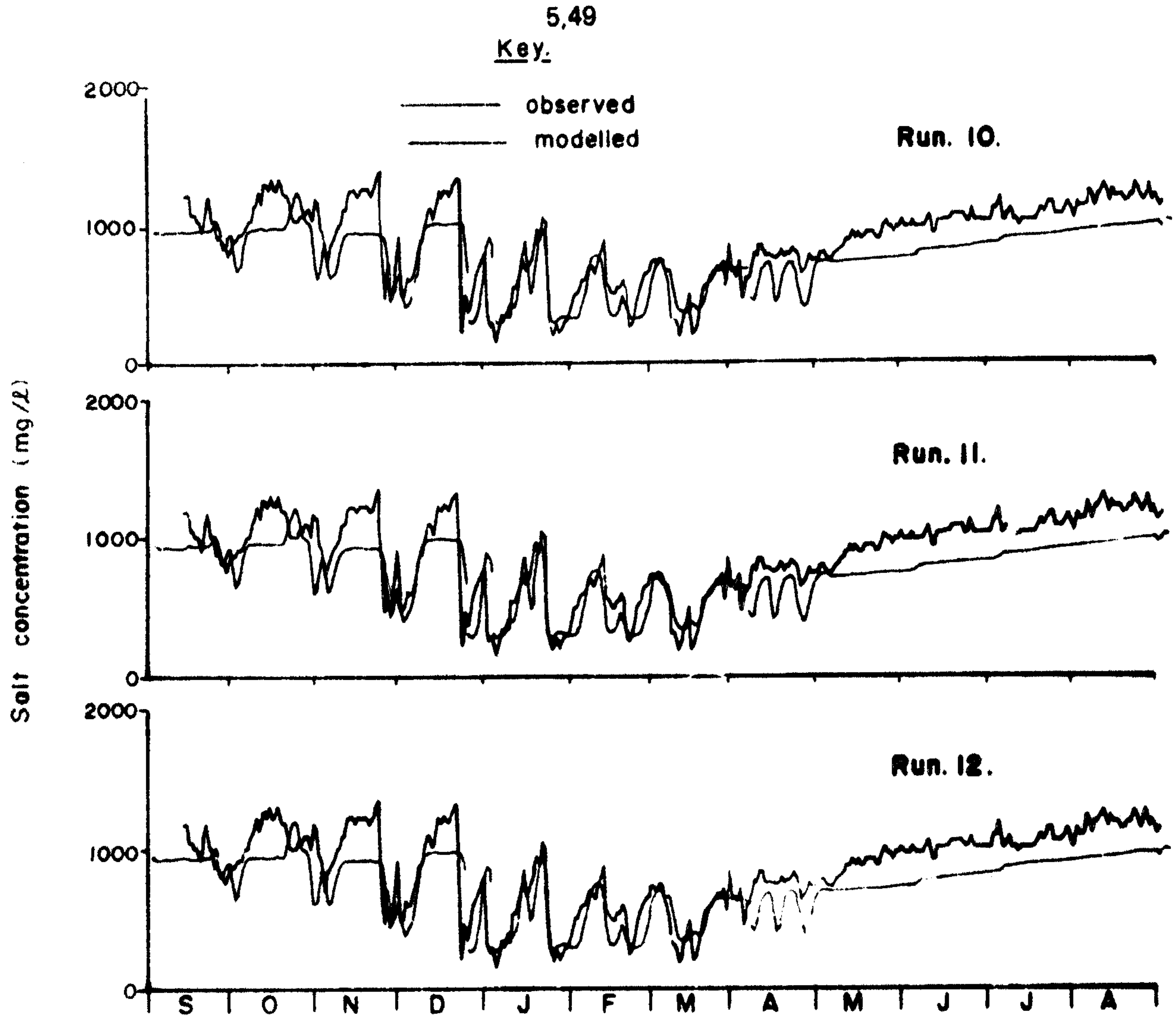

Fig. 5.10: Model calibration for the Rietspruit at C2M05 salt concentrations.

ZMAXN is therefore increased, say to 12 mm/h and SE is increased, say to 220 mm.

The flood recession limbs appear to be too steep, therefore increase TL, say to 1,0.

Run 4: Fig. 5.8 shows that the modelled flood recession limbs are about parallel with those observed, therefore TL need not be adjusted. The balance between early and late season flood peaks is also much improved, but Table 5.11 shows that the modelled mean is a little low. This can be improved by increasing SE, say to 222 mm.

Fig. 5.8 also shows that the modelled base flows during the period September - December, 1977 are too high. This cannot be improved upon, however, as the observed discharges (30 Ml/d) are in fact lower than the observed effluent point inputs, which enter the stream close to the Rietspruit weir (station RV2) and the geology of the area does not support the assumption of high bed losses. (This portion of the Rietspruit is situated in an alluvial plain for which Brink (1978) estimates permeabilities in the range 0,36 - 0,0036 mm/h).

Run 5: Table 5.11 and Fig. 5.8 indicate a reasonable fit between modelled and observed daily discharges. Water quality parameters can therefore now be optimised. Fig. 5.9 and Table 5.12 show that the modelled salt loads are too high. A large imbalance between initial and final salt storages is also evident.

Using equation 5.6, SALTU becomes:

$$SALTU' = 100.\frac{1109}{670}.\frac{1,0}{1,0}.\frac{1,0}{1,0}$$
$$= \underline{165}\ t/km^2$$

Equation 5.4 is used to adjust BPARR:

$$BPARR' = 0,0903 + \frac{(184,1-186,3)}{1116}$$
$$= \underline{0,0436}\ t/km^3/d$$

Using equation 5.5, SALTR becomes:

$$SALTR' = 72.\frac{81670}{80352}.\frac{1,0}{1,0}.\frac{0,0436}{0,0903}$$
$$= \underline{35}\ t/km^2$$

And finally CONCS is adjusted using equation 5.13:

$$CONCS' = 500.\left[\frac{1 + \frac{112955}{33312}}{\frac{112955}{33312}.\frac{1,0}{1,0} + \frac{0,8}{0,8}}\right]\frac{299031}{208430}.\frac{1,0}{1,0}.\frac{0,0436}{0,0903}$$

$$= 346\ (\text{say}\ \underline{350}\ mg/\ell)$$

Run 6: Fig. 5.9 shows an improvement in the modelled daily salt loads, but Table 5.12 shows that the mean daily salt load is now too low. It is also clear from Fig. 5.10 that modelled salt concentrations during floods are too high, while those during base flow conditions are too low. This imbalance can be rectified to some extent by reducing PINTM, say to 0,6, thereby reducing the interflow component of surface runoff.

By simple proportionality the new value of BPARR becomes:

$$\text{BPARR}' = 0{,}0436 + \frac{(134{,}1-125{,}1)}{(186{,}3-125{,}1)} \cdot (0{,}0903-0{,}0436)$$

$$= \underline{0{,}0505} \quad t/km^2/d$$

Figs. 5.9 and 5.10 show that the modelled salt loads during the early season floods are too low, implying that the impervious area salt recharge rate should be increased (see section 5.2.2(b)), say to 1,2 $t/km^2/d$.

BPARR must therefore be adjusted to compensate for the increase in BPARU. With equation [illegible], BPARR then becomes:

$$\text{BPARR}' = 0{,}0505 - (1{,}2-1{,}0) . 0{,}006$$

$$= \underline{0{,}0492} \quad t/km^2/d$$

From equations 5.5 and 5.6 the new estimates of SALTR and SALTU become 40 and 199 t/km^2 and from equation 5.13 CONCS becomes 570 mg/l.

Run 7: Table 5.12 shows that the modelled and observed mean salt loads are in good agreement and the balance between initial and final salt storage states is reasonable. Figs. 5.9 and 5.10, however, still show base flow salt concentrations that are too low. Comparison of Run 6 with Run 7 reveals that the reduction in PINTM has only marginally improved the base flow salinities. Further reduction of PINTM will therefore serve little purpose and might even lead to a deterioration of the fit between modelled and observed peak salt loads.

A reduction of PDEPS, say to 0,7, should have the desired effect of increasing base flow salinities.

BPARR, SALTR and CONCS are adjusted as before and the new values are given in Table 5.12.

Run 8: From Table 5.12 and Fig. 5.10 it can be seen that the base flow salt concentrations still fail to recover quickly enough after the rainy season. It could be that the soil moisture storage is too deep. It might be possible to improve the fit by reducing ST, say to 300 mm. Reducing ST should enhance the effect of evaporation on soil moisture salt concentrations, resulting in a more rapid rise in base flow salinities during the winter period.

To maintain the correct water balance, SE must be reduced by the same amount as ST, i.e. to 122 mm. FT will probably have to be increased, but this should be done in the following step so as to avoid the confusion arising from altering too many parameters at the same time.

The routine salt balance adjustments to parameters BPARR, SALTR and CONCS are indicated in Table 5.12.

Run 9: From Fig. 5.8 it can be seen that base flow discharges are now too low. FT is therefore increased to 0,12 mm/d. The mean discharge has also declined (see Table 5.11). This can be rectified by increasing SE, say by 10 mm. The mean salt load is very close to that observed, therefore BPARR and SALTR are not altered. The initial soil moisture salt storage, however, is too low. From equation 5.13 CONCS becomes 680 mg/l.

Run 10: Fig. 5.8 and Table 5.11 show a large improvement in the fit between modelled and observed daily discharges. The comparison between runs 5 and 10 (see Table 5.11) shows that the best fit using ST = 300 mm is superior to that with ST = 400 mm.

The modelled mean salt load is as yet too high. The adjustments made to the streamflow parameters during runs 9 and 10 make it difficult to estimate the change required in BPARR. The change in mean salt load due to the alteration of BPARR from run 7 to run 8 (see Table 5.12) can be used to estimate BPARR':

$$BPARR' = 0{,}0492 - \frac{(139{,}3-134{,}1)}{(135{,}2-131{,}5)}.(0{,}0493-0{,}0487)$$

$$= \underline{0{,}0484}\ t/km^2/d$$

The routine adjustments to SALTR and CONCS are shown in Table 5.12.

Run 11: Table 5.12 shows that BPARR has not been sufficiently reduced. By simple proportionality (using the results of runs 10 and 11) the new estimate of BPARR becomes 0,0469 $t/km^2/d$. The adjustments to SALTR and CONCS are shown in Table 5.12.

Run 12: The error between observed and modelled mean daily salt loads has now been sufficiently reduced, although the modelled standard deviation is a little high (Table 5.12). This can be attributed to the fact that the modelled base flow salinities (although higher than in run 8) are still too low.

The base flow salt load could be increased by means of a further reduction of ST, but this would increase the standard deviation of the modelled daily discharges (compare runs 5 and 10 of Table 5.11) with a consequent deterioration of the fit. Further parameter adjustment therefore cannot be justified, especially in view of the inconsistency between observed discharges at RV2 and the point inflow immediately upstream of the weir. (See the discussion on run 4).

Any further attempt to improve the base flow salinities could, in view of the above data inconsistencies, lead to unrealistic parameter values. The values used in run 12 are therefore accepted as representing the optimum calibration.

CHAPTER 6 CONCLUSION

A mathematical model to generate daily catchment runoffs and associated salinities using daily rainfall and evaporation data as basic input together with a channel routing model has been successfully developed and tested.

The model can be used to patch and extend records of daily streamflows and salt loads, provided that sufficient data are available for the model parameters to be properly calibrated. Once the model has been calibrated it can be run for a wide range of hydrological conditions, limited only by the availability of rainfall data. The modelled daily discharges and salt loads can then be used to simulate the effectiveness of various pollution control strategies, thereby facilitating selection of the optimum solution.

The strong correlation found between diffuse source generation rate and industrial water consumption introduces a degree of prediction ability which can be used to estimate likely future pollution levels. In comparing water management and planning options a comparison based on present-day conditions alone may not suffice. The behaviour of alternative systems subject to expected future conditions may prove a more appropriate decision-making criterion, especially where costly capital works with long service lives are involved. The model provides a means of simulating likely future conditions. If necessary a spectrum of possible future conditions could be simulated ranging between extreme high and extreme low salt generation growth rates.

As the model is applied to more catchments it may be possible to improve the confidence with which the model can be used to predict the environmental impact of new catchment developments. As yet it is not possible to predict the effect of any particular type of catchment development, such as a new residential area. This could be facilitated by in-depth studies of a large number of smaller homogeneously developed catchments. Such studies, however, would prove costly and time-consuming and the dominance of one or two special elements in small catchments, such as a canning factory in an industrial area, might make generalisation of the results impracticable.

The study of other catchments similar in size to those in the PWV region might prove to be a more fruitful approach. Correlation between catchment characteristics and salt generation rates for a much larger number of catchments should prove a worthwhile exercise.

The model in its present form is designed to simulate the movement of total dissolved solids. Provided sufficient data can be accumulated it should prove possible to adapt the model to simulate the behaviour of individual conservative chemical constituents as they move through the system.

LIST OF REFERENCES

Ackerman, W.C., Allee, D.J., Amorocho, J., Haimes, Y.Y., Hall, W.A., Meserve, R.A., Patrick, R. and Smith, P.M., 'Scientific and Technological Considerations: Water Resources Policy'. Transactions, American Geophysical Union, 59 No. 6: 516-527, 1978.

Andren, A.W., Lindberg, S.E. and Bate, L.C., 'Atmospheric input and geochemical cycling of selected trace elements in Walker Branch watershed'. Pub.728, Oak Ridge Nat. Lab., Environ. Sci. Div., Oak Ridge, Tenn., 1975.

Army Corps of Engineers, Urban Storm Water Runoff - STORM, Computer Program 723 SB L2520, Hydrologic Engineering Center, California, 1975.

Barker, H.M. and Whitmore, J.S., Correlation of evaporation from Symons pans and storage reservoirs. Research Technical Note No. 6, South African Department of Water Affairs, Division of Hydrology, 1965.

Betson, R.P., 'Bulk precipitation and streamflow quality relationships in an urban area'. Water Resources Research, 14, No. 6: 1165-1169, 1978.

Bower, C.A., Spencer, J.R. and Weeks, L.O., 'Salt and water balance, Conchella Velley, California'. J. Irrig. Drain. Div.Amer.Soc. Civ. Engrs., 95 No. 1 : 55-64.

Brink, A.B.A., 'Estimates of soil permeability in the southern PWV area', Report to Messrs. Stewart, Sviridov and Oliver, Johannesburg, February 1978.

Browatt, J.G. and Hart, T., Projections of the urban population of the southern PWV for the years 1980, 1990 and 2000. Occasional paper No. 19, Urban and Regional Research Unit, University of the Witwatersrand, Johannesburg, June, 1978.

Bryan, E.H., Quality of Stormwater Drainage from Urban Land. Paper presented at 7th Conf. Amer. Water Resources Assn., 1971.

Chow, Ven te (Ed.), Open-channel Hydraulics. McGraw-Hill, New York, 1959.

Clausen, H.T. 'Mine shaft water pumped', Pollution control sub-committee circular No. 22/76, Chamber of Mines of South Africa, Johannesburg, May, 1976. (Unpublished).

Clausen, H.T., 'Trends in some waters in the Vaal barrage system', Memorandum to the Chairman of the Pollution control sub-committee, Chamber of Mines of South Africa, Johannesburg, 1977, (Unpublished).

LIST OF REFERENCES - cont.

Cogbill, C.V. and Likens, G.E., 'Acid precipitation in the north-eastern United States'. Water Resour. Res., 10 NO. 6; 1133-1137, 1974.

Computer Centre, CALCOMP Software manual users guide. University of the Witwatersrand.

Council on Environmental Quality, Third Annual Report, Washington DC 1972.

Donigian, A.S. and Crawford, N.H., Modelling Nonpoint Pollution from the Land Surface. Office of Research and Development, EPA-600/3-76-083, Environmental Protection Agency, 1976.

Fritz, P., Cherry, J.A., Weyer, K.V. and Sklash, M.G., 'Runoff analyses using environmental isotope and major ions'. In Interpretation of Environmental Isotope and Hydrochemical Data in Groundwater Hydrology. I.A.E.A., Vienna, pp. 111-130, 1976.

Gel'bukh, T.M., 'Evapotranspiration from overgrowing reservoirs'. Publ. Intern. Assoc. Sci. Hydrol., 62:87, 196[illegible]

Giddens, J., 'Contamination of water by air pollutants, especially ammonia from animal manures'. Rep. ERC 1275, Dep. of Agron., Univ. of Ga., Athens, 1975.

Hall, G.C. and Gorgens, A.H.M.(Ed.), 'Studies of mineralisation in South African rivers'. South African National Scientific Programs Report No. 26, Council for Scientific and Industrial Research, Pretoria, 1978.

Hall, G.C., 'Forecast of end-of-century water demands for the PWVS Complex', Report to the Water Research Commission, Pretoria, April 1980.

Hart, T., Browett, J.G., 'Projections of manufacturing industry employment in the southern PWV region,1970-2000, Occasional paper No. 21, Urban and Regional Research Unit, University of the Witwatersrand, Johannesburg, December, 1978.

Herold, C.E.,'A model to compute on a monthly basis diffuse salt loads associated with runoff. Report No. 1/80, Hydrological Research Unit, University of the Witwatersrand, Johannesburg, March, 1980.

Herold, C.E., Mileikowsky, R.N., Hall, G.C. and Midgley, D.C., 'Numerical Modelling of Salinity Fluctuations in the Vaal System.' Paper presented at Focus on the Vaal Symposium, Vaal River Catchment Association, March, 1980.

Herold, C.E., A model to simulate daily river flows and associated diffuse-source conservative pollutants. Report No. 3/81, Hydrological Research Unit, University of the Witwatersrand, Johannesburg, March 1981.

Huff, F.A. (Ed.), 'Summary report of Metromex studies, 1971-1972'. Rep. of Invest. 74, Ill. State Water Surv., Urbana, 1973.

Hydrocomp International, Inc., Hydrocomp Simulation Programming Operations Manual. 4th Ed., California, 1975.

LIST OF REFERENCES - cont.

Israelson, O.W. and Hansen, V.E., 'Irrigation principles and practices. 3rd Ed. New York: John Wiley & Sons, Inc., 1962.

Kennedy, V.C., 'Hypothesis to explain the rapid release of solutes from soil during storm runoff'. Transactions American Geophysics Union, 58:386, 1977.

Kreil, J.P. Recent investigations on the evaporation from large water surfaces and evaporation tanks in South Africa. Technical Report No. 29, South African Department of Water Affairs, Division of Hydrology, 1963.

Lester, W.F., 'Pollutant River ; River Trent, England', In 'River Ecology' (Ed. Whitton, B.A.), Studies in Ecology Volume 2. Oxford: Blackwell, 1975.

Linacre, E.T., Hicks, B.B., Sainty, G.R. and Grauze, G., 'The evaporation from a swamp'. Agri. Meteorol., 7:375-386, 1970.

Litwin, Y.J. and Donigian, A.S., 'Continuous Simulation of Nonpoint Pollution'. Journal of Water Pollution Control Federation, 50 No. 10: 2348-2361, October 1978.

Lund, B.G.A.,'Relationship between screened and unscreened Class A and Symons Evaporation Pans', Trans. S.A.I.C.E., 12 No. 8: 195-196, 1970.

Metcalf and Eddy, Inc., Storm Water Management Model, Volume 1, Final Report, Environmental Protection Agency, Washington, D.C., 1971.

Midgley, D.C., Lee, R.E., Blok, T. and Weiss, H.W., 'Hydraulic, botanic and dredging aspects', Southern Regional Park proposed Klipriver Lake. Report to City Engineers Dept., Johannesburg, 1974.

Midgley, D.C., 'Flood protection for open-cast mining in the Taaibosspruit valley'. Feasibility study for Anglo American corporation, Hydrological Research Unit, University of the Witwatersrand, Johannesburg, December, 1978.

Migahid, A.M., Further observations on the flow and loss of water in the 'Sudd' swamps of the upper Nile. Fouad I University Press, Cairo, 1952.

Mileikowsky, R.N., A mathematical model for simulating daily salinity fluctuations in the Vaal Barrage. Report No. 4/80, Hydrological Research Unit, University of the Witwatersrand, Johannesburg, April, 1980.

LIST OF REFERENCES - cont.

Murphy, K.O.H., 'Flow-rating tables for stations C2M21 and C2M70', Personal communication, Department of Water Affairs, Pretoria, 1978.

Olivier, H., Irrigation and Climate. London : Edward Arnold Ltd., 1961.

Olivier, H., Irrigation and Water Resources Engineering. London: The Cameolot Press Ltd., 1972.

Penman, H.L., 'Vegetation and hydrology'. Commonwealth Bur. Soil Sci. (Gt. Brit.) Tech. Commun., 53: 64-65, 1963.

Pitman, W.V., A mathematical model for generating monthly river flows from meteorological data in South Africa. Report No. 2/73, Hydrological Research Unit, University of the Witwatersrand, 1973.

Pitman, W.V., A mathematical model for generating daily river flows from meteorological data in South Africa, Report No. 2/76, Hydrological Research Unit, University of the Witwatersrand, Johannesburg, March 1976.

Rijks, D.A., 'Evaporation from a papyrus swamp'. Quart. J.R. Met. Soc., 95: 643-649, 1969.

Rouse, H., Engineering Hydraulics. New York : John Wiley & Sons, Inc., 593, 1949.

Rupert, H., 'Geochemical investigations on atmospheric precipitation in a medium-sized city : Water Air Soil Pollut., 4 : 447-463, 1975.

Secretary for Water Affairs, Fourth supplementary report on the proposed Tugela-Vaal Government Water Project. White Paper No. R-77, ISBN 0 621 03757 5, Republic of South Africa, 1977.

Sklash, M.G., 'The role of groundwater in storm and snowmelt runoff generation'. Ph.D. Thesis, University of Waterloo, Ontario, 1978.

Sklash, M.G. and Farvolden, R.N., 'The Role of Groundwater in storm runoff'. Journal of Hydrology, 43 (1979) : 45-65.

Stewart, Sviridov and Oliver, 'PWV project southern catchment drawings', Project Managers report to the Water Research Commission, Johannesburg, 1978.

LIST OF REFERENCES - cont.

Swank, W.T. and Henderson, C.S., 'Atmospheric input of some cations and anions to forest ecosystems in North Carolina and Tennessee'. Water Resour. Res., 12 No. 3 : 541-546, 1976.

Tennessee Valley Authority, 'A continuous daily streamflow model'. Res. Pap.8, Knoxville, 1972.

Tordiffe, E.A.W., 'Die geohidroligiese opname van die Visrivierbekken met betrekking tot die Oranjerivierprojek'. Report to the Working Group for Mineralization, National Program for Environmental Sciences, 1973.

U.S. Corps of Engineers, Engineering procedure as applied to flood control by reservoirs with reference to the Muskingham flood control project. Appendix 8, Engineer school Fort Belvair, 1936.

Vitale, A.M. and Sprey, P.M., Total Urban Water Pollution Loads: The Impact of Storm Water. Enviro-Control, Inc., Council on Environmental Quality, 1974.

Weibel, S.R., Anderson, R.J. and Woodward, R.L., 'Urban Land Runoff as a factor in Stream Pollution'. Journal of Water Pollution Control Federation, 63: 914, 1964.

Weiss, H.W., An integrated approach to mathematical flood plain modelling. Report No. 5/76, Hydrological Research Unit, University of the Witwatersrand, Johannesburg, September 1976.

Whipple, W., 'Unrecorded Pollution from Urban Land Runoff'. Journal of Water Pollution Control Federation, 46: 873, 1974.

PART II

THE DAILY FEEDBACK MODEL

TABLE OF CONTENTS

TABLE OF CONTENTS - cont.

LIST OF FIGURES

LIST OF FIGURES - cont.

LIST OF FIGURES - cont.

LIST OF TABLES

LIST OF TABLES - cont.

SYNOPSIS

This report describes a numerical model designed to simulate on a monthly basis the fluctuations of salinity and storage state of the reservoirs of the Vaal river water supply system.

Inputs to the model comprise: output from the monthly washoff model described in HRU Report no. 1/80, along with the matrix of annual water demands, the monthly rainfalls, the mean monthly potential evaporations, the physical characteristics of the reservoirs, the model parameters defining the operating rules and, finally, the assumptions associated with each of the simulations.

The feed-back effects of return flows of mineralised effluents which re-enter the water supply system are modelled on the assumption that steady-state conditions persist throughout each month simulated. Functions relating operational and maintenance costs to the TDS concentrations in the water supply have been incorporated so that the approximate costs associated with different levels of pollution can be assessed and to provide a basis of comparison and appraisal of different ameliorative measures.

The computer programs have been written in such a way that a wide variety of management and planning options can be modelled without recourse to programming changes. The behaviour of the system is simulated for several of these options in order to demonstrate the power and versatility of the model.

A comprehensive user manual is provided for guidance in the handling of the various computer programs.

CHAPTER 1 : INTRODUCTION

1.1 Motivation

The Pretoria-Witwatersrand-Vereeniging (PWV) complex constitutes the largest and most highly developed concentration of human activity in southern Africa. For its water supply it is dependent upon the Vaal river and this source is also the sink for much of the pollution generated in the southern portion of the PWV region. Polluted water passes on down river to the detriment of other users of Vaal river water, such as the Western Transvaal Regional Water Company, the O.F.S. Goldfields Government Water Scheme and the Vaalharts Government Irrigation Scheme. Figure 1.1 shows the location of the PWV region and identifies the most significant components of the system.

The major impoundments of the present Vaal system are the Vaal, Bloemhof, Grootdraai and Sterkfontein Dams. The last-mentioned is a component of the Tugela-Vaal scheme and provides reserve storage for water transferred from the Tugela river, thus allowing the Vaal Dam and other storages in the system to be drawn upon at higher rates than normally would be risked. Possible future components include a dam at Schoemansdrift on the Vaal river near Parys on the farm Welkom (referred to subsequently as Welkom Dam) and a second reserve storage reservoir (referred to as New Dam) in the upper reaches of the Vaal upstream of Grootdraai Dam to hold water transferred from the Usutu catchment.

The major concerns regarding the water supply potential of the Vaal system are, first, the timeous implementation of suitable augmentation schemes to meet growing demands, and second, the implementation of appropriate ameliorative measures to ensure the supply of water of acceptable quality to all users. Techniques for estimating the assured yield of a river system are already well established and consequently planning the sizing and timing of augmentation schemes presents little difficulty. Selection and design of suitable ameliorative measures to improve the quality of

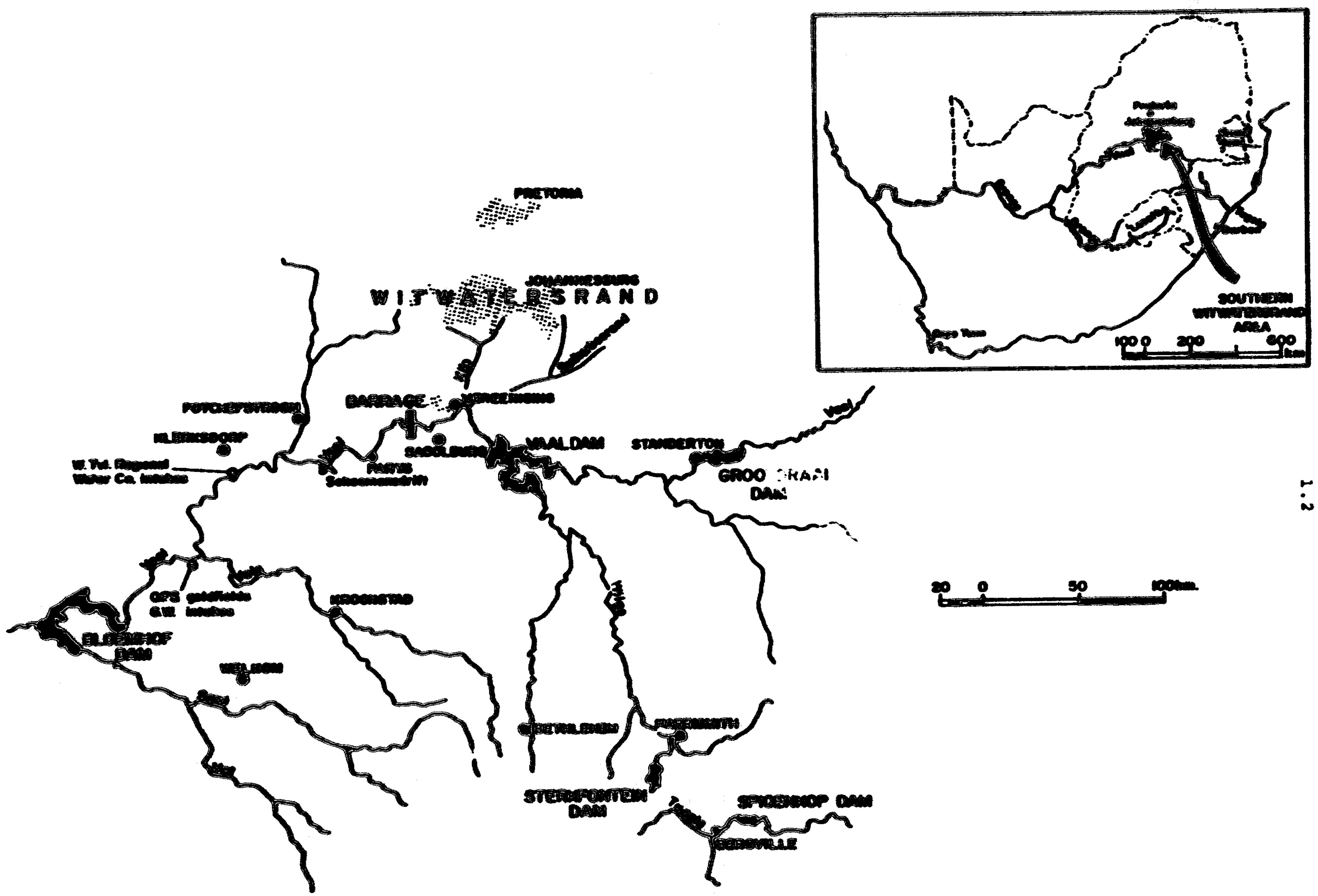

Fig.1.1: Location of PWV region and major reservoirs of the Vaal basin

water supplies, however, constitute a much more complex problem requiring an entirely different approach.

Increasing mineralisation of the water resources of the Vaal system has become a cause for concern, both because of health hazards and because of the high costs associated with damage to industrial and domestic equipment.

In 1975 the Water Research Commission initiated a study of the PWV complex in regard to existing and incipient problems of water supply, waste water management and pollution control, with special reference to mineral pollution. The Hydrological Research Unit of the University of the Witwatersrand, funded by the Water Research Commission, undertook to develop a set of numerical models which could be used to simulate the fluctuations of salinity at key points in the system and to compare various options for ameliorating undesirable future salinity conditions. Models which have previously been documented are the monthly washoff model (Herold, 1980), which simulates monthly diffuse salt loads washed off a catchment using monthly runoff volumes as basic input, and the daily washoff model (Herold, 1981a) which, with daily rainfall and mean monthly potential evaporation data as basic input, simulates daily catchment runoffs and associated diffuse-source salt loads and routes these together with effluent point inputs, through the channel system. Output from these two models serves as input to the daily feed-back model (Herold, 1981b), the purpose of which is to simulate daily fluctuations of storage state and salinity in all reservoirs of the Vaal water supply system. The daily model also simulates the feed-back effect whereby water abstracted from Vaal Dam and Vaal Barrage is supplied to users in the southern PWV region, discharged into the tributaries of the Vaal Barrage (at increased TDS levels) and re-enters the Vaal river from where it is again abstracted. The daily feed-back model is extremely complex (requiring up to 38 separate input and output files) and is consequently expensive to run. This daily model is therefore best suited for the simulation of relatively short hydrological sequences, of the order of two to three years. Much longer sequences can of course be simulated, but at high cost in terms of computer time.

The model discussed in this report is a simplified version of the daily feed-back model and operates at a monthly time step. As a consequence it is more economical to run. The purpose of the monthly model is two-fold. In the first place, it can be run for a number of years in order to establish starting conditions (in terms of both storages and initial salt concentrations in the reservoirs) to be used as input to the daily model. If, for example, it is desired to compare the performance of several system options under 1990 conditions of demand and catchment development, the monthly model can be used to simulate the years from the present date until the beginning of 1990 and the daily model need then be run only for the remaining one year. This exercise could then be repeated for several hydrological sequences in order to establish either the most likely or the most severe 1990 salinity conditions associated with the option being tested. In the second place the monthly model can, at relatively low cost, simulate a large number of hydrological sequences for each proposed option thus allowing an initial comparison to be drawn between options. Many obviously poor options can then be eliminated without recourse to the more expensive daily model. For some options, indeed, it may not be necessary to run the daily model at all because in many such cases the day-to-day fluctuations of TDS concentrations in the Vaal Barrage are of little consequence. Options 4C, 5A and 5B discussed in Chapter 3 are cases in point.

Brief descriptions of the computer programs comprising the monthly feed-back model follow.

1.2 Program RESØØ1

Program RESØØ1 is the main computational program which solves the water and salt mass balance equations for all reservoirs in the system and computes salt concentrations at key points. Costs to users associated with TDS in the water supply in various demand centres are computed month by month using the relationship between TDS and operational and maintenance costs derived by Heynike (1980).

The structure of program RESØØ1 is described in Chapter 2. Appendix A has the details of the data used as input to the model and a program user manual is to be found in HRU report no. 4/81 (Herold, 1981b).

1.3 Program RESØØ3

RESØØ3 is a program which plots monthly reservoir storages and monthly salt concentrations at key points in the system simulated by program RESØØ1. This program is designed to be used in conjunction with a CALCOMP plotter.

1.4 Program RESØØ4

RESØØ4 plots duration curves of simulated monthly salt concentrations at key points in the system using a CALCOMP plotter.

All programs are written FORTRAN IV and have been developed for an IBM 360 or 370 system.

CHAPTER 2 MODEL STRUCTURE

2.1 Introduction

Figure 2.1 is a system diagram showing the major elements of the model. Those features indicated in red are as yet not in existence. Input to the model comprises monthly catchment runoffs and salt loads, monthly rainfalls, mean monthly potential evaporations, annual reservoir demands and physical features of the reservoirs. The model operates to a monthly time step.

For each month simulated, the water mass balance equations are solved for each reservoir in the system according to user-specified operating rules. The equations are solved for reservoir status in the following order: New Dam, Grootdraai, Sterkfontein, Vaal Dam, Vaal Barrage, Welkom and Bloemhof. Whenever a reservoir experiences a supply shortfall, a call is made upon the next upstream dam to make good the shortfall. If Sterkfontein Dam cannot meet Vaal Dam shortfalls, then the system can be considered to have failed and the deficit is printed. To enable the simulation to proceed the deficit is assumed to be met from some unprescribed source.

A decision block has been built into the program which enables the user, by means of minor changes of the coding, to re-distribute the PWV demands between Vaal Dam, Vaal Barrage and Welkom Dam when Vaal Dam or Sterkfontein Dam fail. Storage equations for each reservoir are then solved again using the adjusted demands for the month concerned. In this manner a number of water supply options may be tested.

Once the water balance equations for the month have been solved, solution of the salt mass balance equations for Grootdraai, Sterkfontein and Vaal Dam proceeds. Salt concentrations of water supplied to the PWV region, of effluent return flows and of water in Vaal Barrage are then established assuming steady-state conditions during each month. Allowance is made for channel losses and irrigation abstractions and

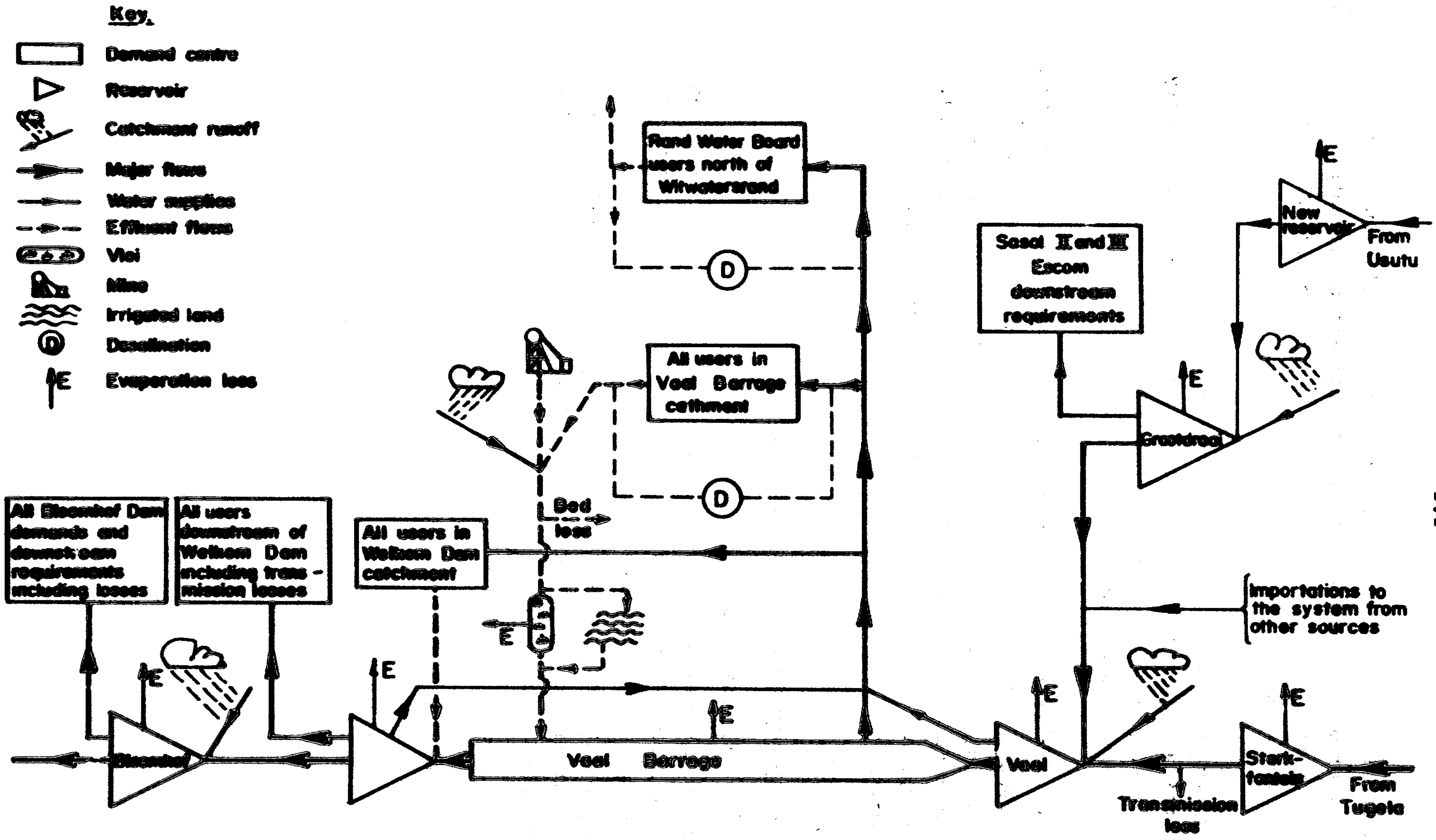

Fig.2.1: System diagram of the PWV monthly model.

return flows. Provision is made for the inclusion in the model of direct reclamation and desalination elements. Finally the salt balance equations for Welkom and Bloemhof Dams are solved.

End-of-month water and salt storages and water and salt fluxes are printed for each reservoir, together with monthly water supply salt concentrations. Accumulated totals are printed at the end of the simulation.

Reservoir water and salt mass balance equations are discussed in sections 2.2 and 2.3, while the steady-state equations governing the salt concentrations of water supplied and that returned from the PWV region are given in section 2.4. The operation of the entire system model is described in section 2.5.

2.2 Reservoir water mass balance

2.2.1 Storage-area relationship

The storage-area relationship for each reservoir is defined by a table of surface areas which are specified for various storages. Surface areas for any given storage are interpolated linearly between the specified values. From Fig. 2.2 it can be seen that the surface area, A (km^2) for storage S ($m^3 \times 10^6$) is given by:

$$A = A_n + (A_{n+1} - A_n) \cdot \frac{(S - S_n)}{(S_{n+1} - S_n)} \quad \ldots\ldots\ldots\ldots\ldots\ldots\ldots (2.1)$$

where A_n, A_{n+1}, V_n and V_{n+1} are defined in Fig. 2.2.

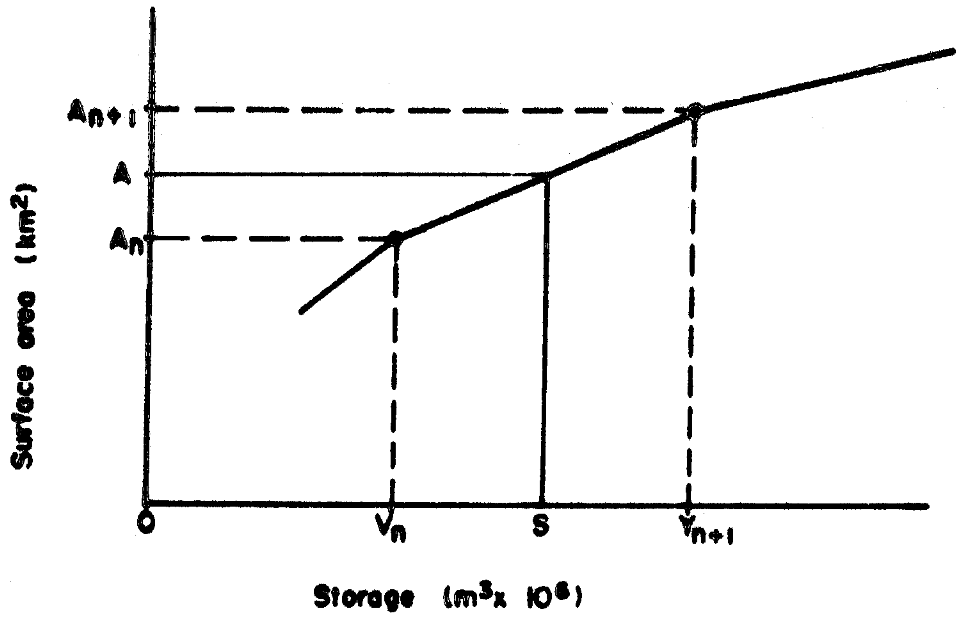

Fig. 2.2: Reservoir storage-area relationship.

2.2.2 Evaporation

Evaporation from the lake surface is computed in one step so as to reduce computational time. If evaporations are computed using initial reservoir storages only, then a systematic over-estimation of evaporation losses will occur. This is because during most months reservoir outflows exceed inflows. For this reason the average storage during the month is estimated as follows:

$$SCALC = \tfrac{1}{2}.(S_i+S'_{i+1}) \quad \ldots\ldots\ldots\ldots\ldots\ldots\ldots\ldots\ldots (2.2)$$

where SCALC = estimated average storage during month (m^3x10^6)

S_i = storage at start of month i (m^3x10^6)

S'_{i+1} = estimated storage at end of month i (m^3x10^6)

and S'_{i+1} is given by:

$$S'_{i+1} = S_i + QIN_i - QOUT_i - E_{i-1} \quad \ldots\ldots\ldots\ldots\ldots (2.3)$$

where QIN_i = total inflow during month i (m^3x10^6)
$QOUT_i$ = total outflow during month i (excluding evaporation loss) (m^3x10^6)
E_{i-1} = total evaporation loss during previous month (m^3x10^6).

In order to compute the evaporation loss during the current month that of the previous month is thus used to approximate the average storage during the month. In this manner a long term systematic error in calculated evaporations is avoided.

Net evaporation during the month is computed as:

$$E_i = (PE_i-R_i).THOU.\{A_n+(A_{n+1}-A_n).\frac{(SCALC-S_n)}{(S_{n+1}-S_n)}\}..(2.4)$$

where E_i = net evaporation during month i (m^3x10^6)
PE_i = mean potential lake evaporation for month i (mm)
R_i = rainfall during month i (mm)
THOU = constant (=0,001)

2.2.3 Water demands

For each reservoir annual demands are read as input data and these are disaggregated according to a specified annual pattern. Monthly demands are thus given by:

$$D_i = PMONTH_i.DEM_j.10^{-2} \quad ....(2.5)$$

where D_i = demand for month i (m^3x10^6)
$PMONTH_i$ = mean monthly demand as percentage of annual demand
DEM_j = annual demand for year j (m^3X10^6).

2.2.4 Water balance equations

The water balance for the month is given by:

$$S_{i+1} = S_i + QUP_i + QCAT_i + CALLU_i - E_i - D_i - CALLD_i \quad \ldots(2.6)$$

where S_{i+1} = storage at end of month i (m^3x10^6)
QUP_i = total spillage from upstream reservoirs less transmission losses during month i (m^3x10^6)
$QCAT_i$ = catchment runoff during month i (m^3x10^6)
$CALLU_i$ = call made on upstream reservoir during month i (m^3x10^6)

If S_{i+1} as obtained by equation 2.6 is greater than SCAP, the reservoir capacity, then the spillage from the reservoir, SPILL (m^3x10^6), is calculated as:

$$SPILL = S_{i+1} - SCAP \quad \ldots\ldots(2.7)$$

and S_{i+1} is set equal to SCAP.

At the beginning of every month $CALLU_i$ and $CALLD_i$ are set equal to zero. Starting at the upstream end, the water balance equations for each dam are calculated. If S_{i+1} as given by equation 2.6 is less than SRES, the reservoir reserve storage, then $CALLU_i$ is calculated as:

$$CALLU_i = SRES - S_{i+1} \quad \ldots\ldots(2.8)$$

and S_{i+1} is set equal to SRES.

Starting with Welkom Dam, and working upstream, each reservoir is again examined. If $CALLD_i$ (which is equal to $CALLU_i$ for the next downstream dam) is greater than zero, then the water mass balance for the reservoir is re-calculated. If $CALLD_i$ is equal to zero, then the next upstream reservoir is checked until the furthest upstream reservoir, Sterkfontein Dam, is reached.

2.3 Reservoir salt mass balance

At the beginning of each time step the reservoir is completely mixed to form a single cell. The aggregated inflow to the reservoir during the time step then forms a second cell at the upstream end of the reservoir. Assuming plug-flow through the reservoir two distinct cases may arise:

Case I $\qquad QOUT_i < S_i$

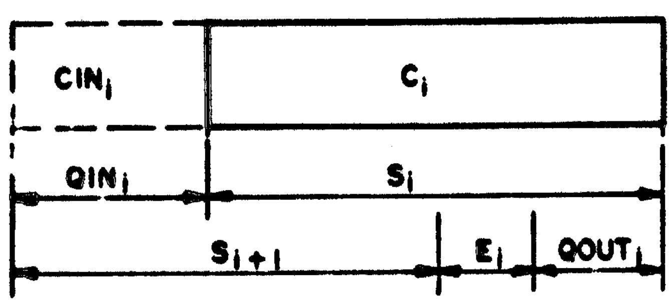

Fig.2.3: Illustration of Case I

In this case $COUT_i$, the salt concentration of the water leaving the reservoir (mg/l), is set equal to C_i, the reservoir salinity at the end of the previous month.

The reservoir salt concentration at the end of month i, C_{i+1} (mg/l), is calculated as:

$$C_{i+1} = \frac{QIN_i.CIN_i+C_i(S_i-QOUT_i)}{S_{i+1}} \quad \text{.............(2.9)}$$

where $\quad CIN_i$ = average salt concentration of inflow to reservoir during month i (mg/l)

Case II

$$QOUT_i \geq S_i$$

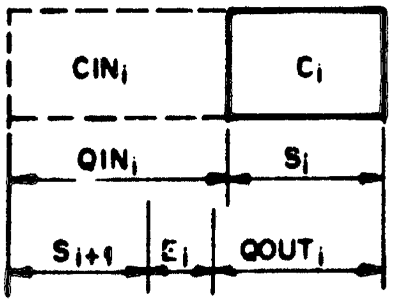

Fig.2.4: Illustration of Case II

In this case the salinity of the water leaving the reservoir is given by:

$$COUT_i = \frac{C_i.S_i + CIN_i.(QOUT_i - S_i)}{QOUT_i} \quad \ldots\ldots\ldots\ldots\ldots\ldots (2.10)$$

The reservoir salt concentration at the end of the month is then calculated as:

$$C_{i+1} = \frac{CIN_i.\{QIN_i - (QOUT_i - S_i)\}}{S_{i+1}} \quad \ldots\ldots\ldots\ldots\ldots\ldots (2.11)$$

The assumption implicit in equations 2.9 to 2.11 is that evaporation losses are deducted at the end of each time step. The volume of water remaining in the reservoir is usually very much greater than the outflow during a single time step. The error introduced by this assumption should therefore be insignificant.

2.4 Steady-state Vaal Barrage feedback element

This portion of the model is used to compute salt concentrations in the Vaal Barrage and in the PWV supply water. Steady-state conditions are assumed during the month. Inputs to the Vaal Barrage include releases from Vaal Dam, mine pumpage, catchment runoffs and effluent return flows from demand centres located south of the Witwatersrand catchment divide. Water supplied to users in the PWV region is abstracted from Vaal Dam and Vaal Barrage. The model also makes provision for possible future abstractions from the proposed Welkom Dam. In computing salt concentrations, allowance must therefore be made for indirect recycling of effluent return flows via the RWB Vaal Barrage intakes.

Channel and irrigation losses are accounted for and provision is made for demineralisation of sewage effluents with, or without, direct reclamation. ('Direct' reclamation is here defined as the recycling of treated sewage effluent directly into supply in a controlled manner, as opposed to the prevailing situation in which effluent returns are recycled in an uncontrolled manner via the Barrage intakes).

2.4.1 PWV region water supply

The PWV region has been divided into three distinct demand zones:

a) users north of the Vaal catchment divide;
b) users within the Vaal catchment downstream of Vaal Barrage;
and c) users within the Vaal catchment upstream of Vaal Barrage.

All three zones are supplied at present from Vaal Dam and Vaal Barrage with no significant direct reclamation. For the purposes of this model it is assumed that all users are supplied with the same mixture of Vaal Dam and Vaal Barrage water. Provision is made for the blending of water from the proposed Welkom Dam into the PWV supply.

Fig. 2.5 shows the Vaal Barrage abstraction points. Under normal circumstances flows in the Vaal Barrage are from east to west, with the result that salt concentrations upstream of the confluence of the two tributaries draining the southern PWV region (the Klip and Suikerbosrand) are virtually the same as Vaal Dam water (viz. of the order of 120 mg/l). Salinities downstream of the tributaries, however, are much higher due to the highly mineralised return flows. Reversals of flow occur in the Vaal river between the confluence of the tributaries and abstraction points 8 and 9 when releases from Vaal Dam are restricted and when the Klip and Suikerbosrand are in spate.

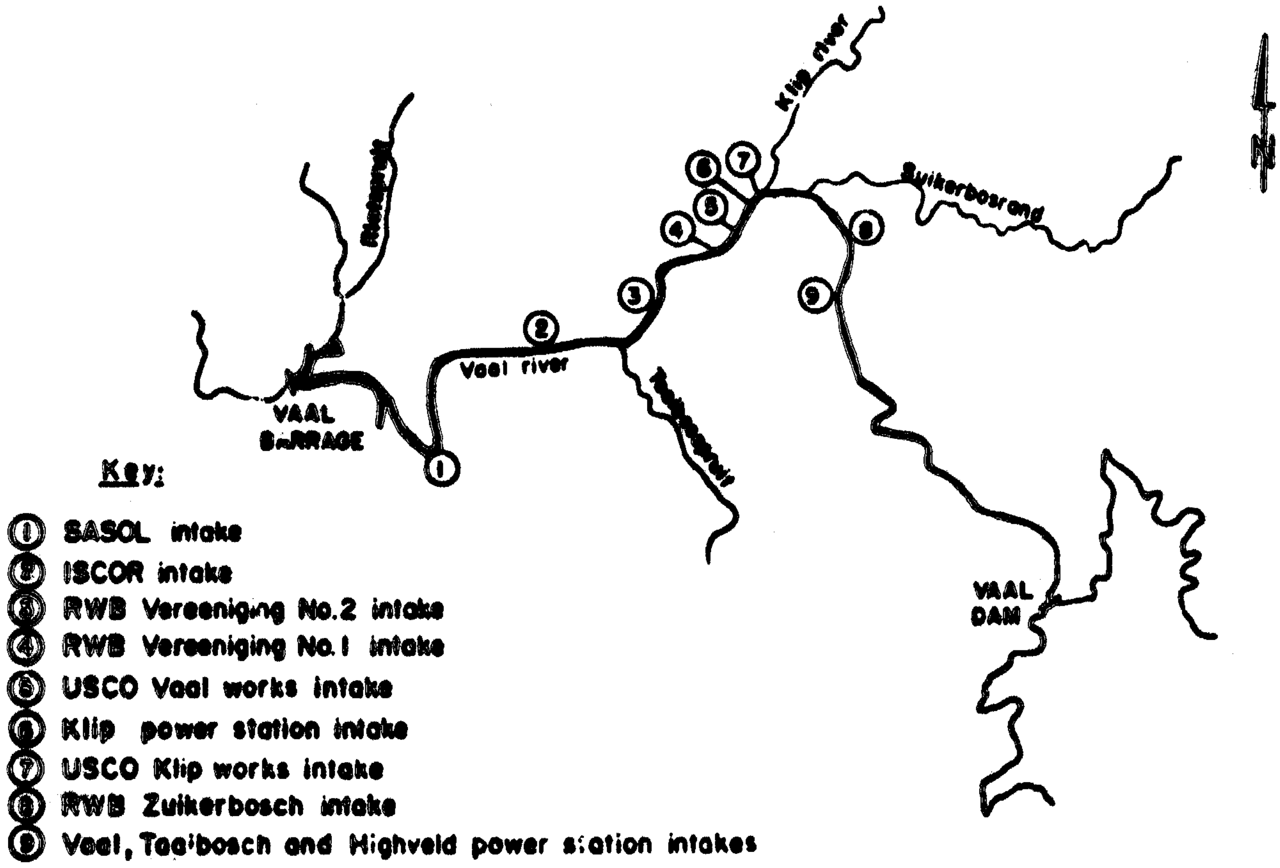

Fig.2.5: Location of Vaal Barrage abstraction points

The distinct difference between water qualities upstream and downstream of the tributaries demanded adoption of a two-cell model for the Vaal Barrage. The Vaal Barrage cell configuration is shown in Fig. 2.6. In the diagram DA is the monthly demand totalled for all abstraction points upstream of the tributaries (i.e. intakes 8 and 9) while DB is that for all abstraction points downstream of the tributaries (i.e. intakes 1 to 7). The quantities of water to be abstracted from Vaal Dam, Vaal Barrage cell A, Vaal Barrage cell B and Welkom Dam during each year simulated are specified as percentages of the nett PWV demand. During any month simulated the demands made on each of the above sources are given by:

$$DV = DNET.PV.10^{-2} \quad (2.12)$$

$$DA = DNET.PA.10^{-2} \quad (2.13)$$

$$DB = DNET.PB.10^{-2} \quad (2.14)$$

and $$DW = DNET-DV-DA-DB \quad (2.15)$$

where DV = demand on Vaal Dam during current month ($m^3 x10^6$)

DA = demand on Vaal Barrage cell A ($m^3 x10^6$)

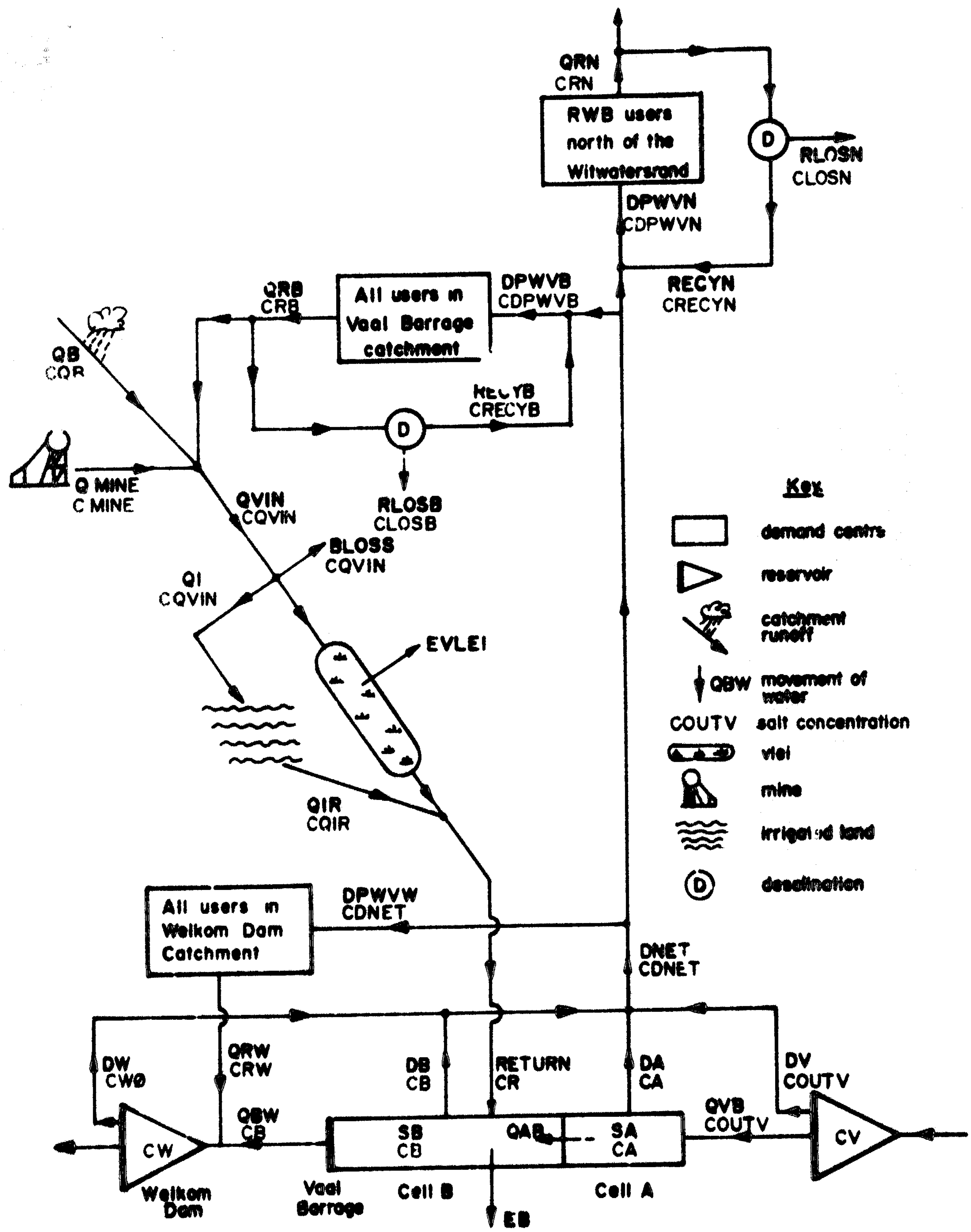

Fig.2.6: Diagram showing the movements of water and salt in the PWV region

DB = demand on Vaal Barrage cell B ($m^3 x 10^6$)

DW = demand on Welkom Dam ($m^3 x 10^6$)

PV = demand of Vaal Dam as percentage of net PWV demand

PA = demand of Vaal Barrage cell A as percentage of net PWV demand

PB = demand of Vaal Barrage cell B as percentage of net PWV demand

DNET = net PWV demand during current month ($m^3 x 10^6$)

and DNET is given by:

$$DNET = DPWVN - RECYN + DPWVB - RECYB + DPWVW \quad (2.16)$$

where DPWVN = monthly demand in northern catchment ($m^3 x 10^6$)

RECYN = quantity of water directly reclaimed in northern catchment ($m^3 x 10^6$/month)

DPWVB = monthly demand in Barrage catchment ($m^3 x 10^6$)

RECYB = quantity of water directly reclaimed in Barrage catchment ($m^3 x 10^6$/month)

DPWVW = monthly demand in demand zone downstream of Vaal Barrage ($m^3 x 10^6$)

DPWVN, DPWVB and DPWVW are in turn given by:

$$DPWVN = PMONTH_i . ADPWVN_j . 10^{-2} \quad (2.17)$$

$$DPWVB = PMONTH_i . ADPWVB_j . 10^{-2} \quad (2.18)$$

and

$$DPWVW = PMONTH_i . ADPWVW_j . 10^{-2} \quad (2.19)$$

where $ADPWVN_j$, $ADPWVB_j$ and $ADPWVW_j$ are annual demands in the northern catchment, Barrage catchment and the catchment downstream of Vaal Barrage during year j.

The salt concentration of the blended water supply CDNET (mg/l), is thus given by:

$$CDNET = \frac{DV.COUTV + DA.CA + DB.CB + DW.CW\emptyset}{DNET} \quad (2.20)$$

where COUTV = salt concentration of water leaving Vaal Dam during month (mg/l)

CA = salt concentration in Barrage cell A during month (mg/l)

CB = salt concentration in Barrage cell B during month (mg/l)

CWØ = salt concentration in Welkom Dam at start of month (mg/l)

The salt concentration of water abstracted from Welkom Dam during the month may be approximated to that at the start of the month because of the plug-flow assumption used to solve the reservoir salt balance. Under most conditions the outflow from the reservoir during any given month is much smaller than the reservoir storage,(i.e. Case I of section 2.3 usually applies). The effect of feedback of effluents from the large reservoir of Welkom Dam therefore becomes a long term effect and need not be considered when solving the Barrage salinity steady-state equations for a single month.

2.4.2 Effluent return flows

For each of the three water demand zones it is assumed that a constant proportion of the water supplied is returned to the stream as effluent. For any month simulated the return flow quantities are thus given by:

$$QRB = PRETB.DPWVB.10^{-2} \quad \ldots\ldots(2.21)$$
$$QRN = PRETN.DPWVN.10^{-2} \quad \ldots\ldots(2.22)$$
$$QRW = PRETW.DPWVW.10^{-2} \quad \ldots\ldots(2.23)$$

where PRETB, PRETN and PRETW are the percentages of water supplied to users in the Barrage, northern and Welkom Dam catchments that are returned to the stream, and QRB, QRN and QRW ($m^3 x10^6$) are the corresponding monthly return flows.

Users in each of the three catchments are assumed to increase the salt concentration of effluent water by a constant amount above that supplied. Effluent salt concentrations are therefore computed as:

$$CRB = CDPWVB + CADDB \quad \ldots\ldots(2.24)$$
$$CRN = CDPWVN + CADDN \quad \ldots\ldots(2.25)$$
$$CRW = CDNET + CADDW \quad \ldots\ldots(2.26)$$

where CRB, CRN and CRW are effluent salt concentrations in the Barrage, northern and Welkom Dam catchments respectively; CDPWVB, CDPWVN and CDNET are corresponding influent salt concentrations; and CADDB, CADDN and CADDW are the corresponding increases in salt concentrations. All units are mg/1.

Referring to Fig. 2.6 it can be seen that by applying the principle of continuity CDPWVB and CDPWVN are computed as:

$$CDPWVB = \frac{(DPWVB-RECYB).CDNET + RECYB.CRECYB}{DPWVB} \quad ....(2.27)$$

and $$CDPWVN = \frac{(DPWVN-RECYN).CDNET + RECYN.CRECYN}{DPWVN} \quad ......(2.28)$$

where RECYB and RECYN are water quantities directly reclaimed in the Barrage and northern catchments respectively, and CRECYB and CRECYN are the corresponding salt concentrations of the treated effluent.

2.4.3 Demineralisation and direct reclamation

The quantity of water reclaimed (i.e. the actual quantity re-introduced to supply) for each demand centre is specified as a proportion of the mean monthly demand for each year simulated. For each year simulated an upper limit is set upon the quantity of water that may be directly reclaimed in the Barrage and northern catchments. These values, RCAPB and RCAPN (m^3x10^6/month), can thus be considered as being the reclamation plant capacities during each simulation year. Provision is made for demineralisation of the recycled water. For each demineralisation works it is assumed that a constant proportion of the influent is bled off as brine).

In computing the actual quantity of water reclaimed in the Barrage catchment two distinct cases may arise:

<u>Case I</u> : $QRB \geq \frac{RCAPB}{(1-PLOSB.10^{-2})}$

$$RECYB = RCAPB \quad ....(2.29)$$

Case II : $QRB < \frac{RCAPB}{(1-PLOSB.10^{-2})}$

$$RECYB = QRB.(1-PLOSB.10^{-2}) \qquad (2.30)$$

where PLOSB = brine bleed-off for the Barrage catchment demineralisation works as percentage of influent discharge.

In both cases the brine bleed-off, RLOSB (m^3x10^6), is given by:

$$RLOSB = \frac{PLOSB.RECYB}{(100-PLOSB)} \qquad (2.31)$$

The actual quantity of water reclaimed in the northern catchment is computed in similar manner:

Case I : $QRN \geq \frac{RCAPN}{(1-PLOSN.10^{-2})}$

$$RECYN = RCAPN \qquad (2.32)$$

Case II : $QRN < \frac{RCAPN}{(1-PLOSN.10^{-2})}$

$$RECYN = QRN.(1-PLOSN.10^{-2}) \qquad (2.33)$$

where PLOSN = brine bleed-off for the northern catchment demineralisation works as percentage of influent discharge.

The brine bleed-off, RLOSN (m^3x10^6), is given by:

$$RLOSN = \frac{PLOSN.RECYN}{(100-PLOSN)} \qquad (2.34)$$

The assumption is made that the demineralisation works reduce salt concentrations by a constant percentage. The salt concentrations of recycled water in the Barrage and northern catchments, CRECYB and CRECYN, are then given by:

$$CRECYB = CRB.(1-PSUBB.10^{-2}) \qquad (2.35)$$

and

$$CRECYN = CRN.(1-PSUBN.10^{-2}) \qquad (2.36)$$

where PSUBB = percentage by which salt concentration is reduced by the Barrage catchment demineralisation works (mg/l)

PSUBN = percentage by which salt concentration is reduced by the northern catchment demineralisation works (mg/l).

The salt loads of the brine produced by the Barrage and northern catchment demineralisation works, LLOSB and LLOSN, are computed as:

$$LLOSB = CRB.(RLOSB + RECYB.PSUBB.10^{-2}) \quad \ldots\ldots\ldots\ldots\ldots (2.37)$$

$$LLOSN = CRN.(RLOSN + RECYN.PSUBN.10^{-2}) \quad \ldots\ldots\ldots\ldots\ldots (2.38)$$

From equations 2.24, 2.25, 2.27, 2.28, 2.35 and 2.36 the steady-state values of CDPWVB and CDPWVN can be expressed in terms of CDNET as:

$$CDPWVB = \frac{CDNET.(DPWVB-RECYB)+CADDB.RECYB.(1-PSUBB.10^{-2})}{DPWVB-RECYB.(1-PSUBB.10^{-2})} \quad ..(2.39)$$

and

$$CDPWVN = \frac{CDNET.(DPWVN-RECYN)+CADDN.RECYN.(1-PSUBN.10^{-2})}{DPWVN-RECYN.(1-PSUBN.10^{-2})} \quad ..(2.40)$$

If the desalination option is not required, then RCAPB, RCAPN, PSUBB and PSUBN are set equal to zero.

2.4.4 Mine pumpage

The pumping rate, QMINE ($m^3 x 10^6$/year), and the salt concentration, CMINE (mg/l), of water pumped from mine workings in the Barrage catchment are assumed to remain constant during each year simulated.

2.4.5 Catchment runoff

Monthly catchment runoffs, QB ($m^3 x 10^6$), and average monthly runoff salt concentrations, CQB (mg/l), are read as input data to the model. These values are generated by program NACLØ1 (Herold,1981a) or by program NACLM1 (Herold, 1980). Runoffs from all sub-catchments of the Barrage catchment are aggregated and treated as a single input and the tributaries draining the Barrage basin are idealised as a single river (see Fig. 2.6) where PSUBB = percentage by which salt concentration is reduced by the Barrage catchment demineralisation works (mg/l)

PSUBN = percentage by which salt concentration is reduced by the northern catchment demineralisation works (mg/l).

The salt loads of the brine produced by the Barrage and northern catchment demineralisation works, LLOSB and LLOSN, are computed as:

$$LLOSB = CRB.(RLOSB + RECYB.PSUBB.10^{-2}) \quad \ldots\ldots\ldots\ldots\ldots (2.37)$$

$$LLOSN = CRN.(RLOSN + RECYN.PSUBN.10^{-2}) \quad \ldots\ldots\ldots\ldots\ldots (2.38)$$

From equations 2.24, 2.25, 2.27, 2.28, 2.35 and 2.36 the steady-state values of CDPWVB and CDPWVN can be expressed in terms of CDNET as:

$$CDPWVB = \frac{CDNET.(DPWVB-RECYB)+CADDB.RECYB.(1-PSUBB.10^{-2})}{DPWVB-RECYB.(1-PSUBB.10^{-2})} \quad \ldots (2.39)$$

and

$$CDPWVN = \frac{CDNET.(DPWVN-RECYN)+CADDN.RECYN.(1-PSUBN.10^{-2})}{DPWVN-RECYN.(1-PSUBN.10^{-2})} \quad \ldots (2.40)$$

If the desalination option is not required, then RCAPB, RCAPN, PSUBB and PSUBN are set equal to zero.

2.4.4 Mine pumpage

The pumping rate, QMINE ($m^3 x 10^6$/year), and the salt concentration, CMINE (mg/l), of water pumped from mine workings in the Barrage catchment are assumed to remain constant during each year simulated.

2.4.5 Catchment runoff

Monthly catchment runoffs, QB ($m^3 x 10^6$), and average monthly runoff salt concentrations, CQB (mg/l), are read as input data to the model. These values are generated by program NACLØ1 (Herold,1981a) or by program NACLM1 (Herold, 1980). Runoffs from all sub-catchments of the Barrage catchment are aggregated and treated as a single input and the tributaries draining the Barrage basin are idealised as a single river (see Fig. 2.6)

The total inflow to the idealised river reach, QVIN ($m^3 x 10^6$) is given by:

$$QVIN = QB + QMINE + QRB - RECYB - RLOSB \quad \text{.............(2.41)}$$

The corresponding salt concentration, CQVIN (mg/l), is computed as:

$$CQVIN = \frac{QB.CQB+QMINE.CMINE+(QRB-RECYB-RLOSB).CRB}{QVIN} \quad \text{....(2.42)}$$

2.4.6 Channel seepage losses

Water is assumed to be lost from the channel at a constant rate, BLOSS ($m^3 x 10^6$/month). The salt concentration of the water lost is taken as being equal to CQVIN (mg/l). Seepage losses are therefore assumed to occur before evaporation losses, i.e. at the upstream end of the river.

2.4.7 Irrigation losses

The irrigation application during any given month, QI ($m^3 x 10^6$), is computed as:

$$QI = AIRRIG.(EB.FIRRIG-RB).THOU \quad \text{..............(2.43)}$$

where AIRRIG = irrigated area (km^2)
EB = mean monthly potential evaporation for Barrage catchment (mm)
FIRRIG = irrigation demand factor
RB = rainfall during month on Barrage catchment (mm)

RB as used in equation 2.43 should in fact be effective rainfall (i.e. actual rainfall multiplied by a reduction factor) in order to account for the fact that precipitation is not predictable and therefore may on occasion follow a full irrigation application. Furthermore, the rainfall is not evenly distributed over the month. It was not considered worthwhile incorporating such a factor in the equation, however, in view of the uncertainty in FIRRIG (e.g. little is known about the water requirements of crops being cultivated in the region) and the uncertainty in AIRRIG (irrigated areas had to be estimated from maps and it is not known what percentage of the land would be lying fallow at any given time). The uncertainties would tend to bring the reduction factor close to unity.

If QI as given by equation 2.43 is negative, then QI is set equal to zero.

The salt concentration of water applied to irrigated lands is taken as CQVIN mg/l. Irrigation losses are therefore also assumed to occur at the upstream end of the river.

Monthly irrigation return flows are calculated as:

$$QIR = QI.PIQRET.10^{-2} \qquad (2.44)$$

where QIR = irrigation return flow (m^3x10^6)

PIQRET = irrigation return flow as percentage of irrigation application.

A constant percentage of the salt load applied to irrigated lands, PILLOS, is assumed to be retained, the remainder returning to the stream. The salt concentration of effluent return flows is thus calculated as:

$$CQIR = \frac{QI.CQVIN.(100-PILLOS).10^{-2}}{QIR} \qquad (2.45)$$

2.4.8 Evaporation loss

Account is taken of the evaporation loss from the extensive vlei systems of the southern PWV region. Evaporation losses, EVLEI (m^3x10^6), are calculated for each month as:

$$EVLEI = AVLEI.(EB.FEVAP-RB).THOU \qquad (2.46)$$

where

AVLEI = average vlei water surface area during month (km^2)

FEVAP = vlei evaporation factor

and AVLEI is computed as:

$$AVLEI = A1V.QCAL^{A2V} \qquad (2.47)$$

where A1V and A2V are constants defining the discharge-area-relationship and QCAL (m^3x10^6) is the mean discharge in the channel which is approximated by:

$$QCAL = QVIN - \tfrac{1}{2}(BLOSS-QI+QIR-EVLEI_O) \qquad (2.48)$$

where

$EVLEI_O$ = vlei evaporation computed for previous month.

2.4.9 Return flow to Vaal Barrage

The tributary input to the Vaal Barrage during each month simulated, RETURN (m^3x10^6), is calculated as:

$$RETURN = QVIN - BLOSS - QI + QIR - EVLEI \qquad (2.49)$$

and the corresponding salt concentration, CR (mg/l), becomes:

$$CR = \frac{CQVIN.(QVIN-BLOSS-QI) + CQIR.QIR}{RETURN} \qquad (2.50)$$

2.4.10 Barrage mass balance

The Vaal Barrage is modelled as a two-cell reservoir, the boundary between the two cells being immediately downstream of the RWB Zuikerbosch intakes (intake No. 8 of Fig. 2.5). The storage in the upstream cell is ignored for purposes of modelling water qualities. This assumption is well justified for a monthly steady state model as the flow through this portion of the Barrage even during a dry month is very much greater than the storage. (For instance, at Barrage capacity the storage of this cell is $4,6x10^6m^3$, while the 1977/78 average monthly abstraction from the Zuikerbosch intakes alone is $20,4\ x10^6m^3$). The storage effect of the downstream cell ($48\ x10^6m^3$), however, cannot be ignored.

The water mass balance for the entire Barrage reservoir is solved in a manner similar to that described in section 2.2.1.

Applying the principle of continuity to cell A (which has zero storage) allows QAB(m^3x10^6), the discharge between cells A and B, to be calculated as:

$$QAB = QVB - DA \qquad (2.51)$$

where QVB (m^3x10^6) is the release from Vaal Dam during the month.

2.4.11 Steady-state equations to solve for Barrage salt concentrations

In solving for salt concentrations in the PWV region two distinct cases can arise, solutions for which follow:

<u>Case I</u> : QAB $\geq$ 0

In this case salt concentrations in cell A are independent of those in cell B. The salt concentration in cell A is equal to the concentration of water released from Vaal Dam. Thus:

$$CA = COUTV \quad \text{.......} (2.52)$$

Substitution in equation 2.20 yields:

$$CDNET = X1 + Y1.CB \quad \text{.......} (2.53)$$

where
$$X1 = \frac{COUTV.(DV+DA)+DW.CW\emptyset}{DNET} \quad \text{.......} (2.53a)$$

$$Y1 = \frac{DB}{DNET} \quad \text{.......} (2.53b)$$

From equations 2.39 and 2.53:

$$CDPWVB = X2 + Y2.CB \quad \text{.......} (2.54)$$

where
$$X2 = \frac{X1.(DPWVB-RECYB)+CADDB.RECYB.(1-PSUBB.10^{-2})}{DPWVB-RECYB.(1-PSUBB.10^{-2})} \quad \text{.......} (2.54a)$$

$$Y2 = \frac{Y1.(DPWVB-RECYB}{DPWVB-RECYB.(1-PSUBB.10^{-2})} \quad \text{.......} (2.54b)$$

From equations 2.24 and 2.54:

$$CRB = X3 + Y2.CB \quad \text{.......} (2.55)$$

where
$$X3 = X2 + CADDB \quad \text{.......} (2.55a)$$

From equations 2.42 and 2.55:

$$CQVIN = X4 + Y3.CB \quad \text{.......} (2.56)$$

where
$$X4 = \frac{QB.CQB+QMINE.CMINE+(QRB-RECYB-RLOSB).X3}{QVIN} \quad \text{.......} (2.56a)$$

$$Y3 = \frac{(QRB-RECYB-RLOSB).Y2}{QVIN} \quad \text{.......} (2.56b)$$

From equations 2.45 and 2.56:

$$CQIR = X5 + Y4.CB \quad \text{.......} (2.57)$$

where
$$X5 = \frac{X4.QI.(100-PILOS).10^{-2}}{QIR} \quad \text{.......} (2.57a)$$

$$Y4 = \frac{Y3.QI.(100-PILOS).10^{-2}}{QIR} \quad \text{.......} (2.57b)$$

From equations 2.50, 2.56 and 2.57:

$$CR = X6 + Y5.CB \quad \text{.......} (2.58)$$

where
$$X6 = \frac{X4.(QVIN-BLOSS-QI)+X5.QIR}{RETURN} \quad \text{.......} (2.58a)$$

$$Y5 = \frac{Y3.(QVIN-BLOSS-QI) + Y4.QIR}{RETURN} \quad \text{.......} (2.58b)$$

The salt mass balance equation for cell B is given by:

$$CB1.SB1 = CB\emptyset.SB\emptyset.+CA.QAB+CR.RETURN-CB.DB-CB.QBW \quad ..(2.59)$$

where CB1 = salt concentration of cell B at end of month (mg/l)

SB1 = water storage of cell B at end of month ($m^3 x10^6$)

CBØ = salt concentration of cell B at end of previous month (mg/l)

SBØ = water storage of cell B at end of previous month ($m^3 x10^6$)

QBW = discharge from Vaal Barrage to Welkom Dam during month ($m^3 x10^6$).

Equation 2.59 holds true provided that the steady-state condition is attained near the beginning of the month.

For steady-state conditions the salt concentration at the end of the month is equal to that during the month, i.e. CB1 = CB. The unknown cell salinity, CB, can now be solved from equations 2.58 and 2.59:

$$CB = \frac{CB\emptyset.SB\emptyset+CA.QAB+X6.RETURN}{SB1+DB+QBW-Y5.RETURN} \quad ....(2.60)$$

Case II QAB < Ø

In this case the salt concentration of cell A is dependent upon that of cell B:

$$CA = \frac{COUTV.QVB - CB.QAB}{QVB - QAB} \quad ....(2.61)$$

Coefficients X1 and Y1 of equation 2.52 now become:

$$X1 = \frac{COUTV.(DV+QVB) + CW\emptyset.DW}{DNET} \quad ....(2.53c)$$

$$Y1 = \frac{DB - QAB}{DNET} \quad ....(2.53d)$$

Equations 2.54 to 2.58 remain unaltered, but the salt mass balance equation for cell B becomes:

$$CB1.SB1 = CB\emptyset.SB\emptyset+CR.RETURN-CB.DB-CB.QBW+CB.QAB \quad .....(2.62)$$

Substituting CB1 = CB and using equation 2.58 yields:

$$CB = \frac{CB\emptyset.SB\emptyset+X6.RETURN}{SB1+DB+QBW-QAB-Y5.RETURN} \quad ....(2.63).$$

The salt mass balance equation for cell B is given by:

$$CB1.SB1 = CBØ.SBØ.+CA.QAB+CR.RETURN-CB.DB-CB.QBW \quad ..(2.59)$$

where CB1 = salt concentration of cell B at end of month (mg/l)

SB1 = water storage of cell B at end of month (m^3x10^6)

CBØ = salt concentration of cell B at end of previous month (mg/l)

SBØ = water storage of cell B at end of previous month (m^3x10^6)

QBW = discharge from Vaal Barrage to Welkom Dam during month (m^3x10^6).

Equation 2.59 holds true provided that the steady-state condition is attained near the beginning of the month.

For steady-state conditions the salt concentration at the end of the month is equal to that during the month, i.e. CB1 = CB. The unknown cell salinity, CB, can now be solved from equations 2.58 and 2.59:

$$CB = \frac{CBØ.SBØ+CA.QAB+X6.RETURN}{SB1+DB+QBW-Y5.RETURN} \quad \ldots\ldots\ldots\ldots\ldots\ldots\ldots(2.60)$$

<u>Case II</u> QAB < Ø

In this case the salt concentration of cell A is dependent upon that of cell B:

$$CA = \frac{COUTV.QVB - CB.QAB}{QVB - QAB} \quad \ldots\ldots\ldots\ldots\ldots\ldots\ldots\ldots\ldots(2.61)$$

Coefficients X1 and Y1 of equation 2.52 now become:

$$X1 = \frac{COUTV.(DV+QVB) + CWØ.DW}{DNET} \quad \ldots\ldots\ldots\ldots\ldots\ldots\ldots(2.53c)$$

$$Y1 = \frac{DB - QAB}{DNET} \quad \ldots\ldots\ldots\ldots\ldots\ldots\ldots\ldots\ldots\ldots\ldots\ldots(2.53d)$$

Equations 2.54 to 2.58 remain unaltered, but the salt mass balance equation for cell B becomes:

$$CB1.SB1 = CBØ.SBØ+CR.RETURN-CB.DB-CB.QBW+CB.QAB \quad .....(2.62)$$

Substituting CB1 = CB and using equation 2.58 yields:

$$CB = \frac{CBØ.SBØ+X6.RETURN}{SB1+DB+QBW-QAB-Y5.RETURN} \quad \ldots\ldots\ldots\ldots\ldots\ldots\ldots(2.63).$$

In the program, provision is made for simulating options where water supplied to users in the PWV region is composed of a blend of Vaal Barrage and Vaal Dam water proportioned in such a manner that the TDS concentration never exceeds a specified upper limit, CTARG (mg/l), while at the same time maximising the proportion abstracted from the Barrage. This is achieved by initially setting PV, PA and PW to zero and PB to 100 per cent. If the salt concentration of the supply to the PWV region, CDNET, as given by the equation 2.20 exceeds CTARG, then new percentage abstractions from Vaal Dam and Vaal Barrage cell B are computed as follows:

$$PB' = 100.\frac{(CTARGX - COUTV)}{CB - COUTV} \qquad (2.64)$$

where PB' = new estimate of PB(%)

CTARGX = target salt concentration set slightly lower then CTARG in order to reduce the number of iterations required to achieve a concentration lower than CTARG (mg/l)

and $$PV' = 100 - PB' \qquad (2.65)$$

The water and salt mass balance equations for all reservoirs are then re-computed for the month using the adjusted PB and PV values. More than one iteration is often required because the changes in PB and PV can sometimes increase the value of CB.

2.4.12 Quality of water supplied to users between Vaal Barrage and Bloemhof Dam

Most of the Vaal river intakes providing water to users in this region are situated at a point in the Vaal river above which approximately 40 percent of the runoff from the intervening Bloemhof catchment has already entered. For the sake of simplicity in the computation of dilution factors, it has been assumed that all transmissior losses and irrigation abstractions are also centred on the same point.

The salt concentration of Vaal river water immediately upstream of the point of abstraction during each month simulated is thus given by:

$$CDWD = \frac{RW.COUTW+PCWTVL.QBL.CQBL.10^{-2}}{RW+PCWTVL.QBL.10^{-2}} \quad \ldots\ldots\ldots\ldots (2.66)$$

where CDWD = salt concentration in Vaal river at point of abstraction (i.e. supply TDS to users downstream of the potential Welkom Dam site) (mg/l)

RW = total release from Welkom Dam (m^3x10^6)

COUTW = salt concentration of water leaving Welkom Dam (or in the Vaal river at this location for options in which Welkom Dam does not exist) (mg/l)

PCWTVL = percentage of Bloemhof catchment runoff entering the Vaal river upstream of the intakes (approximately 40 percent)

QBL = catchment runoff between Welkom Dam and Bloemhof Dam

CQBL = average monthly TDS of runoff from the Bloemhof catchment (mg/l)

The quantity of water entering Bloemhof Dam during the month, QINBL (m^3x10^6), is computed as:

$$QINBL = RW + QBL - DWD \quad \ldots\ldots\ldots\ldots (2.67)$$

where DWD = total of all abstractions and transmission losses between Welkom Dam and Bloemhof Dam (m^3x10^6)

Finally, the salt concentration of water entering Bloemhof Dam, CQINBL (mg/l), is given by:

$$CQINBL = \frac{RW.COUTW+QBL.CQBL-DWD.CDWD}{QINBL} \quad \ldots\ldots\ldots\ldots (2.68)$$

CHAPTER 3: MODEL APPLICATIONS

This chapter demonstrates the versatility of the model and describes how it can be used to compare the merits of various pollution control strategies. Section 3.1 gives suggestions as to the criteria by which ameliorative measures can be objectively compared, while in section 3.2 initial comparisons are drawn among the various options that have been suggested. It must be stressed that the comparisons made in section 3.2 are merely preliminary and should not be allowed to eliminate any of the options. A much more rigorous analysis has yet to be performed, including testing the options against many other hydrological sequences, detailed investigations of the water resources (which are beyond the scope of this report) and feasibility studies, including costs of implementation, of each option. Moreover, the assumptions made regarding reservoir operating rules and projected water demands have to be checked. The simulations described should therefore be regarded as no more than examples of how the model can be used.

3.1 Suggested criteria for the comparison of pollution control strategies

The output from the model comprises a simulated record of monthly reservoir storages and monthly TDS concentrations in each reservoir and in the water supply to various demand centres for any given sequence of hydrology and demand pattern.

The basic philosophy behind hydrological modelling is that the hydrology (in particular the rainfall patterns) observed over a sufficiently long period of the past are representative of what may be expected in the future. If this assumption is made, and provided the hydrological record is long enough, the system can be simulated for several hydrological sequences, thereby facilitating the estimation of the probability of the occurrence of various events. In a water resources study the "event" for which an estimation of the probability of occurrence is required would be the failure of a reservoir to meet a specified demand . In the present study, however, we are more interested in the likely salt concentrations in the water supply.

TDS concentrations can be presented in several different forms. In the first instance, a time series of monthly concentrations can be plotted (see, for example, Fig. 3.3). Such a plot (or series of plots for different hydrological sequences) is, however, extremely difficult to interpret. A more convenient means of expressing the data is the cumulative frequency (or duration) curve, an example of which is given in Fig. 3.4. Several different duration curves can in fact also be compiled. Fig. 3.4 is a duration curve for one particular 20-year sequence of hydrology (1914/15 to 1933/34) corresponding to projected demand conditions for the period 1980/81 to 1999/2000. If several such simulations were to be run, using other hydrological sequences as input data, it would be possible to compile a duration curve for each of the demand years 1980/81, 1981/82...., 1999/2000. Fig 3.1 shows how such a set of duration curves could be used to estimate the most likely exceedance levels for a given option over the next 20 years.

Representations of the monthly TDS concentrations, such as those shown in Figs. 3.1 and 3.4, are much easier to interpret than Fig. 3.3. Difficulty still remains, however, in placing a value upon the improvement in water quality achieved by any given ameliorative measure as opposed to that resulting from other options. Of what significance, for example, is the difference in the distribution of TDS concentrations reflected in Figs. 3.4 and 3.10 (i.e. options 1 and 3A)?

With this problem in mind the Water Research Commission appointed Mr. J J C Heynike to conduct research into the economic costs to users in the PWV region of different TDS concentrations in the supply water. Various industries and

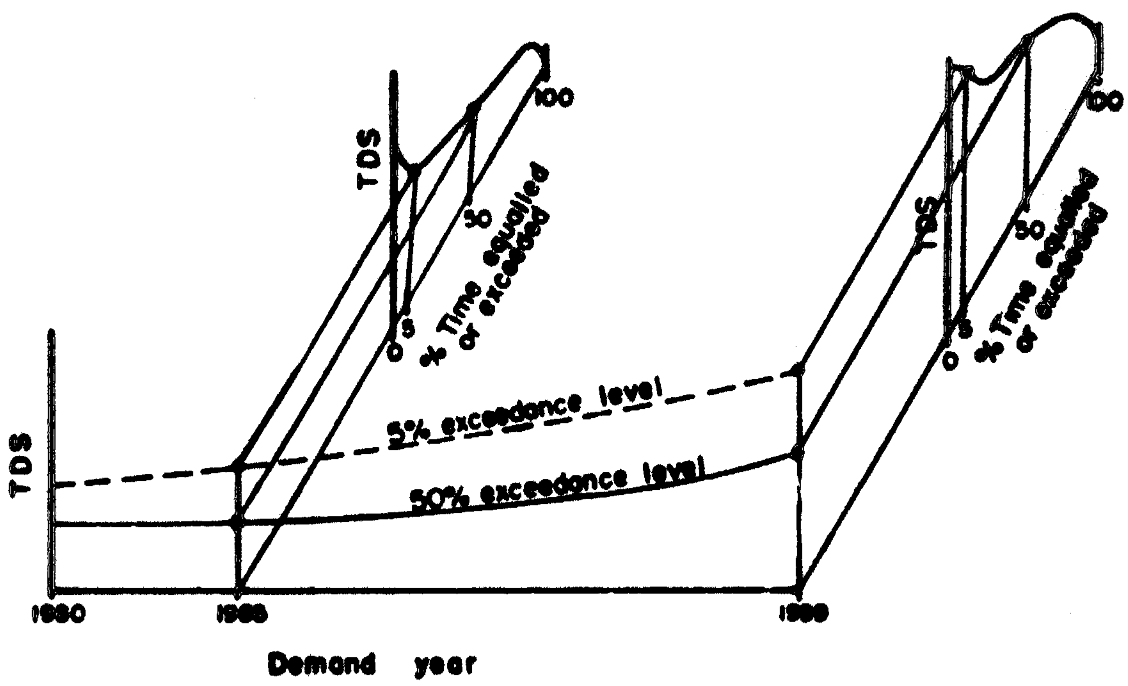

Fig.3.1. Representation of duration curves as a time series of probable exceedance levels.

local authorities were asked to produce a break-down of costs, both running (including such factors as corrosion, additional water, power costs and additional chemicals) and capital (such as additional plant and increased reservoir storage). The costs to private householders were also estimated (e.g. electric geysers, pipework replacement, detergents and reduced life of washable fabrics).

Estimates of marginal costs as outlined above were estimated assuming increases in TDS concentrations from the present 300 mg/l to 500-600 and 800 mg/l respectively. The marginal costs, as estimated by Heynike (1980) are tabulated in Table 3.1.

Table 3.1 : Marginal costs associated with dissolved solids in water supply (millions of rands)

Average TDS (mg/l)	500-600 mg/l	800 mg/l
Running costs (relative to cost at 300 mg/l TDS)		
Private household (European)	19,5	40,0*
" " (other)+	15,0+	22,0+
Local authorities (corrosion in distribution network)	0,3	1,1
Industry and power stations (O & M)	25,1≠	35,1
Sub-total	59,9	98,2
Capital costs (additional plant and reservoir storages, etc)		
Water supply authority (RWB) (Additional plant capacity)	4,6	11,4
Industry and power stations (Capital costs)	14,9≠	20,9
(Additional reservoir capacity)	1,2	2,9
Sub-total	20,7	35,2
Total	80,6	133,4

* Revised figure (Heynike, 1981)

\+ Costs of Asian, Coloured and Black householders. These values became available for the first time in 1981 (Heynike,1981)

≠ The split between capital and running costs was assumed to be the same as for the 800 mg/l level, i.e. running costs were taken as being 62,7% of the total cost to industries of R40 million estimated by Heynike (1980).

The costs given in Table 3.1 are total annual costs to users in the PWV region for the 1980 level of demand (i.e. 874 x $10^6 m^3$ p.a.). The total costs were then expressed as expenditure per million cubic metres of water supplied and are given in Table 3.2.

Table 3.2 : Marginal costs per million cubic metres of water consumed (rand x 10^3)

Average TDS (mg/l)	running cost	capital cost	total cost
100	-59,7 +	-20,3 +	-80,0
300	0	0	0
425	37,3 *	12,7 *	50,0
550	68,5	23,7	92,2
675	93,5 *	32,9 *	126,4
800	112,4	40,3	152,6
1000	142,6 +	52,1 +	194,7

* These values have been interpolated using a second order equation

\+ These values have been extrapolated linearly.

The costs given in Table 3.2 are plotted in Fig. 3.2.

It is of importance to note that there is a difference between the manner of calculating running costs and that of capital costs.

Running costs can be estimated by simulating one or more representative hydrological sequences for a given set of demand conditions and then computing the cost incurred in each month as follows:

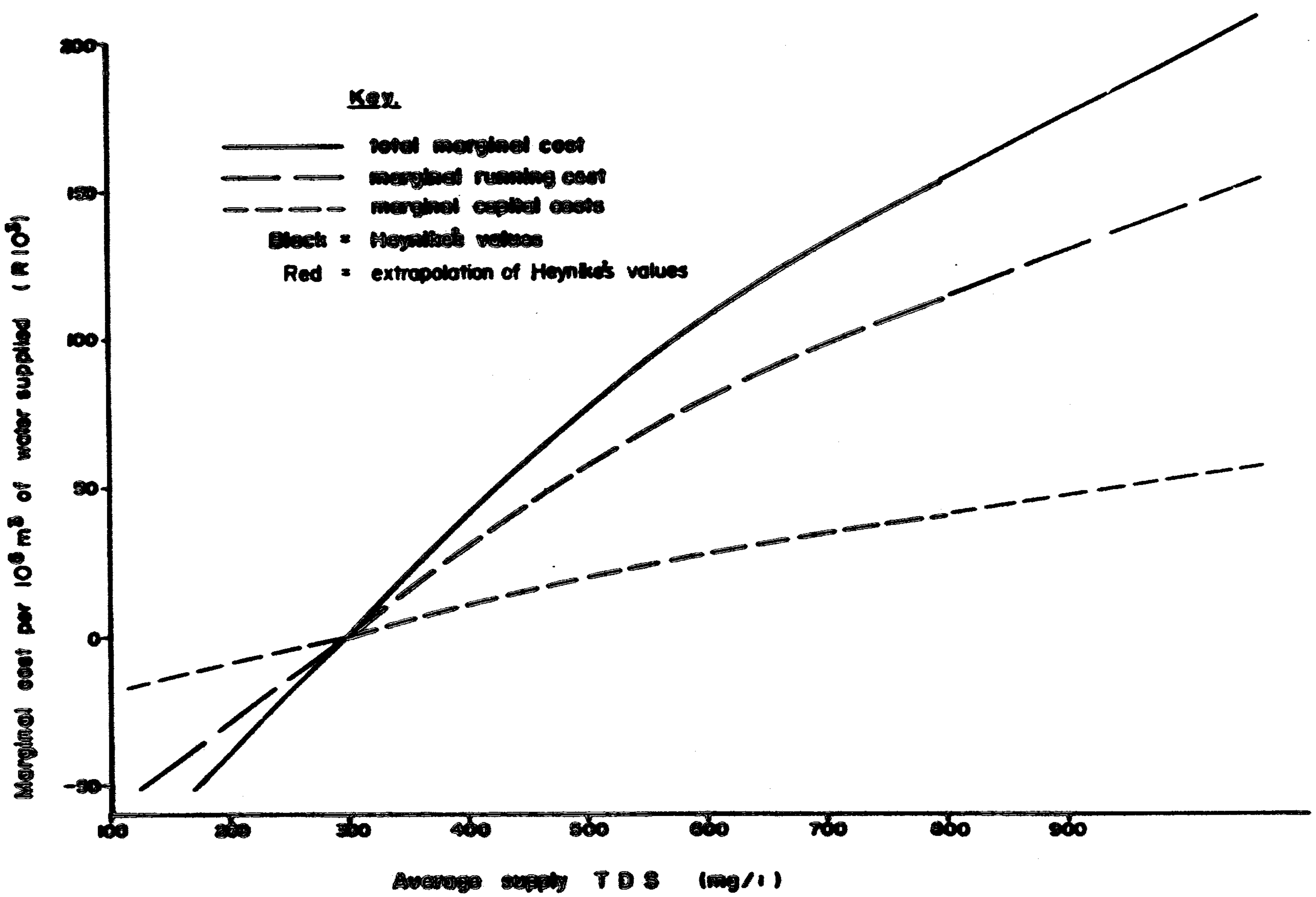

Fig. 3.2: Relationship between marginal costs and average water supply TDS

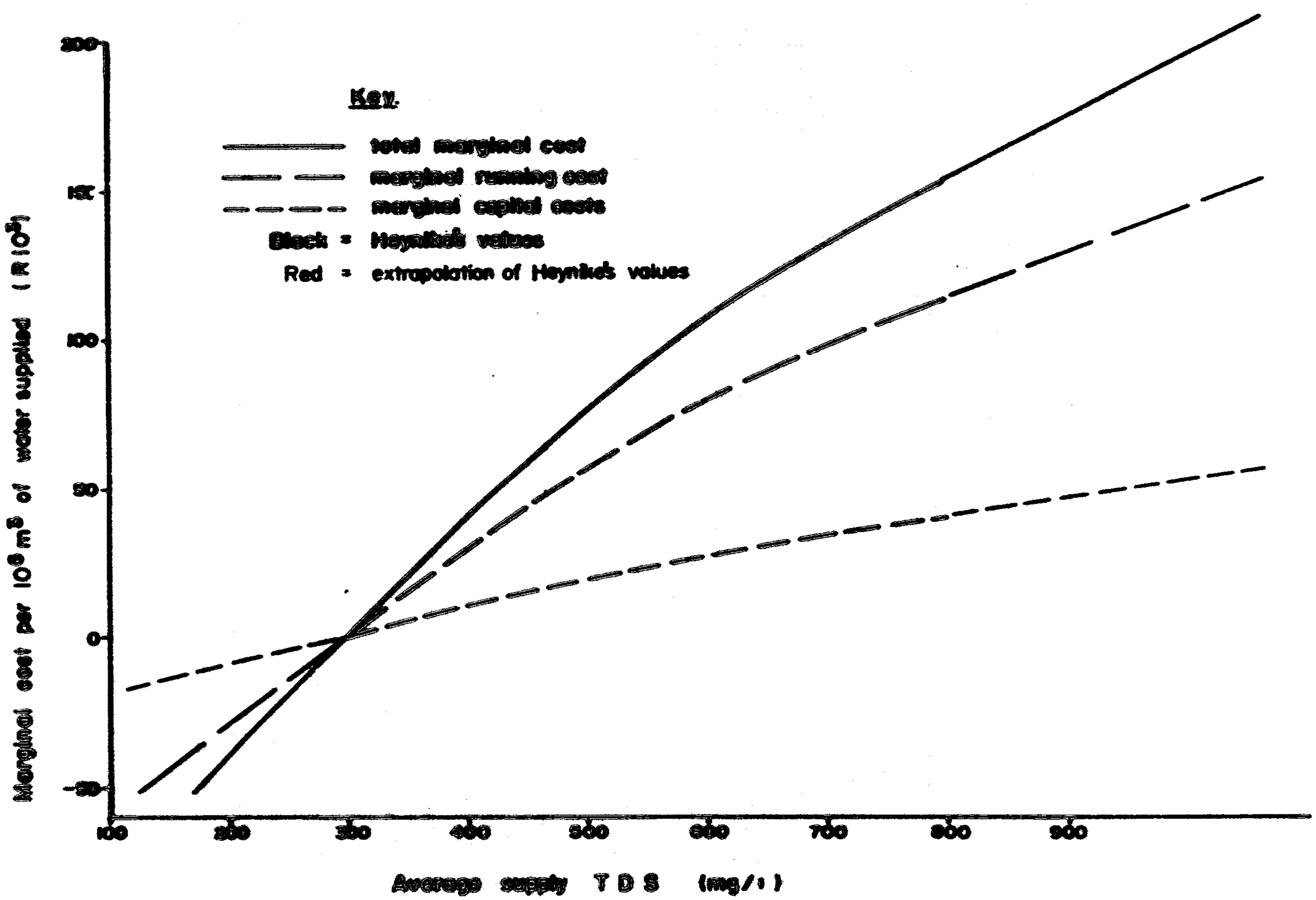

Fig.3.2: Relationship between marginal costs and average water supply TDS

$$CR_{i,j} = D_{i,j}.RR(TDS_{i,j}) \quad \ldots\ldots\ldots\ldots\ldots\ldots\ldots\ldots (3.1)$$

where $CR_{i,j}$ = running cost incurred in month j of the ith year simulated (rands x 10^3)

$D_{i,j}$ = water demand in month j of the ith year simulated ($m^3 x 10^6$)

$RR(TDS_{i,j})$ = cost per million cubic metres of water consumed given an average monthly TDS of $TDS_{i,j}$ mg/l (obtained from Fig. 3.2) where $TDS_{i,j}$ is the average TDS during month j of the ith year simulated

This cost can then be expressed as an equivalent present value capital cost:

$$PV_{i,j} = \frac{CR_{i,j}}{(1+I)^i} \quad \text{(rands x } 10^3) \ldots\ldots\ldots\ldots\ldots\ldots (3.2)$$

where $PV_{i,j}$ = present (1980) value of the running cost incurred in month j of year i

I = interest rate (%)

The total present value running cost for the entire period simulated can then be expressed as a present value annual cost as follows:

$$AR = \left[\sum_{i=1}^{n} \sum_{j=1}^{12} PV_{i,j}\right] \cdot \frac{I.(1+I)^N}{(1+I)^N-1} \quad \ldots\ldots\ldots\ldots\ldots\ldots (3.3)$$

where AR = annual present value running cost (randsx10^3)

n = total number of years simulated

N = number of years over which the costs are to be discounted.

The above approach, however, cannot be used to estimate the capital investment costs to users of the water because there are no capital cost savings during months when the TDS concentrations drop below the level for which the plant was designed. In order to assess the capital costs during each demand year it is necessary to establish the most probable average TDS to be expected in that year. This can be achieved by running each option for several hydrological sequences and then computing the mean TDS for each demand year. The capital cost incurred in each year can then be estimated as the incremental change in the marginal capital cost for the year (i.e. care must be taken not to re-invest erroneously the entire marginal cost for each year).

The procedure involved in computing incremental capital costs is complex and is best demonstrated by means of an example. Let us consider a hypothetical option which results in most probable average annual TDS concentrations during the next 4 years as indicated in Table 3.3. Projected annual demands (see Appendix A) are also given in Table 3.3.

Table 3.3 : Hypothetical average annual TDS concentrations

year	1980	1981	1982	1983	1984
average TDS (mg/l)	300	400	450	350	400
annual demand ($m^3 x 10^6$)	874	916	959	1005	1052

Incremental cost during 1981

Plant already exists to cope with 874 x $10^6 m^3$ at 300 mg/l. The incremental cost for the first 874 x $10^6 m^3$ is thus calculated as:

Cost = $(RC(400) - RC(300)).874.10^{-3}$ (million rands)

where RC(400) and RC(300) are the marginal capital costs corresponding to average TDS concentrations of 400 and 300 mg/l respectively (see Fig. 1).

i.e. cost = $(10 - 0).874.10^{-3}$

= R8,74 million